SOCIAL INTERACTIONS IN NATURAL POPULATIONS OF WEAKLY ELECTRIC FISH

DISSERTATION
der Mathematisch-Naturwissenschaftlichen Fakultät
der EBERHARD KARLS UNIVERSITÄT TÜBINGEN
zur Erlangung des Grades eines
Doktors der Naturwissenschaften
(Dr. rer. nat.)

vorgelegt von
Dipl. Biol. Jörg Henninger
aus Heide

Tübingen
2015

Gedruckt mit Genehmigung der Mathematisch-Naturwissenschaftlichen Fakultät der
Eberhard Karls Universität Tübingen.

Tag der mündlichen Prüfung	29.9.2015
Dekan:	Prof. Dr. Wolfgang Rosenstiel
1. Berichterstatter:	Prof. Dr. Jan Benda
2. Berichterstatter:	Prof. Dr. Rüdiger Krahe
3. Berichterstatter:	Prof. Michael R. Markham

All men by nature desire to know. An indication of this is the delight we take in our senses – for even apart from their usefulness they are loved for themselves ...

Aristotle in *Metaphysics*, Book 1, 980a

Contents

List of Figures

List of Tables

Abstract

Animals and their sensory systems evolved in specific environments and in the context of their particular ethological niches. It is often found that sensory neurons are tuned to the statistics of the natural scenes that they likely to experience. Accordingly, the importance of knowledge of natural stimuli and the problems faced and solved by sensory systems in their natural environments for the understanding of neural processing is increasingly recognized.

Weakly electric fish are successful model organisms for studying the neural mechanisms underlying sensory processing in vertebrates. These mostly nocturnal animals evolved an active electric sense employed in navigation, foraging and communication. Nocturnal conditions, murky water, and the tropical environment make their natural habitats challenging study sites. Therefore, most data on their natural behavior and their communication signals have been acquired under restricted lab conditions or remain anecdotal. However, their permanently active electric organ discharges provide an excellent opportunity to monitor the movements and communication of individual unrestrained fish. The central goal of the present thesis has been to establish and to apply a method for the non-invasive quantification of electrocommunication stimuli while animals roam and interact in their natural environment.

In Chapter 2, we present an automated tracking system allowing for the reliable and continuous tracking of wave-type electric fish based on the individual-specific frequency of the electric organ discharge. The system extracts frequency modulations of the EOD on short and long time scales, and estimates location and orientation of the tracked fish.

We acquired data on natural communication of the ghost knifefish, *Apteronotus rostratus*, during its reproductive period, by deploying our tracking system in the Panamanian rain forest (Chapter 3). We tracked individuals and characterized dyadic interactions and the corresponding electro-communication scenes. We showed that a specific communication signal, independent of context, was almost exclusively emitted in close proximity to a conspecific. During courtship, the communication of males was precisely locked to that of females. Our data also showed that competing male intruders can be detected and responded to over larger distances of up to 170 cm, even in the presence of a much stronger EOD of a nearby female conspecific. For the observed interactions we extracted frequency differences and estimated effective signal intensities, and related those to the response properties of the P-unit electroreceptors. Surprisingly, we found that in many relevant communication situations the electro-receptors will be driven only weakly by electric communication signals, either because of a frequency mismatch in courtship or because of large interaction distances in agonistic contexts. This study is the first account for the detailed monitoring and characterization of electric fish movement and communication in their natural habitat.

To determine the behavioral context of the male-female interaction observed in Panamá, we conducted a long-term breeding experiment in the laboratory with the closely related species *A. leptorhynchus* (Chapter 4). We used our tracking software to identify male-female communication scenes similar to those observed in the field and demonstrated its relationship to courtship and spawning. Sequence and dynamics of the chirping during courtship closely matched that observed in the field. We found that both the female long chirp signaling spawning and the quick and precisely timed male echo response to female chirps are conserved across species.

Applying our tracking system we revealed the properties of natural communication situations. We then demonstrated how our system can be used to further characterize the behaviors observed in the field in a tailor-made long-term laboratory study.

Deutschsprachige Zusammenfassung

Tiere und ihre Sinnessysteme sind in einer für sie spezifischen Umwelt evolviert. Es wurde oft festgestellt, dass die Kodierungseigenschaften sensorischer Neurone an die Statistik natürlicher Umweltsituationen angepasst sind. Die Bedeutung des Verständnisses natürlicher Signale und der spezifischen sensorischen Herausforderungen, denen die Tiere in ihrer natürlichen Umwelt ausgesetzt sind, wurde dementsprechend zunehmend anerkannt.

Schwachelektrische Fische sind erfolgreiche Modellorganismen für die Erforschung der neuronalen Mechanismen, die der sensorischen Verarbeitung in Vertebraten zu Grunde liegen. Diese meist nachtaktiven Tiere entwickelten einen aktiven elektrischen Sinn, der für die Orientierung, den Beutefang und die Kommunikation eingesetzt wird. Durch die Nachtaktivität der Tiere, sowie oftmals trübes Wasser und die tropischen Bedingungen sind die natürlichen Habitate dieser Tiere schwierige Studienorte. Deshalb waren bisherige Studien zum natürlichen Verhalten und insbesondere der Kommunikation dieser Tiere entweder auf das Labor beschränkt oder haben anektodischen Charakter. Dennoch sind diese Tiere wegen ihrer permanenten elektrischen Entladungen hervorragend für Studien über Ihre Bewegung und Kommunikation unter unbeschränkten Bedingungen. Das zentrale Ziel dieser Promotionsarbeit ist die Entwicklung und Anwendung einer neuartigen Methode zur nichtinvasiven Quantifizierung der Elektrokommunikationssignale von freilebenden und -interagierenden elektrischen Fischen in ihrem natürlichen Habitat.

Im zweiten Kapitel stelle ich die Methode zur automatisierten Beobachtung von identifizierten elektrischen Fischen vor, das auf der Verfolgung von elektrischen Entladungen dieser Fische basiert. Diese Methode extrahiert Frequenzmodulationen der elektrischen Entladungen auf verschiedenen Zeitskalen und schätzt den Ort und die Orientierung der Fische.

Im dritten Kapitel wurde diese Methode angewandt, um den Messerfisch Apteronotus rostratus während seiner Fortplanzungsperiode in seinem natürlichen Habitat in Panamá zu untersuchen. Wir haben Individuen automatisch verfolgt und die Kommunikationssituationen von paarweisen Interaktionen charakterisiert. Wir konnten dabei zeigen, dass bestimmte Kommunikationssignale ausschließlich auf kurzen Entfernungen generiert werden, unabhängig vom sozialen Kontext. Während des Paarungsverhaltens senden männliche Messerfische ihre Signale in einem zeitlich präzisen Verhältnis zu denen der Weibchen. Unsere Daten zeigen auch, dass um Weibchen konkurrierende Männchen vom residenten Männchen auf Distanzen bis zu 170 cm entdeckt werden können und auf sie reagiert wird. Für alle beobachteten Interaktionen extrahierten wir die spezifischen Frequenzdifferenzen und schätzen die effektiven Signalstärken. Dabei hat sich gezeigt, dass in vielen relevanten Kommunikationssituationen die Elektrorezeptoren nur schwach von den Elektrokommunikationssignalen aktiviert werden. Dies ist so, entweder weil die Signale und die Übertragungseigenschaften der Rezeptoren beim Paarungsverhalten nicht optimal übereinstimmen, oder weil die Interaktionsdistanzen im Falle agonistischen Verhaltens sehr groß waren. Dieses ist die erste Studie, die Bewegungen und Kommunikationsverhalten von elektrischen Fischen im Freiland detailliert charakterisiert.

Um den Kontext der im Freiland beobachteten Interaktionen zwischen Männchen und Weibchen zu bestimmen, haben wir eine Langzeit Studie zum Paarungsverhalten von Messerfischen mit einem nahen Verwandten von A. rostratus durchgeführt. Mittels unseres automatischen Beobachtungssystems identifizierten wir zum Freiland ähnliche Kommunikationssituationen und konnten eindeutig die Verbindung zwischen der beobachteten Kommunikation und Paarungsverhalten zeigen. In dem beobachteten Kommunikationsverhalten fanden wir exklusive Signale für die Eiablage und, wie im Freiland, zeitlich präzise

auf Weibchen antwortende, von Männchen generierte Signale.

Durch die Anwendung unseres automatischen Beobachtungssystems konnten wir Eigenschaften natürlicher Kommunikationssituationen charakterisieren. Wir haben dann gezeigt, wie unser System benutzt werden kann, um im Freiland beobachtete Verhalten weiter zu analysieren.

Contributions

Some parts of this thesis were created in collaboration with colleagues, whose contributions I here indicate. If not otherwise indicated all data, analyses, visualizations and text has been created by myself. In Chapter 2, the ideale dipole model and the equations for the gradient descent algorithm were developed in collaboration with Dr. Fabian Sinz. Chapter 3 is modified from a manuscript that has been prepared together with Prof. Dr. Jan Benda, Prof. Dr. Rüdiger Krahe and Dr. Jan Grewe. Prof. Benda and Dr. Grewe contributed the whole nerve recordings presented in Figure 3.9 A, B, E. The text has been edited by Prof. Benda and Prof. Krahe. The breeding experiment presented in Chapter 4 was performed in collaboration with Prof. Dr. Frank Kirschbaum from the Humboldt-Universität zu Berlin, who provided his invaluable expertise in fish breeding, the laboratory facilities, and the experimental animals.

Acknowledgements

First of all, I would like to thank my supervisors, Jan Benda and Rüdiger Krahe, for their inspiration and support throughout this thesis – I very much enjoyed learning from and with them. I am very grateful for the encouragements and the vast amount of freedom they gave me, and also for the friendly reminders not to go astray and, eventually, to get things done. Many thanks go to my colleagues who I worked with over the last years, from whom I learned a lot and who often gave me invaluable advice and assistance.

I am grateful to all my friends, who have been patient with me, especially during the last phase of this thesis, and whose splendid company made the sometimes challenging moments of this thesis a lot easier. Especially I want to thank Thorsten Dietzsch, who not only made the effort to read it all, but also sent back great, and often uplifting comments, even on very short notice. I thank my family, for their support and their believe that this thesis will be finished at some point and who kindly stopped asking when precisely this would be the case. Most of all, I want to thank my partner Noémi, who is always there, when I need her and whose patience for me never seizes to astonish me.

This work was supported by the Smithonian Tropical Research Institute that provided a Short Term Fellowship and the invaluable advice and assistance of its local staff at its Naos facility, Panamá. In particular, I am very grateful to Eyda Gomez, Ruth Gisela Reina, and Rigoberto Gonzalez, without whom much of my research in Panamá would not have been possible and who helped helped out, when things did not work out as they were supposed to. Equipment used in this work has been sponsored by the company 'Technoform Caprano + Brunnhofer GmbH', Kassel, Germany, which provided samples of its robust thermoplast-fiberglas profiles.

CHAPTER 1

INTRODUCTION

> *Since the EODs of wave-type electric fish provide individual frequency tags, these animals are ideally suited for behavioral field studies. Large arrays of electrodes could be spread out over a natural habitat during the breeding season and, by fast Fourier analysis executed on a small portable computer, the whereabouts of undisturbed individuals could be monitored on the basis of their individual frequencies. The movement and distribution of specific animals, as well as their electrical communication and responses to playback signals, could thus be recorded continually.*
>
> *From* Hagedorn and Heiligenberg, 1985

1.1 Searching for the neural basis of behavior

The primary function of an animal's brain is to create appropriate behavior in the face of a rapidly changing environment. To this end, a brain must analyze the complex sensory scenes that are provided by its senses, extract relevant information, and, depending on its internal state, decide the appropriate course of action. Understanding this process, and thereby ourselves, is the central goal of neuroscience.

Animals evolved senses, or sensory systems, that allow them to utilize a panoply of physical stimuli, e.g., vision, audition, olfaction etc., and each sense comes with its own challenges (Smith, 2008). The receptor cells of a sensory organ transform the physical stimulus, i.e., those parts of it that are deemed relevant, step by step into an electrical signal that can be processed by the nervous system, thereby shaping a neural representation of the stimulus. The information provided by a sense can be used for different purposes, e.g., orientation, foraging, and communication, and for each purpose different aspects of the sensory scene are relevant (e.g., Lewicki, 2002; Singh and Theunissen, 2003). Accordingly, a sensory system needs to analyze the sensory input for a wide range of features that might be important for an animal. What features are relevant will depend on the species, its current ecological context, and the sensory modality.

Nevertheless, many general characteristics of sensory processing exist, e.g., early processing stages commonly display dense coding, i.e. they encode many aspects of the sensory stimulus. This is important for the feature extraction at subsequent processing stages, because only information that has been captured by the sensory periphery can be analyzed later. In contrast, neurons of central processing stages successively become more selective to specific sensory objects and their properties (Barlow, 1972). Sensory systems, by means of their intricate neural circuitry, provide solutions for problems that occur during the process of feature extraction and scene analysis. Accordingly, for understanding the mechanisms and functions implemented in higher sensory processing stages, it becomes increasingly important to understand an animal's sensory environment, its so-called natural stimuli, and the problems that the sensory system faces in the animal's natural environment and successfully solves (Simoncelli and Olshausen, 2001; Lewicki et al., 2014). In other words, if we want to fully understand *how* a sensory system works, we must know *what* it is that it evolved for and what solutions for what problems it implements.

Several lines of argument support this fundamentally neuroethological view. The first argument is trivial, yet important. Only if one knows what stimulus features are important, can adequate stimulus abstractions be created and used for probing the functioning of the sensory processing. This argument is supported by insightful research revealing the mechanisms of the early processing in the retina (reviewed by Gollisch and Meister, 2010). In higher processing stages natural stimuli proved to be even more important as neurons become more selective for specific aspects of the stimulus, e.g., faces and sounds (Young and Yamane, 1992; Hromadka et al., 2008). Additionally, neurons have been shown to respond differently to natural stimuli than to simplified stimuli (Vinje and Gallant, 2002; Froudarakis et al., 2014). E.g., auditory neurons in the avian forebrain yield different spatiotemporal receptive fields in response to natural stimuli compared to white noise stimuli (Theunissen et al., 2000) and blowfly horizontal cells are driven into a different, non-linear operating regime when stimulated with naturalistic stimuli compared to simplified stimuli (Kern et al., 2005).

Second, sensory systems are often confronted with insufficient information to arrive at a unique solution, i.e., scene analysis problems are often ill-posed (Poggio and Koch, 1985; McDermott, 2009). These ambiguities can only be resolved by employing *a priori* knowledge about scene structure (Kersten et al., 2004). Sometimes, the workings of neural structures mediating such knowledge are revealed, e.g., in the popular examples of visual illusions (Eagleman, 2001). Additionally, sensory processing is also about detecting weak signals embedded in a noisy signal background. It is likely that the neural mechanisms involved in the solutions of such problems can only be unraveled using appropriate, i.e., challenging and naturalistic stimuli.

In light of these arguments, there has been a growing interest in understanding, i.e., quantifying, the statistics of natural sensory scenes (e.g., Schwartz and Simoncelli, 2001). Although much progress has been made in a variety of sensory systems, most of the research to date has been limited to studies in laboratory or semi-natural conditions and/or has required the use of invasive techniques (e.g., Betsch et al., 2004; Fotowat et al., 2013; Knutsen et al., 2008). The central goal of the present thesis has been to establish and to apply a method for the non-invasive quantification of communication stimuli while animals roam and interact in their natural environment. Weakly electric fish, even though they are notoriously hard to observe given their nocturnal life style in often highly turbid rainforest waters, turn out to be an excellent choice for this undertaking.

1.2 Weakly electric fish as a model system in neuroscience

Electric fish are intriguing animals that evolved an active electric sense employed in foraging, navigation and communication. At least two lineages, the African mormyrids and the South American gymnotiforms, each with around 200 described species, independently developed the ability to actively generate electric discharges with a specialized electric organ (Albert and Crampton, 2005; Caputi et al., 2005). The generated electric currents flow through the surrounding water (Fig. 1.3 A; Knudsen, 1975) and are sensed by tuberous electroreceptors distributed over the fish's skin as transdermal potential differences. These receptors are able to sense perturbations of the self-generated electric field caused by surrounding objects with conductivity different than that of the surrounding water, e.g., prey, or the electric discharges of nearby conspecifics (Bullock, 1982). Weakly electric fishes as well as many non-electrogenic animals possess a second class of electroreceptors allowing for passive electrolocation. Ampullary receptors sense the tiny external electric fields created by the muscles of prey animals (Parker and Van Heusen, 1917; Zakon, 1986). Passive electroreception has evolved in a range of animals, e.g., catfish (Bullock et al., 1993; Lavoue et al., 2012), elasmobranchs such as rays and skates (Murray, 1960; Kalmijn, 1966) and mammals such as the duck-billed platypus (Scheich et al., 1985) and the Guiana dolphin (Czech-Damal et al., 2012).

Most electric fish are freshwater fish, because the high conductivity of salt water strongly decreases their signal detection range (Fig. 1.1). However, some strongly electric fish, e.g., the electric stargazer (*Astroscopus*) and some skates and rays (e.g., *Torpedo*), are found in the ocean (Bennett et al., 1961). The probably most prominent strongly electric fish is the gymnotiform electric eel, which is capable of

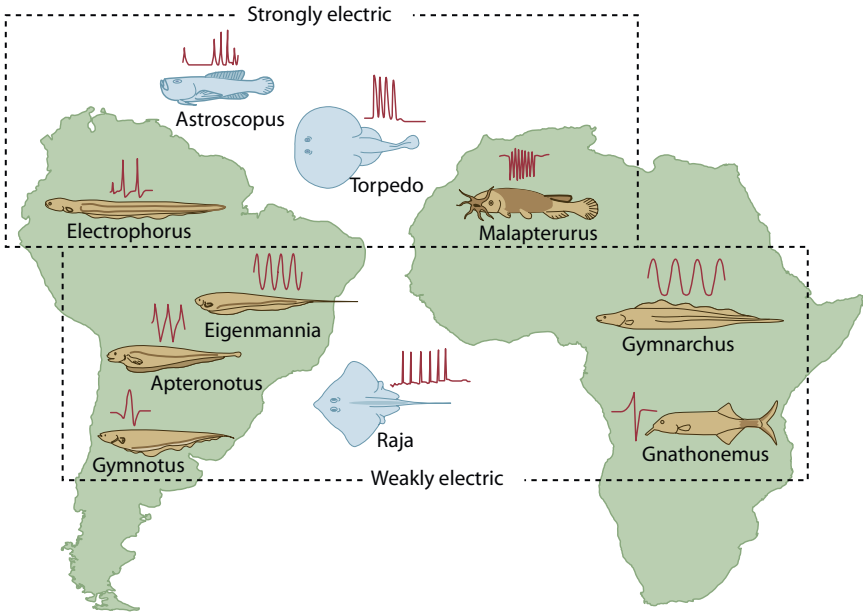

Figure 1.1: DISTRIBUTION OF ELECTRIC FISH SPECIES IN MARINE AND FRESHWATER ENVIRONMENTS. Electric fish species can be found in marine (blue) and freshwater (yellow) environments. Strongly electric fish are capable of stunning their prey. In contrast, weakly electric fish employ their electric sense for prey detection and communication. The temporal waveform of the EOD is illustrated above the fish sketches (red). Taken from Nelson, 2011 after Moller, 1995.

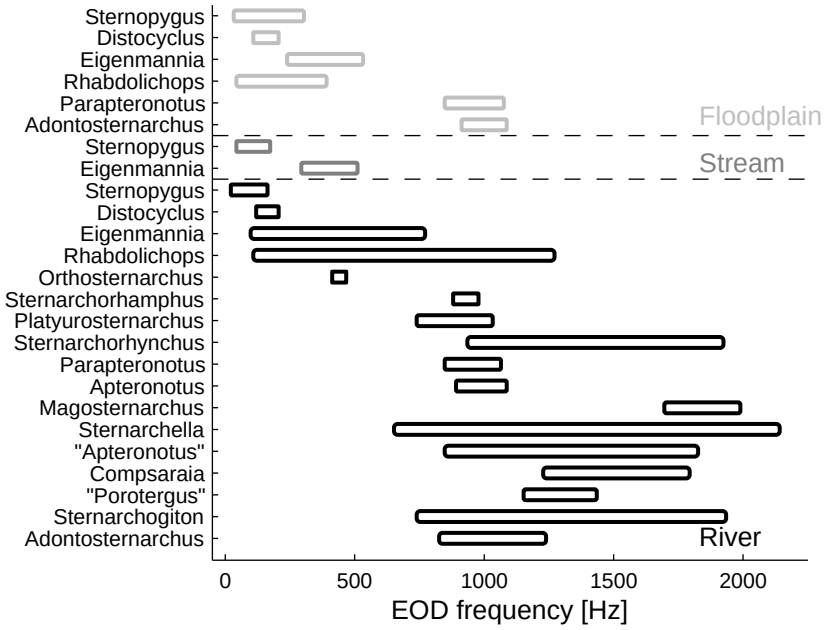

Figure 1.2: SPECIES SPECIFIC EOD FREQUENCY DISTRIBUTIONS OF ELECTRIC FISH. The EOD frequencies (EODf) of wave-type electric fish vary widely between about 40 – 2000 Hz. A relationship between the EODf range covered and the habitat inhabited by a species has been hypothesized, because species found in the floodplain and slow flowing streams were found to exhibit lower EODf than the majority of those found in fast flowing rivers. Reproduced after Crampton and Albert, 2006. Courtesy of Dr. Jan Grewe.

using its electric discharges of up to 600 Volts shock hidden prey (Bauer, 1979; Catania, 2014).

In contrast, weakly electric fish generate much more subtle electric organ discharges (EOD) of only a few millivolts (~ 1 mV/cm) and their abilities remained unnoticed for a long time (Bullock and Heiligenberg, 1986). In a key experiment Lissmann and Machin (1958) demonstrated the ability of the eel-like mormyriform fish *Gymnarchus* to discriminate objects with differing electric properties. Almost at the same time, Möhres (1957) presented evidence for social electric communication in the mormyrid *Gnathonemus*. By now it is well established that weakly electric fish possess an electric sense allowing them to navigate and forage through dark and turbid waters, and providing them with a private communication channel (Maciver et al., 2001; Bullock, 1969; Hopkins, 1974a).

Electric fish of both lineages group into two phenomenological classes. On the one hand, there are so-called 'pulse fish', i.e. species generating an EOD comprised of short pulses separated by often variable pauses in frequencies between about 1 and 120 Hz (Bass, 1986; Albert and Crampton, 2005). The discharge rates, or EOD frequencies (EOD*f*), depend strongly on context and are rapidly sped up if in behavioral demand (e.g., Hagedorn, 1988; Jun et al., 2014a), but do not show obvious individual-specific characteristics. When played back via a loudspeaker, these EODs create a rather sputtering and raspy sound. On the other hand, 'wave fish' are species generating a continuous and quasi-sinusoidal EOD, which is remarkably stable over many hours (Fig. 1.3 B; Bullock, 1970; Moortgat et al., 1998), and which creates a continuous, almost pure tone when played back via a loudspeaker. Wave species show a high diversity with species-specific EOD frequencies ranging between 40 – 2000 Hz (Fig. 1.2; Crampton and Albert, 2006). In habitats with few species of electric fish, EOD*f* has been hypothesized to signal species identity (e.g., Hopkins and Heiligenberg, 1978; Hagedorn, 1986). Within a species, each individual has its own preferred EOD*f* that is under active behavioral control and can be modulated to communicate the fish's motivational status (Zakon et al., 2002). Additionally, for some wave species that show sexual EOD*f* dimorphism and a social hierarchy, EOD*f* has been hypothesized to convey information about the sender's sex and social status (Hagedorn and Heiligenberg, 1985; Dunlap and Oliveri, 2002; Fugère et al., 2011).

Electric fish, beyond being fascinating per se, proved an unique and highly successful model system in neuroscience. Studies on the electrosensory system revealed neural mechanisms that underlie temporal hyperacuity (Rose and Heiligenberg, 1984), redundancy reduction (Bastian et al., 2004), parallel processing (Oswald et al., 2004), context-dependent switching of frequency tuning (Chacron et al., 2003), a neural searchlight mechanism (Berman and Maler, 1999) similar to that proposed for the visual cortex by Crick (1984), and mechanisms of feature extraction and the processing of communication stimuli (Benda et al., 2006; Vonderschen and Chacron, 2011). Studies of electric organs have profoundly increased our knowledge of neurotransmitters (Feldberg et al., 1940) and their synthesis (Whittaker, 1992) and receptors (Changeux, 1993; Galzi et al., 1991), ion pumps (Glynn, 1963) and the evolution of sodium channels (Zakon et al., 2006).

Additionally, electric fish excelled as champions of the field of 'neuroethology', i.e., the integrated study of behavior and brain function. A prominent example for this is the research on the jamming avoidance response (JAR) that is one of the best understood behaviors, from sensory perception and processing to motor output (Heiligenberg, 1991a), and a fascinating example for the convergent evolution of neural processing in African and South American electric fish. A key advantage of these animals is that many of their behaviors are purely 'electrical' and do not involve any mechanical components. This includes the JAR and extends to behaviors like 'active phase coupling' and electrocommunication (Langner and Scheich, 1978; Zakon et al., 2002). Further, electrical behavior of these fish can readily be recorded with electrodes in the water. The large diversity of electric fish and their behavior makes them also interesting from an evolutionary point of view (e.g. Bullock et al., 1975; Metzner, 1999; Carlson et al., 2011).

Several aspects make electric fish and their electric sense a formidable subject for physiological studies. First of all, the electric sense is unfamiliar to us humans – a fact that facilitates a study that is free of preconceptions on its perception. Further, the electric sense combines the spatial properties of vision with temporal properties of audition. Its structure is well described and is similar to mammalian

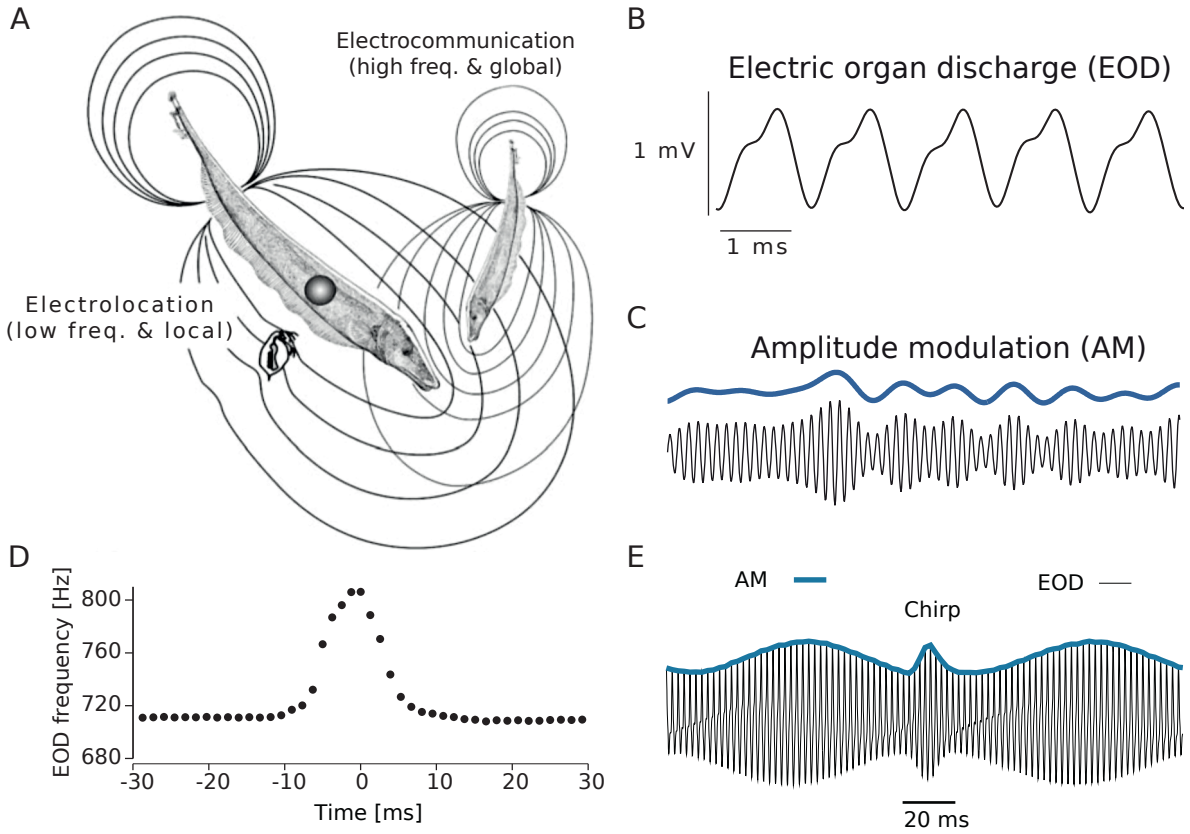

Figure 1.3: ACTIVE ELECTROLOCALIZATION AND ELECTRO-COMMUNICATION. **A**) Illustration of the differing spatiotemporal characteristics of electrolocation and electro-communication in the wave-type electric fish *Apteronotus leptorhynchus*. Prey stimuli, e.g., *Daphnia*, distort the electric field (curved lines) locally and activate few electroreceptors with typically low frequencies that peak at 10 Hz. Communication stimuli are spatially diffuse and can contain high frequencies up to a few hundred Hertz and activate many electroreceptors widely distributed over the fish's body. **B**) Temporal waveform of the electric organ discharge (EOD) of *A. leptorhynchus*. **C**) The EOD amplitude is modulated by nearby objects, e.g., prey. **D**) Wave-type electric fish utilize transient frequency modulations, i.e. decreases and increases, as communication signals. Short modulations, typically shorter than 600 ms, are termed 'chirps', because of their acoustic quality, when played back via loudspeaker. The corresponding behavior is accordingly called 'chirping'. **E**) When two wave-type electric fish are close, their electric fields superimpose and result in a periodic amplitude modulation called the 'beat'. A chirp interrupts the beat and is accordingly detected by the electroreceptors that encode EOD amplitude. **A** modified from Bastian and Zakon, 2005, **C** modified from Krahe and Gabbiani, 2004, **D** and **E** modified from Walz et al., 2013.

sensory systems in many respects. Several successive processing steps in different brain areas are readily accessible to physiological study. Electric stimuli are well defined and mimics of natural stimuli can easily be generated in the laboratory, allowing for studying the basic principles and mechanisms of neural encoding and feature extraction (for recent reviews, see Chacron et al., 2011; Krahe and Maler, 2014).

The ghost knifefish

Among the South American electric fishes, the ghost knifefishes (*Apteronotidae*) are the most speciose family with more than 60 species (Albert and Crampton, 2005; Crampton and Albert, 2006) and they are special in several aspects. Ghost knifefishes replaced their myogenic electric organ, derived from muscle cells and present only in larvae, by one derived from the axons of spinal motor neurons allowing them to discharge faster than any other electric fish. Their neural pre-motor circuits controlling the EOD*f* exclusively use electrical synapses, thereby forming the fastest and most stable neural oscillator known (Metzner, 1999; Bullock, 1970; Moortgat et al., 1998). During social encounters ghost knifefishes are known to transiently modulate their EOD*f*, thereby shaping specific communication signals called 'chirps' and 'rises' that convey their motivational status (Zakon et al., 2002). Both EOD*f* and communication signals vary widely across sexes and species (Turner et al., 2007). Some species are morphologically and electrically dimorphic, e.g., male black ghost knifefish, *Apteronotus albifrons* have lower EOD*f* than females, whereas in *A. leptorhynchus* males have higher EOD*f* than females, (Dunlap et al., 1998; Meyer et al., 1987). Even within the same species, the strength of the EOD*f* dimorphism can vary across populations and habitats (Ho et al., 2013). These characteristics make this family an ideal candidate for research on the evolution and functioning of the neural circuits underlying the generation and processing of social signals. The brown ghost knifefish, *A. leptorhynchus*, is the most intensively studied apteronotid species and much is known about the neuroanatomy and physiology of their electrosensory system as well as their electric behaviors. Additionally, many electric fish, including the ghost knifefish, are well suited for behavioral experiments, allowing to probe their sensory performance using discrimination and detection tasks (e.g., Lissmann and Machin, 1958; Knudsen, 1974; Stamper et al., 2012).

In general, species of *Apteronotus* tend to be territorial and are found solitary or in small groups (Hagedorn, 1986; CD Santana, personal communication). During daylight the fish hide beneath rocks, leaf debris or within roots below river banks, whereas at night the fish leave their hiding places and roam through their habitat. Apteronotid males show a dominance hierarchy, while females appear to lack a distinct dominance relationship (Hagedorn and Heiligenberg, 1985). Apteronotid fish have a cyclic reproduction that is controlled by environmental factors. These factors are related to the transition from dry to wet season and include the increase of water level, the decrease of water conductivities, and the occurrence of rain (Kirschbaum and Schugardt, 2002; Hopkins, 1974b,a). With the transition to the wet season the fish's gonads mature, female fish become gravid and male fish develop visible testes. Juveniles reach the minimum size to obtain first maturity after about one year (Kirschbaum and Schugardt, 2002).

Apteronotids choose their spawning sites very carefully to hide their sticky eggs. All available data indicate that brown ghosts are partial and irregular spawners, and external fertilizers, with 1-100 eggs spawned in intervals of 3-17 days (Kirschbaum and Schugardt, 2002). Hagedorn and Heiligenberg (1985) observed courtship in *A. leptorhynchus* in laboratory tanks, and no parental care has observed. Courtship is initiated by long bouts of chirping by a dominant male, which may last a whole night. When ready to spawn females start chirping and may continue so while squeezing out an egg. The female chirping elicits an approach behavior in the male, which hovers close to the female and presumably fertilizes the egg when it leaves the cloacal opening. In this process, females were reported to elicit a single long duration chirp. Hagedorn and Heiligenberg (1985), for the first time, provided a qualitative description of apteronotid courtship behavior. However, because many aspects of courtship behavior and the associated communication were disregarded, their results should be considered anecdotal.

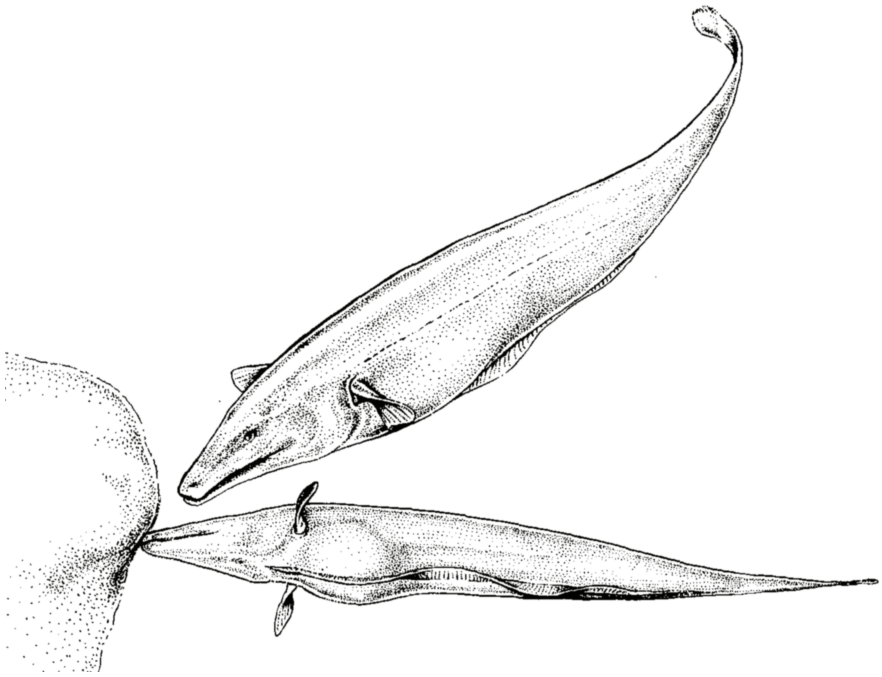

Figure 1.4: COURTSHIP AND SPAWNING OF *Apteronotus leptorhynchus*. During courtship males were reported to generate long bouts of chirps for many hours. When ready to spawn females approach substrate and swim on their side, while at the same time generating chirps. The male hovers close to the female that squeezes out a single egg that then sticks to the substrate. Because most of the caudal part of the bodies of electric fish is taken up by the muscles driving the ribbon fin, their visceral organs including their cloaca and gonads are concentrated in their rostral body. Taken from Hagedorn and Heiligenberg, 1985.

1.3 The electrosensory and -motor system

The tuberous electroreceptors of *Apteronotus* are subdivided in P-type receptors that encode EOD amplitude modulations (AM) and T-type receptors that encode EOD frequency modulations. Apteronotids possess about 15.000 P-type receptors distributed over the body that are phase-locked to the EOD, but uncorrelated to each other, and discharge with rates between 100 –500 spikes per second (Nelson et al., 1997; Benda et al., 2006).

All receptors project onto pyramidal cells in the electrosensory lateral line lobe (ELL) that is divided into four topographical maps. Ampullary receptors project exclusively to the medial map and are not further considered here. In contrast, the tuberous receptors trifurcate and synapse onto pyramidal cells of the three remaining maps (Fig. 1.5 A, B), the centromedial (CMS), centrolateral (CLS), and lateral segment (LS). Each map consists of six pyramidal cell classes that differ in their spatiotemporal properties and the feedback they receive. This architecture results in multiple topographical representations of the electrosensory activity over the body surface (Krahe and Maler, 2014). The ELL can be considered as a preprocessing stage: whereas electroreceptors encode stimuli using a dense code, the encoding by the ELL pyramidal cells is already more selective and sparser (Vonderschen and Chacron, 2011). The maps have been demonstrated to have distinct functional roles. (Juranek and Metzner, 1997). The pyramidal cells are the main ELL output neurons and fall into two major classes of On and Off center-like cells, called E- and I-cells (Saunders and Bastian, 1984; Krahe and Gabbiani, 2004).

Some pyramidal neurons (deep cells) project to the nucleus praeeminentialis (nP) that mediates feedback, whereas all project to the midbrain torus semicircularis (TS). nP mediates direct and indirect feedback (via cerebellar granule cells, EGp) to the ELL that influences the spatiotemporal processing properties of the pyramidal cells (Fig. 1.5 B, C). E.g., the direct feedback is implicated in a ‘sensory searchlight’ mechanism (Berman and Maler, 1999), whereas one function of the indirect pathway is to remove redundant global low-frequency input caused by self-movement (Bastian et al., 2004). TS contains both dense coding and sparse coding neurons that respond selectively to specific beat frequencies, different types

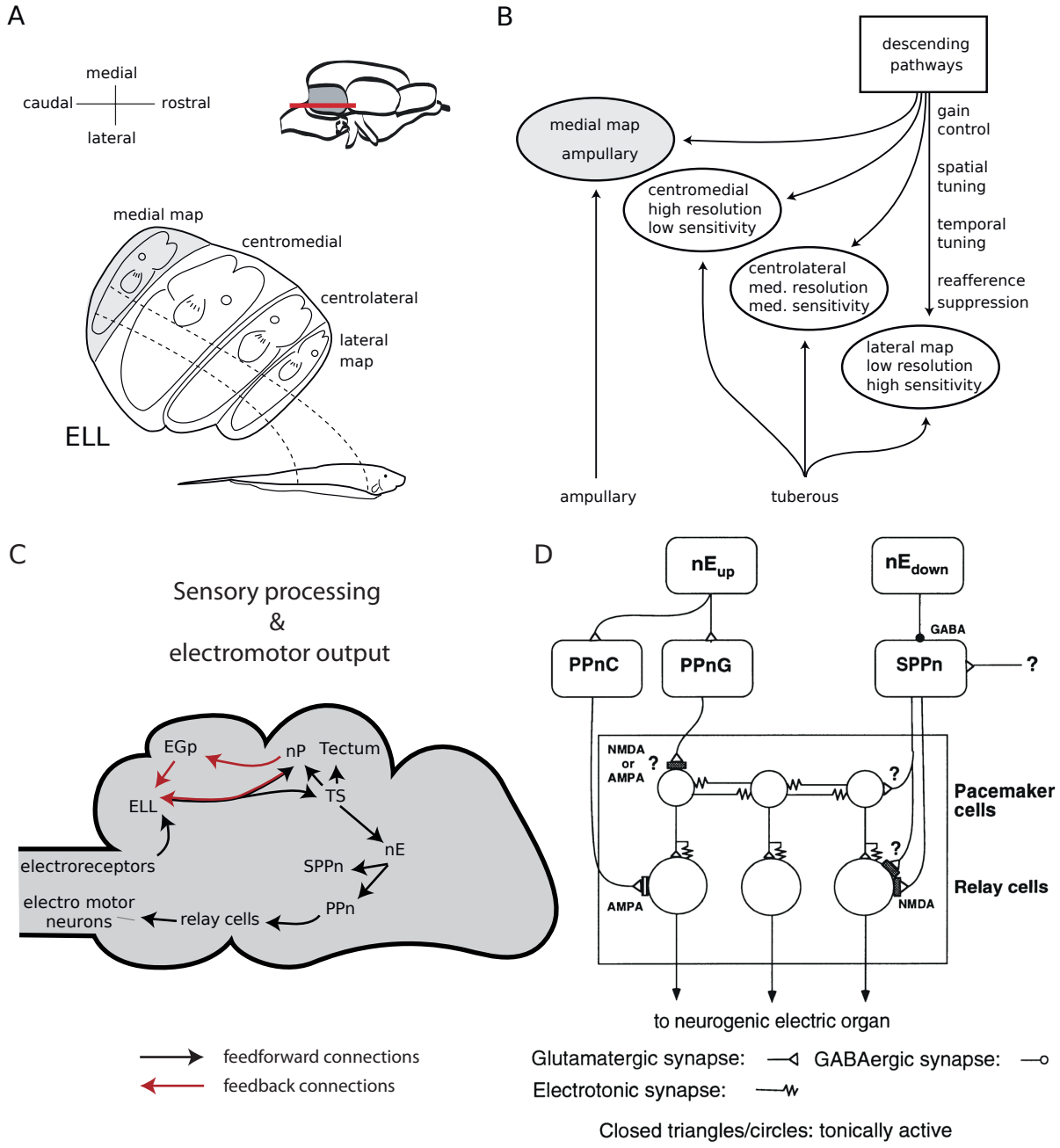

Figure 1.5: NEURAL PROCESSING OF ELECTROSENSORY INFORMATION **A**) Dorsoventral slice (red line) of the right ELL. Electrosensory input is distributed to four somatotopic maps. Gray: ampullary input, unshaded: tuberous input. **B**) Ampullary input is processed exclusively by the medial map. Three maps are dedicated to tuberous inputs and differ in their resolution and tuning characteristics. Feedback connections from EGp and nP control gain, spatiotemporal tuning, and provide information to suppress redundant information. **C**) Schematic of the electrosensory pathways involved in the processing of electro-communication. Black arrows indicate feedforward and red arrows feedback projections. **D**) Schematic representation of premotor circuitry in *Apteronotus*. The medullary pacemaker controls the EOD*f* and is composed of pacemaker and relay cells. Relay cells project to the spinal motor neurons that in *Apteronotus* comprise the electric organ. Pacemaker cells are connected reciprocally and with relay cells via mixed chemical and electrical synapses. Pacemaker and relay cells spike in one-for-one manner with the spinal electromotor neurons. Several modulatory projections to the pacemaker from prepacemaker nuclei are known. **A** and **B** modified from Nelson, 2005. **C** modified from Walz et al., 2013. **D** modified from Juranek and Metzner, 1997. ELL: electrosensory lateral line lobe; EGp: eminentia granularis pars posterior; nP: nucleus praeeminentialis; TS: torus semicircularis; $nE_{up/down}$: nucleus electrosensorius; SPPn: sublemniscal prepacemaker nucleus; PPn: prepacemaker nucleus.

of chirps, movement direction and higher-order signal envelopes (Fortune and Rose, 1997; Chacron and Fortune, 2010; Vonderschen and Chacron, 2011). However, the mechanisms underlying the transformation from dense to a selective and sparse response remain elusive, and are subject of ongoing and fascinating research.

The electric organ discharge

In apteronotids the electric organ is composed of modified axons of spinal electromotor neurons that exit the caudal spinal chord and, bundled together and expanded to large diameters of up to 100 µm, form the electric organ (Bennett, 1971). Long (~ 50 µm), passive nodes create the currents of the EOD, driven by action potentials that are renewed at so-called hair-pin turns with active nodes, that also have an important role in shaping the EOD's specific waveform. Interestingly, apteronotids begin their life with a myogenic organ that is gradually replaced by the neurogenic one during their first months (Kirschbaum, 1983). During that period, the EOD is generated by the two organs in parallel, while the neurogenic organ continuously grows larger, whereas the contribution of the myogenic organ slowly decreases. Two separate sets of electromotor neurons, one for each organ, are connected to the pacemaker's relay cells, such that the two organs fire in perfect synchrony.

The frequency of the EOD is controlled by the medullary pacemaker nucleus and its prepacemaker nuclei, i.e. the thalamic prepacemaker, PPnC and PPnG, and the sublemniscal prepacemaker, SPPn (Fig. 1.5 D; Metzner, 1999). The pacemaker cells are extensively electrically coupled and oscillate intrinsically with constant frequency. These cells are electrically and chemically connected to relay-cells that synapse onto the spinal electromotor neurons. Rapid and transient EOD*f* modulations, i.e. chirps of various types, have been generated by glutamatergic stimulation of the PPnC (Dye, 1987; Kawasaki et al., 1988). PPnG projects to pacemaker cells and mediates the 'unselective response' and slow and gradual gradual EOD*f* modulations, so-called rises. The SPPn controlls mainly the jamming avoidance response, but strong electrical stimulation can also cause rapid high-frequency modulations that appear similar to high frequency chirps (Heiligenberg et al., 1996).

1.4 Electrocommunication signals

EODs are direct motor outputs of the fish's brain, and its externally measurable modulations are the expression of an internal behavioral state. Accordingly, the EODs of conspecifics and their modulations are an important part of the sensory scene that the electrosensory system has to analyze. Gymnotiform wave-type electric fish generate at least three classes of signals with communicative function, first of all, the EOD itself with its baseline frequency. A second signal are fast transient EOD*f* modulations in the range between tens to hundreds of milliseconds (Fig. 1.3 D, E and 1.6 A–D). These signals are commonly called 'chirps', because of their acoustic quality when played back via loudspeaker, and the associated behavior 'chirping'. A third signal are slow EOD*f* modulations in the range of seconds to minutes that are commonly called 'rises' (Fig. 1.6 E). Their properties are highly variable across species and individuals, and, while their function remains unclear, these modulations are hypothesized to signal social stress (Smith, 2013).

The EOD*f* varies between ~ 500 – 2000 Hz in apteronotid species and is hypothesized to carry information about species, social status and, in species with sexually dimorphic EOD*f*, sex of the generating fish. Within a species EOD*f* commonly spans 200 – 600 Hz(Kramer et al., 2013; Turner et al., 2007). The function of EOD*f* as an indicator of sex is supported by the observation that, in species with sexually dimorphic EOD*f*, fish chirp differently in response to male versus female playbacks. At least for *A. leptorhynchus* the EOD*f* is also hypothesized to act as a signal of social rank, because it is often found to be positively correlated with body size (Cuddy et al., 2012; Dunlap, 2002; Fugère et al., 2011), and because large animals were found to be dominant in social interactions (Hagedorn and Heiligenberg, 1985; Dunlap and Oliveri, 2002).

Whereas the EOD of a wave-type electric fish is a permanent signal that is continuously active from

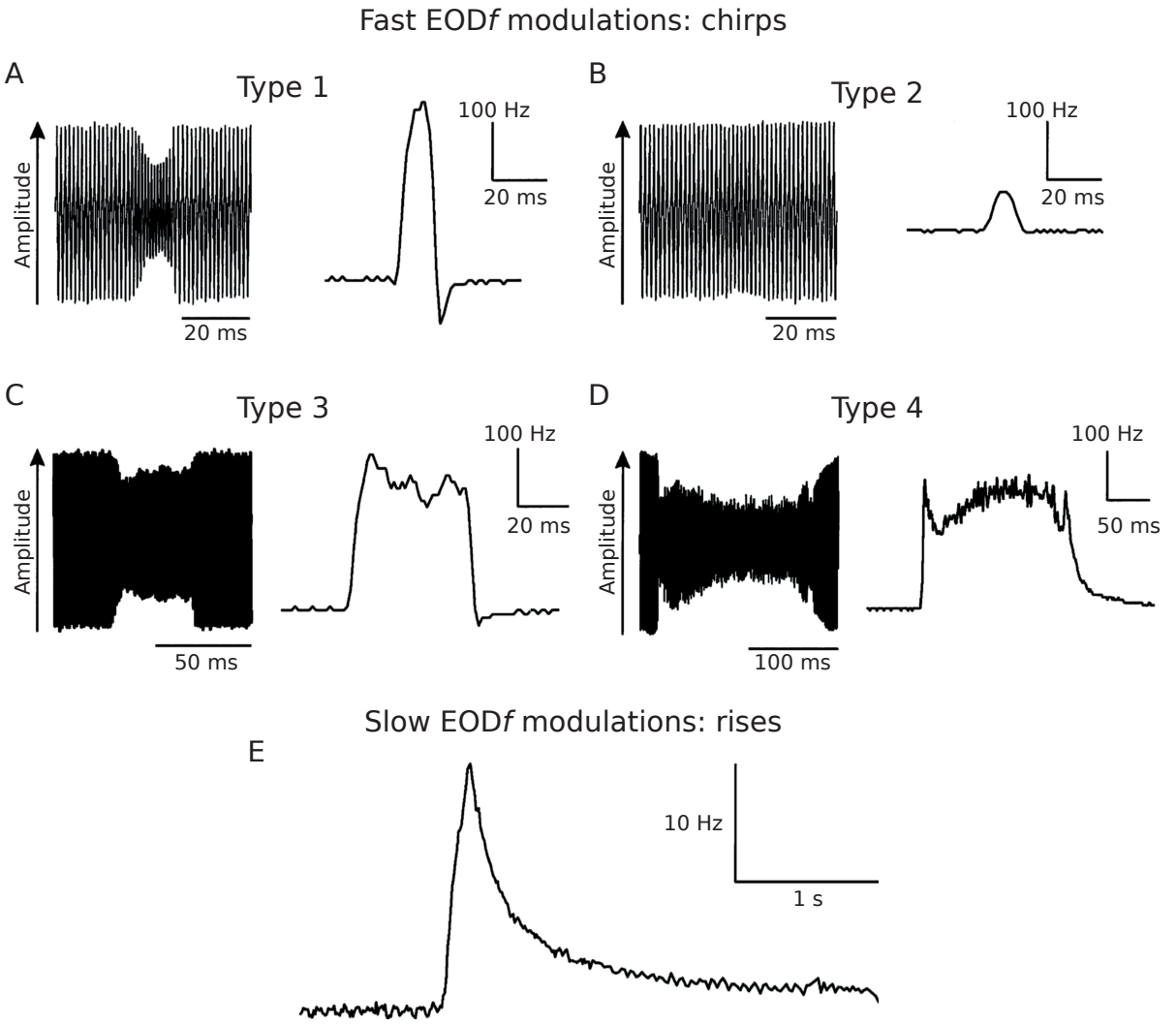

Figure 1.6: EOD MODULATIONS OF *Apteronotus leptorhynchus*. **A**–**D**) Temporal EOD waveforms (left) and frequency traces of spontaneous chirps as classified by Engler et al., 2000. Chirps with large frequency excursions (types $1, 2, 4$) show pronounced amplitude decreases of the EOD waveforms, whereas small, or type 2, chirps show almost none decrease in EOD amplitude. In how far the classification of chirps in discrete categories is justified is an ongoing and controversial debate. **E**) Apteronotids and many other wave-type electric fish also generate slow frequency modulations in the range of seconds to minutes. Their function remains unclear. Taken from Zupanc, 2002.

a few days after hatching until eventual death, chirps and rises are almost exclusively emitted during social interactions. Chirps are best-studied in *A. leptorhynchus*, where they have been classified into distinct types (Fig. 1.6; Engler et al., 2000. However, the validity of this classification remains unclear, and most often chirps are referred to as low and high frequency chirps. Low frequency, or small, chirps have frequency excursions between ~ 20 – 150 Hz, durations of about 10 – 20 ms and very little amplitude modulation (Bastian et al., 2001). These chirps have been related to agonistic behavior between same-sex fish (Hupé and Lewis, 2008; Triefenbach and Zakon, 2008), but it remains unclear, if they signal aggression or appeasement (see Smith, 2013 for a review). In contrast, high frequency chirps have frequency excursions up to 400 Hz, varied durations of up to 500 ms and amplitude decreases of about 75%. High frequency chirps of short duration (~ 20 – 30 ms) are often called big chirps (Benda et al., 2006; Vonderschen and Chacron, 2011), and are believed to function as courtship signals (Hagedorn and Heiligenberg, 1985) that are emitted by males towards low-frequency females. Almost all information on chirp structure and their function has been extracted from laboratory experiments of restrained fish or staged interactions in small tanks, settings that strongly limit the animal's behavioral options. It is therefore unclear to what degree these results can be generalized.

Because chirps are commonly emitted during dyadic interactions, their generation and sensory processing is often considered in this context. When two wave-type electric fish are close, their EODs interfere and create a beating amplitude envelope, the frequency of which is given by the difference between the EOD frequencies of the two fish. The beat amplitude is well encoded by the tuberous electroreceptors, i.e. by the P-units, and by the pyramidal neurons in the ELL (Walz et al., 2014; Marsat and Maler, 2012). The beat frequency and amplitude are the decisive signal background for chirp encoding. A chirp disrupts and resets the beat envelope because of the change in frequency and, in the case of the high frequency chirps, the reduction of the sender's EOD amplitude (Fig. 1.3 E). Previous studies found that small chirps synchronize the P-unit receptor population, while big chirps cause a strong desynchronization mediated by the strong decrease in EOD amplitude (Benda et al., 2006). However, a recent study demonstrated that this view is simplified and the effect of small chirps on the receptor population strongly depends on the sign and frequency of the beat (Walz et al., 2014).

Chirps are well encoded by pyramidal cells in the lateral segment of the ELL. Superficial E-type pyramidal cells haven been shown to clearly encode the occurrence of small chirps on the background of slow beats that indicate same-sex interactions with bursts of spikes (Marsat et al., 2009). In contrast, high frequency chirps of various durations are well encoded by a heterogeneous population of I-type pyramidal cells from all layers and from all three maps of the ELL that respond to the desynchronization of tuberous input (Marsat and Maler, 2010). However, these results did not yet consider the results of Walz et al. (2014) that suggest that the same signal, i.e. small chirps, is encoded differently in dependence of the beat frequency and that these different encodings will likely persist in the ELL. In the next processing step, the midbrain torus semicircularis, information about the occurrence and properties of chirps are encoded in separate populations of dense and sparse coding cells (Vonderschen and Chacron, 2011). The shortest pathway to electromotor output is to the nucleus electrosensorius (nE) that projects to the prepacemaker nuclei, PPn and SPPn (Fig. 1.5 C, D). However, so far no chirps could be elicited by stimulation of nE (e.g. Keller et al., 1990), so that it appears as if nE does not function as a chirp-controlling command nucleus, despite the suggestive connection indicated in Fig. 1.5 D.

1.5 The goal of this study

Knowledge of the signals and their contextual background that a sensory system evolved to process is a prerequisite for understanding the principles and neural mechanisms underlying its functioning. In this thesis, I will focus exclusively on the electrocommunication of ghost knifefish and its natural context.

In general, much is known about apteronotid electrocommunication signals (Zakon et al., 2002; Turner et al., 2007; Serrano-Fernandez, 2003), and in particular about chirps in *A. leptorhynchus*. However, most information on electrocommunication was extracted from laboratory studies on captive fish using playbacks of EOD mimics, from staged interactions, and from a study on breeding fish (Dunlap and

Larkins-Ford, 2003; Hupé and Lewis, 2008; Triefenbach and Zakon, 2008; Hagedorn and Heiligenberg, 1985). These studies provided a strong basis, but also resulted in much conflicting evidence concerning the context and the function of chirps (Smith, 2013), which may be caused in large part by the limitations of working within the spatial constraints of aquaria.

Elaborating on these results, physiological studies on the processing of chirps narrowed down on a small set of chirp-types, beat frequencies, and signal intensities used to characterize the electrosensory system's response characteristics. Mostly two types of chirps are used in these studies, i.e. small chirps with low frequencies and short duration (60 – 150 Hz; ~ 15 ms) and 'big' chirps with high frequency and short durations (200 –900 Hz; $<$ 45 ms) (e.g., Benda et al., 2006; Marsat et al., 2009; Marsat and Maler, 2010; Vonderschen and Chacron, 2011). Because small chirps, according to the laboratory results on chirping, are assumed to occur during same-sex interactions, they are presented on top of slow beats (mostly $<$ 60 Hz), whereas big chirps are assumed to be courtship signals and are therefore presented on top of fast beats (100 – 400 Hz). Signal intensities, i.e. the amplitude of the background beat stimulus, are often fixed to 15 – 20% contrast. However, the validity of such simplifications remains unclear and is one of the topics of this thesis.

This thesis has two goals. The main goal is to learn about natural stimuli for the electrosensory system, i.e. to better understand the properties and the context of natural electric communication. Who communicates with whom using what signals? What are the relevant signal intensities and backgrounds and how does this relate to previous studies? The second, supporting goal is to provide the technical means for studying the behavior and interactions of undisturbed individual wave-type electric fish over extended periods of time and space. Nocturnal activity patterns, turbid water, the vast area of the streams, and tropical rainforest conditions make natural habitats challenging study sites (e.g. Hopkins, 1974b; Hagedorn, 1988). However, as stated by Hagedorn and Heiligenberg (1985), the permanently active EOD of wave-type electric fish poses a great opportunity to monitor the behavior of unrestrained fish in natural environments. We aim to provide a tracking system that enables new types of studies in the laboratory, where everything is neatly controlled for, and also allows for a novel type of field study, where we can find out whether things really work the same in nature as they do in the laboratory. At the same time, electric fish with their well characterized electrosensory system become available for approaching new exciting research questions from the areas of ecology and evolution that can now be accessed in the wild. Finally, by providing the ability to acquire and automatically analyze large datasets of electric fish behavior, electric fish become subject of the newly emerging and exciting field of Computational Ethology (Anderson and Perona, 2014).

This thesis is structured as follows. Being the prerequisite for achieving our main goal, we will first discuss the EOD-based tracking of electric fish behavior in Chapter 2. In Chapter 3 we applied our tracking system in a natural habitat of a close relative of *A. leptorhynchus* during its reproductive season and analyzed its natural intra-species interactions. In Chapter 4 we studied the interactions observed in the wild in a laboratory-based breeding study, again profiting from our tracking system. Finally, in Chapter 5, we discuss the results of the previous chapters in a broader scope.

CHAPTER 2

AUTONOMOUS TRACKING OF WEAKLY ELECTRIC FISH

This chapter describes the methods used for the automated spatiotemporal tracking of individual wave-type weakly electric fish and their behavior on a large scale and over long periods of time. Our description is separated in several parts. (i) Development of equipment for the recording of EODs, (ii) detection and discrimination of wave-type EODs, (iii) continuous tracking of EODs over multiple electrodes and time, (iv) the detection of electro-communication, (v) the estimation of fish location.

2.1 EOD-based tracking of individual electric fish

Visual tracking of fish movement and behavior are well established for laboratory setups (Hughes and Kelly, 1996; Noldus et al., 2001), including electric fish (Fotowat et al., 2013; Hofmann et al., 2014). However, the natural habitats of weakly electric fish and their electro-communication are often inaccessible to visual tracking methods. During daylight electric fish remain hidden under river banks, groves, in roots and leaf debris and leave their hiding places at night to roam rivers and streams, which often are turbid. Technically, visual tracking commonly relies on the processing of high contrast images, which are not easily generated under field conditions. Tracking based on the fish's self-generated EODs provides a powerful alternative to visual approaches and first basic attempts for the tracking of diurnal movements of weakly electric fish have been published by Steinbach (1970) for south American gymnotids and by Friedman and Hopkins (1996) for pulse-type African mormyrids. The proposal to systematically track individual wave-type electric fish based on their EOD*f* using large arrays of electrodes was raised at least as early as 1985 by Hagedorn and Heiligenberg. However, only recent technological advances provided the means for a comprehensive implementation of this tracking strategy.

EOD-based tracking provides several advantages to visual tracking approaches. First, EODs are well suited markers for the tracking of individual wave-type electric fish. They are generated continuously from a few days after hatching until the end of their lifespan (Kirschbaum and Westby, 1975; Kirschbaum, 1983) and directly distinguish electric fish from other non-electric fish. Second, EODs convey cues about species (Turner et al., 2007; Zupanc and Bullock, 2005), sex (Meyer et al., 1987), and dominance (Fugère et al., 2011). Third, EODs can be used to estimate the fish's position, to extract electro-communication behavior and, eventually, interactions and social relations of individual electric fish, without the need for a direct line of sight between the fish and the sensor. For pulse-type electric fish an EOD-based method for tracking their position in shallow water in a laboratory setup has been published recently (Jun et al., 2013, 2014b).

The tracking system presented here allows for the tracking of wave-type electric fish recorded with electrode arrays in the wild (see Chapter 3), and also for continuous monitoring of fish behavior over many months in holding tanks using a multi-electrode setup (see Chapter 4).

EOD frequency as an individual identifier for electric fish

Three characteristics of the EOD are potential identifiers for the discrimination of wave-type electric fish: frequency, amplitude and the shape of the waveform. EOD frequency (EOD*f*), the single most important parameter for individual discrimination in wave-type electric fish, is known to be remarkably stable over time. The pacemaker nucleus driving the EOD on a cycle-by-cycle base is one of the most stable biological oscillators known (Bullock, 1970) and its precision has been shown to be under behavioral control (Moortgat et al., 1998). EOD*f* is mostly stable over hours and days, but is subject to temperature-related changes (Dunlap et al., 2000) and behavioral modulations both on short, medium and long time scales (sub-second: chirps; several to hundreds of seconds to hours: rises, Zakon et al., 2002; Smith, 2013).

EOD amplitude has been shown to be subject to circadian rhythms in both pulse and wave-type electric fish with myogenic electric organs (*Brachyhyppopomus*, pulse-type: Franchina and Stoddard, 1998; Stoddard et al., 2007; *Sternopygus macrurus*, wave-type: Markham et al., 2009). In species with neurogenic electric organ, i.e. all apteronotid species, no circadian EOD amplitude changes have been described. Thus, it might be useful for discrimination of individual EODs over short periods of time, if used in conjunction with EOD*f*.

The shape of the EOD waveform is the least suited parameter for the discrimination of individual electric fish. The head-to-tail waveforms are highly stereotypical for each species (Bennett, 1971; Bass, 1986; Turner et al., 2007), but the waveform recorded at different locations around the fish can differ strongly from the head-to-tail waveform, in particular close to the fish's body surface (Hoshimiya et al., 1980; Rasnow et al., 1993; Assad et al., 1998; Jun et al., 2012). The spatiotemporal dynamics of the electric field depend strongly on the anatomic plan and the location of the electric organ within the fish. Concentrated organs generate fields with the same temporal waveform everywhere, while organs distributed along the body axes generate fields with complex, site-dependent temporal waveforms that reflect the activation pattern of the electric organ's separate units (Caputi et al., 2005). Accordingly, the harmonic composition of the EOD at different locations around the fish can vary considerably, and in particular close to the fish's electric equator (Knudsen, 1975). Finally, a study of Fugère and Krahe (2010) suggests, that apteronotid fish themselves do not pay much attention to waveform.

We used the EOD*f* as an individual marker of wave-type electric fish. Individual EOD*f* is readily accessible by performing a spectral analysis on EOD voltage traces (Fig. 1.3 B). The spectral analysis, using for example the *Fast Fourier transform* (FFT), transforms a time-varying signal into a frequency representation, a *spectrum*, thereby revealing the signal's frequency composition. By this means, an individual fish's EOD*f* and its amplitude can be determined, even in a signal with EODs of multiple fish superimposed on each other. The temporal extension of the FFT is the spectrogram, which visualizes the spectrum of a signal as it varies over time. Figures 2.1 and 2.2 display spectrograms of EODs recorded in the fish's natural habitat in Panamá and in a breeding tank, respectively. The EOD*f*s of individual fish remain strikingly constant over the course of hours, but show fine modulations over the course of seconds and minutes.

2.2 Tracking equipment

In order to record the EODs of spatially distributed electric fish we developed a portable multi-channel recording system. The EODs of gymnotiform electric fish cover the frequency range of about 30 to 2000 Hz and typically show amplitudes below 10 mV (Fig. 2.3 C). To be able to resolve all naturally occurring EOD frequencies a recording system must sample at least with twice the expected maximum frequency, in the case of EODs about 4 kHz. Then, to cover also the EOD's harmonic frequencies multiples of the expected maximum frequency must be sampled. We therefore designed a recording system with a minimum recording frequency of 10 kHz. In collaboration with npi electronics GmbH (Tamm, Germany) we designed a sensitive headstage with a stainless steel electrode embedded in epoxy resin (Fig.2.3 B). The headstage has an input resistance of 100 MΩ, a flat transfer function beyond 100 kHz,

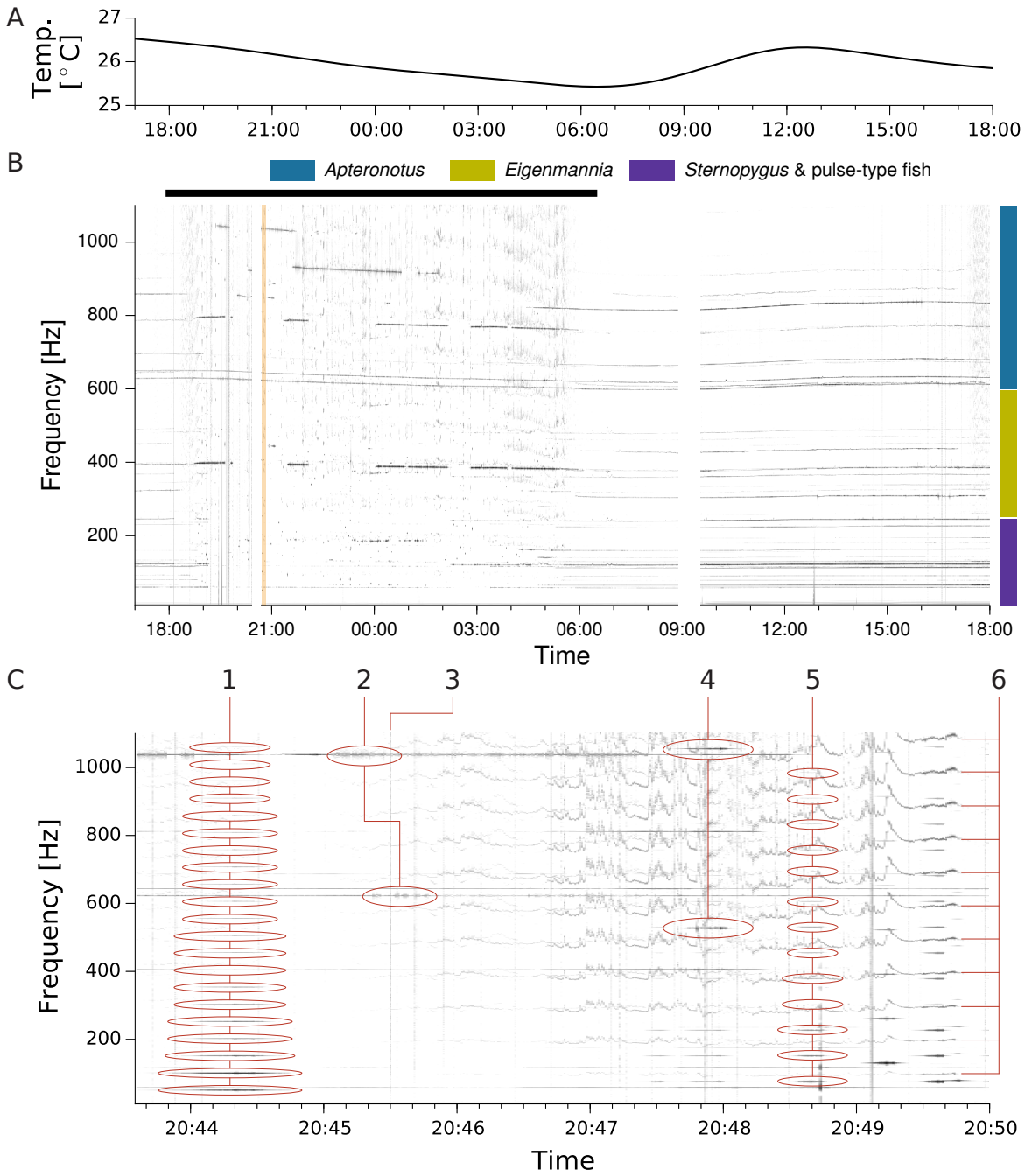

Figure 2.1: FIELD-DATA FROM DARIÉN, PANAMÁ. **A**) Water temperature of the stream at the location of the grid over 25 hours. Temperature decreases at night by about a degree and rises during the day. **B**) Spectrogram of 25 hours of electrode data, recorded with a 64-channel electrode array, collapsed over all channels. EODs are most conspicuous as horizontal traces. This dataset, recorded in Darién, Panamá, contains four sympatric species of electric fish (3 wave-type, at least 1 pulse-type). The fundamental EOD*f*s of the wave-type species are well separated (colored patches) over the range from about 50 to 1100 Hz, whereas the EOD*f* of the present pulse-type species (30 to 100 Hz), *Brachyhypopomus occidentalis*, overlaps with *Sternopygus dariensis* (~40 – 220 Hz). Electric activity varies between daytime and nighttime (black bar). During daylight, electric fish stay at their hiding places, while at nighttime, many electric fish roam the stream and pass the recording area. The vertical orange line indicates the time frame in focus in the bottom plot. Breaks in the time axis indicate maintenance breaks during sequential recording sessions. **C**) Enlarged spectrogram of the same recording. Many electric fish pass the recording area within a few tens of seconds (1, 4, 5, 6). Few fish remain within the recording area for longer periods of time (2). Although the wave-type species' fundamental EOD*f*s are well separated in frequency space, the EOD's harmonics of low-EOD*f* species, e.g., *Sternopygus*, strongly overlap with the EOD*f*-ranges of higher frequency species, i.e. *Apteronotus* and *Eigenmannia*. See 1, 4, 5 for the case of overlapping wave-type harmonics and 6, for the case of overlapping pulse-type harmonics. Blurring and broadening of spectral EOD*f*-traces (2) in wave-type species are often indicators of ongoing chirp-activity. Vertical lines indicate strong environmental noise (3). Frequency resolution: 0.3 Hz. Data were recorded on 2012/05/12.

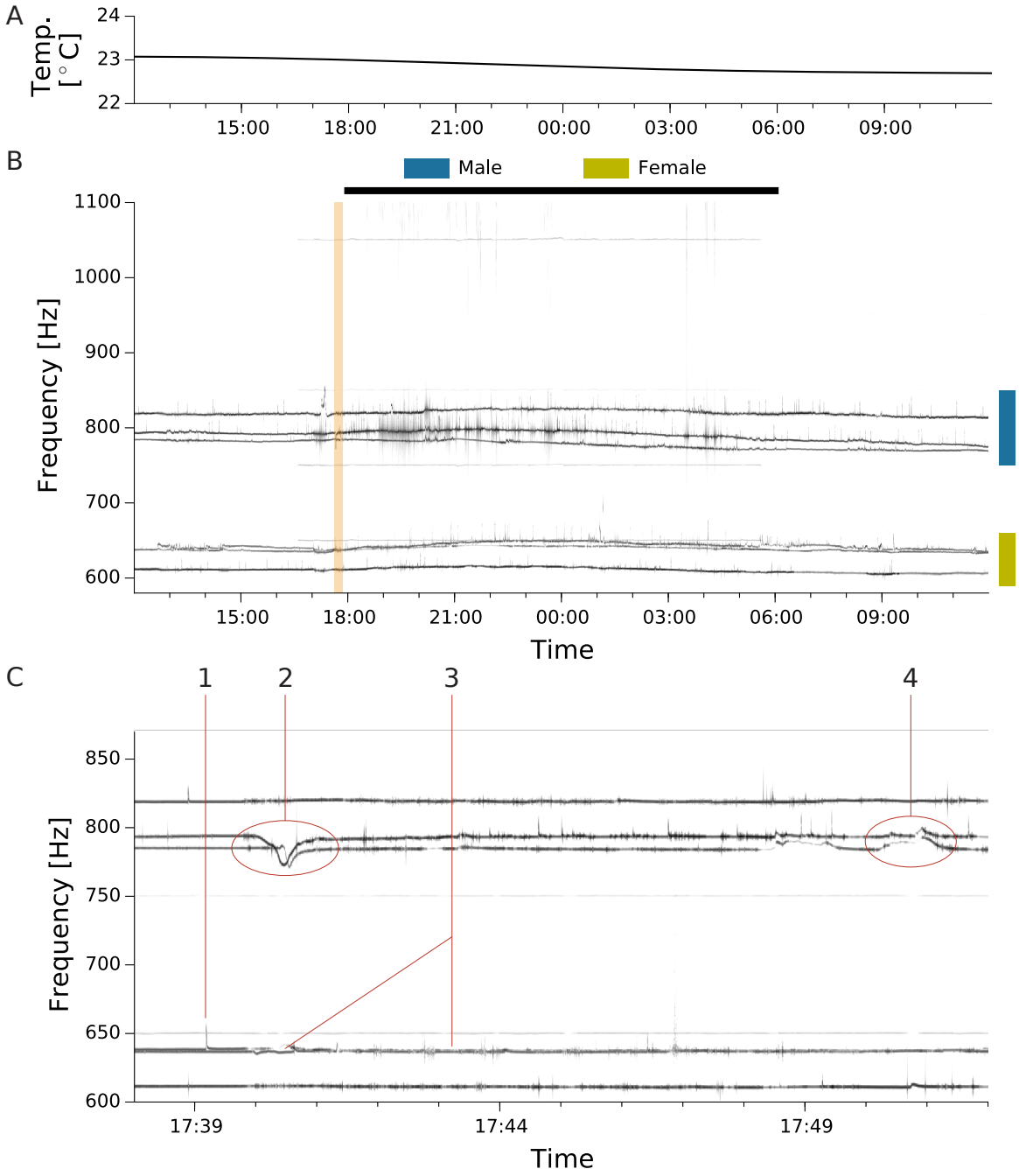

Figure 2.2: DATA FROM A BREEDING EXPERIMENT. **A**) Water temperature over 24 hours. Temperature changes very little over the course of the day. **B**) Spectrogram over 24 hours from a breeding tank housing 6 *Apteronotus leptorhynchus*, 3 male and 3 female fish. The nighttime is indicated by the black bar. These recordings allow for the analysis of EOD traces over a full day and, eventually, months. The EOD*f* of males and females are well separated by about 150 Hz. Overlaps of male and female EOD*f* ranges are extremely rare. EOD*f* changes only slowly over the course of hours and many of the observed changes in EOD*f* do not appear to be correlated to changes in water temperature.The broadening of spectral EOD traces (see male EOD trace in the center during nighttime) is an indicator for high chirp-activity. The vertical orange line indicates the time frame in focus in the bottom plot. **C**) Enlarged spectrogram of the same recording (17:38 PM). EOD modulations of variable length are commonly observed. (1) A short frequency rise over several seconds. (2) EOD*f* drops of two male fish, resulting in the crossing of EOD*f*s, over tens of seconds. (3) EOD*f*s of two individuals can overlap over long periods of time without showing any signs of a jamming avoidance response. (4) EOD*f* rises of two male fish over tens of seconds. Frequency resolution: 0.3 Hz. Data were recorded on 2014/10/26.

a 1-fold amplification, and is able to reliably transfer a measured signal over more than 20 m of cable without relevant signal distortion. The analog-to-digital (A/D) conversion used in this setup required an input signal in the range of ± 10 V. Therefore, the measured EOD signal was amplified by a factor of 1000 by a second set of amplifiers in reference to a single electrode. Over the course of this project we developed and worked with two amplifier versions. A first prototype (Fig. 2.4 A) was designed with 16 input channels and an analog filter layout for recordings with sample rates up to 10 kHz. The built-in A/D conversion device (USB-6211 OEM, 250 kS,16-bit; National Instruments, Austin, Texas, USA) was controlled via USB by a netbook running on a Linux operating system (openSUSE v10.2). The amplifier was powered by a custom-built battery pack allowing for up to 2.5 hours of recording.

The second amplifier (Fig. 2.4 C) was designed with 64 channels and an analog filter layout for recordings with sample rates up to 30 kHz per channel. The amplifier had two built-in A/D conversion boards (PCI-6259, 1.25 MS, 16-bit; National Instruments, Austin, Texas, USA) connected to a custom-built computer system via a PCI-Expansion (EX-1035, Exsys, Steinbach, Germany). Both amplifier and computer system were designed for minimal energy consumption (25 W and 22 W, respectively) and for resistance against rain and high humidity, a common threat to electronics in tropical environments. The system was powered by a set of car batteries (2×70 Ah) allowing for uninterrupted recordings of up to 14 hours. For the computer we chose a headless design (i.e. no monitor connected) with an industry-standard Mini-ITX mainboard (DFI-ACP LR100-N16M) in a sealed metal case. All connections and plugs were sealed with silicon. Recordings were controlled using a standard laptop, which was connected to the recording system via ethernet network in order to start, stop or monitor recordings.

Recordings were controlled with custom-designed software, *'fishgrid'*, written in C++ by Jan Benda and Jörg Henninger and running on a Linux operating system (Ubuntu 11.10 and later). The data acquisition module was based on the comedi framework (www.comedi.org). For each recording we created a separate folder for configuration, log and raw binary data files. Raw data were saved as multiplexed 4-byte floats and analyzed offline.

For mounting the headstages we used two different systems. The first mounting system was built using round standard tubes made of polyvinyl chloride (PVC) and used for plumbing (Georg Fischer GmbH, Albershausen, Germany; 4 cm total diameter, 3 mm wall diameter; Fig. 2.4 B). This system was too flexible for the precise positioning of headstages in streams with strong currents. Therefore, we switched to a much more rigid frame based on fiber-reinforced thermoplast profiles (4×4 cm; 60% polyamid, 40% fiberglass; Fig. 2.4 D) sponsored by Technoform Caprano + Brunnhofer GmbH (Kassel, Germany), which resembled the MB profile system of item Industrietechnik GmbH (Solingen, Germany). Despite its greater weight, this robust and highly adaptable system proved to be ideal for our application. All connectors were custom-designed and made of PVC and polypropylene (PP).

2.3 Tracking electric fish over time

Our EOD tracking system is optimized for identifying and tracking individual wave-type electric fish, to estimate the fish's positions, and to detect communication signals. The signals of pulse-type electric fish are detected, but remain unprocessed for now. EOD tracking is organized in three steps (Fig. 2.5). First, information about electric fish presence, EOD frequency, and approximate position is extracted. Each electrode is analyzed separately in sequential overlapping windows (1.22 s width, 85% overlap). For each window the signal's spectral transform is calculated, frequency peaks above a given threshold are detected, and individual fish are extracted from the list of frequencies. Then, for each analysis window, EOD detections from all electrodes are matched and consolidated. Finally, fish detections in successive time windows are matched, combined, and stored for further analysis. Slow EOD frequency modulations, so-called frequency rises (Zakon et al., 2002), are already detected at this stage.

Because EOD data recorded in natural habitats are noisy (Hopkins, 1973; Fig. 2.1B, (iii), the tracking strategy is optimized with focus on reliable and autonomous processing. This is achieved by combining the application of tolerances, thereby allowing for a certain variation in the data, with the application of thresholds, in order to further process reliably represented data only.

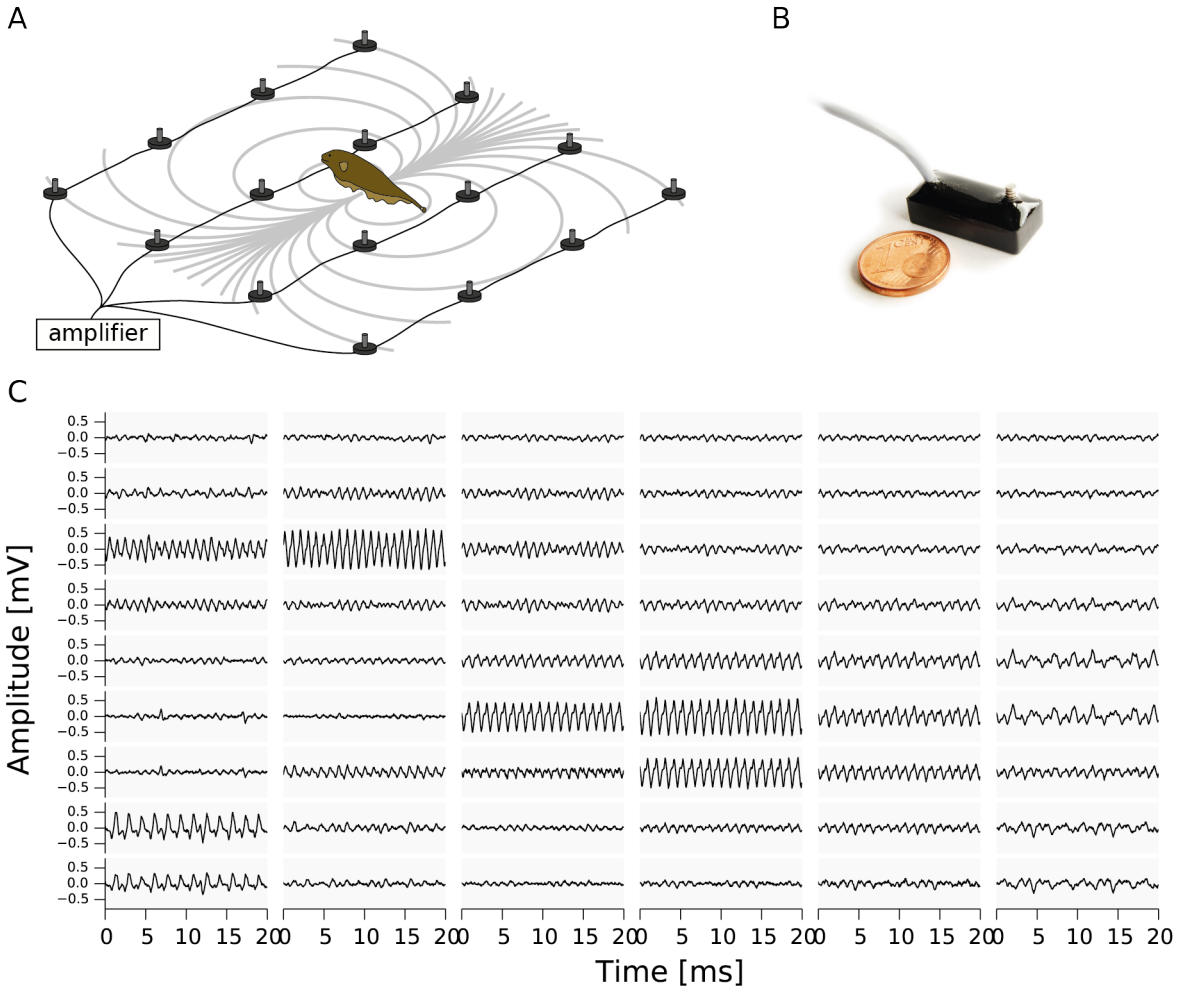

Figure 2.3: MULTI-ELECTRODE RECORDING SYSTEM. **A**) Illustration of the EOD's spatial distribution surrounding an electric fish and our multi-electrode recording system. Recording electrodes are spatially distributed in a tank or the electric fish's natural habitat and allow for recording of EOD signals of numerous freely moving electric fish. **B**) The recording electrode's headstage is small and created from stainless steel to allow for a robust and sensitive recording of EOD signals. **C**) Raw data example recorded with 54 electrodes (gray boxes) with three *A. rostratus* being present, a low frequency female (lower left) and two high frequency males (upper left and center). Commonly, recorded EOD signals of wave-type fish are below 1 mV in amplitude.

Figure 2.4: VERSIONS OF THE RECORDING SYSTEM. Over the course of this project we developed two major implementations of the multi-electrode recording system. **A**) A first, highly portable prototype was designed with 16 channels, powered by standard AA batteries, and successfully deployed at the Panguana research station, Peru. A/D conversion was integrated into the amplifier and controlled via USB by a netbook. **B**) For the prototype, electrodes were mounted on PVC tubes and spacings between 50 – 100 cm were used. **C**) The final, rugged recording system was designed with 64 channels and powered by a set of 12 V car batteries to enable long and uninterrupted recording sessions. **D**) The mounting of electrodes was improved by using a much more rigid frame, which could be adjusted in height and provided a large degree of flexibility. All connectors were custom-designed and made of PVC and PP.

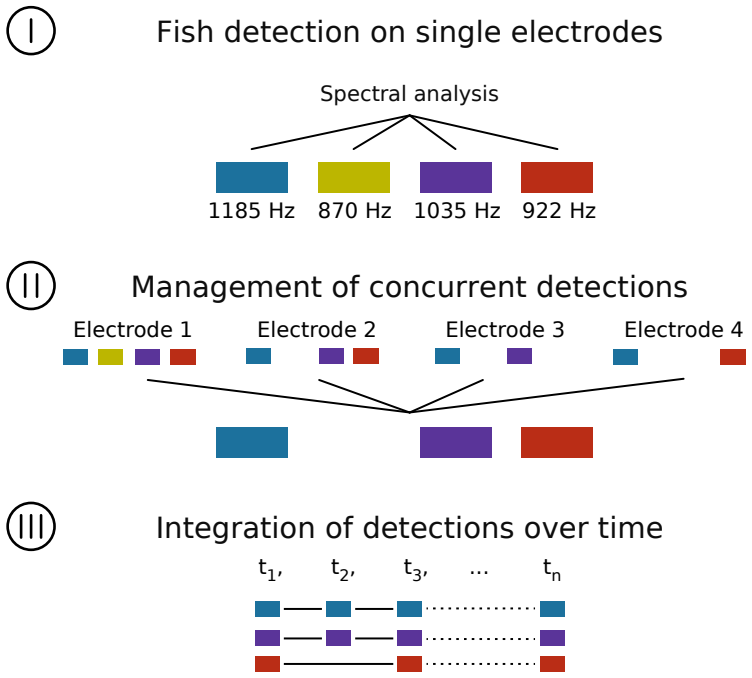

Figure 2.5: EOD TRACKING SCHEME. The tracking of electric fish's EODs over space and time is organized in three steps. **1**) Spectral analysis on single recording electrodes and detection of EODs of present electric fish. **2**) Information on detected EODs is matched and consolidated over all electrodes. Only EODs detected on several electrodes are processed further in order to increase the tracking system's robustness against noise. **3**) Tracking of EODs over time by matching new to previous detections, thereby creating temporal continuation. This process relies on EOD frequency, but allows for small mismatches to follow the EOD frequency modulations commonly observed in electric fish.

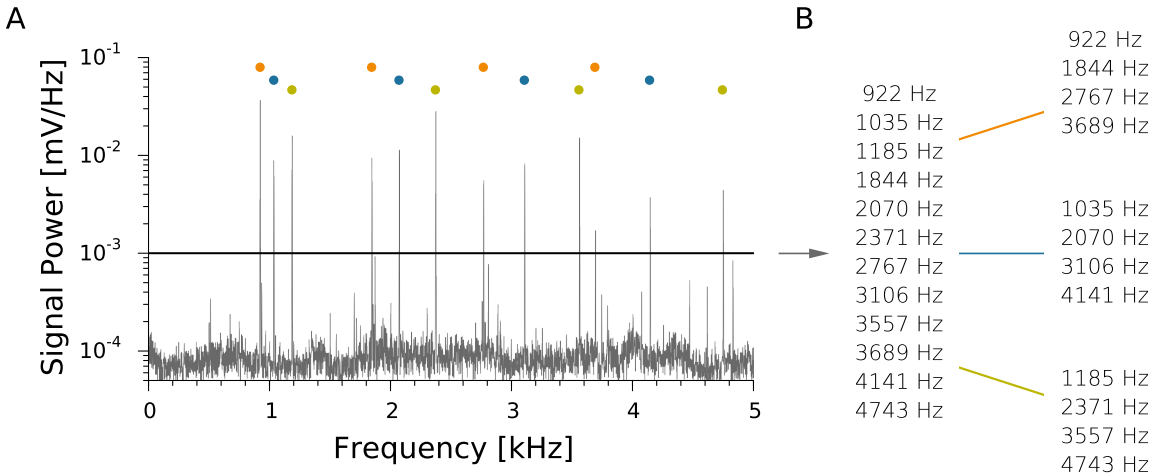

Figure 2.6: EODs ARE DETECTED BASED ON THEIR SPECTRAL REPRESENTATIONS. **A**) The spectrum shows the overlapping spectral representation of the EODs of three concurrently present electric fish (*Sternarchorhynchus spec.*) recorded in Peru. The colored markers code for each EOD's harmonic structure. **B**) Peak detection on the spectrum generates a list of prominent frequencies, which is sorted into the harmonic structures related to each fish's EOD.

Detection of EODs

The spectrum of a single EOD shows a prominent frequency peak at the discharge rate of the electric organ, the so called fundamental frequency, EODf or f_1. Additionally, the spectrum shows frequency peaks at many integer multiples, the so called harmonics or f_n, where n is the order of the harmonic. Together, the fundamental frequency and its harmonics are known as a harmonic series. Often, voltage recordings of electric fish activity, both in the field and in the laboratory, are a superposition of the EODs of multiple fish (Fig. 2.6, A) and, accordingly, the associated spectra contain many frequency peaks. Because EODs cover a vast range from as low as 30 up to 2000 Hz, it is not directly clear, which frequency in the spectrum is an EOD's fundamental and which is a harmonic. However, just this information can be extracted by analyzing the harmonic composition of a frequency spectrum and thereby grouping a spectrum's many frequency peaks into a few EOD-related *harmonic structures* (Fig. 2.6, B). Accordingly, the extraction of harmonic structures is the core of our EOD tracking algorithm. Commonly, EODs of wave-type electric fish contain three or more prominent harmonics, the relative amplitudes of which are related to the specific shape of the EOD's waveform.

Indeed, overlaps of an EOD's fundamental with the harmonics of other EODs are a very common phenomenon in natural habitats. For example, *Sternopygus dariensis* (~ 40 – 220 Hz), can have strong EODs with many harmonics (see Fig. 2.1 B), which fully overlap with the fundamental frequency ranges of both *Eigenmannia humboldtii* (~ 200 – 600 Hz) and *Apteronotus rostratus* (~ 600 – 1100 Hz). Then again, the harmonics of *E. humboldtii* itself overlap with the fundamental frequency range of *A. rostratus*. Interestingly, the overlap of fundamental frequency ranges and harmonics occurs intraspecifically, too. The genus *Sternopygus* exhibits a sexually dimorphic frequency distribution (Hopkins, 1972, 1974b): males cover the range between about 40 – 70 Hz, while females cover the range between about 130 – 220 Hz, the latter of which overlaps with the male EOD's third and fourth harmonic. This observation raises the question, if and how electric fish distinguish between fundamental and harmonic frequencies in order to differentiate species.

Searching for harmonic structures

The recorded electrode data is analyzed in sequential and overlapping fragments referred to as *analysis windows* (time step = 40 ms). For each electrode and analysis window, we calculate the *power spectral density* (PSD, 8192 FFT data points, 5 overlapping sub-windows, overlap 50%, total width = 1.22 s), and

generate two lists of frequency peaks using the peak detector algorithm of Todd and Andrews (1999) on the log transformed PSD. To generate the two lists, we choose a conservatively set high (ht-list) and a less conservatively set low threshold (lt-list).

While the ht-list provides us with a reliable list of frequency detections, the lt-list greatly improves the sensitivity of the EOD detection and discrimination. The ht-list contains frequencies, which were detected using a high threshold and to which we therefore attribute a high confidence to be relevant. All of these frequencies should be to attributed to harmonic structures, i.e. electric fish's EODs, if possible. The lt-list might contain additional frequency detections of lower confidence, some of which might be attributable to noise or spectral side-lobes. This potentially larger list will be used as a resource for filling up the harmonic structures.

EOD detection is based on the prime assumption that wave-type electric fish's EODs possess a harmonic structure with at least three prominent components, i.e. a fundamental frequency and at least two harmonics. Often, but not always, the fundamental frequency is the strongest frequency in an EOD's harmonic group, f_{max}. Therefore, we start searching for a conclusive harmonic structure based on the assumption that f_{max} is the EOD's fundamental, $f_{max} = f_1$, and then continue our search using a small range of integer fractions of f_{max}, $f_1 = f_{max}/n$, thereby assuming that f_{max} is the EOD's nth harmonic ($1 \leq n \leq 4$).

In order to attribute the frequencies to EOD-related harmonic structures, all its frequencies are tested for being harmonics of f_1. When testing for harmonics, we are faced with the fact that all frequencies in the lists are derived from a spectral representation with limited frequency resolution, Δf, onto which the true EOD frequency and its harmonics are mapped. The resulting inaccuracy in frequency representation has several consequences. (i) Generally, when testing for harmonics, allowing for a small frequency tolerance is necessary. The tolerance amounts to half of the spectral frequency resolution of the PSD, $f_{tol} = \Delta f/2$. (ii) The inaccuracy of f_1 affects the testing for harmonics by an implicitly growing frequency tolerance $\Delta f \cdot n$, where n is the order of the harmonic in question. E.g., given a frequency resolution of 1 Hz, the frequency tolerance for the 2nd harmonic ($n = 2$) is 2 Hz, for the 3rd it's 3 Hz and so on. Potentially resulting wrong attributions of frequencies can be avoided by demanding that sequential harmonics are separated by the frequency difference given by $f_1 \pm 2 \cdot f_{tol}$. (iii) Conversely, harmonics can be used to improve our knowledge of the true value of f_1. Our knowledge of harmonics is exactly as imprecise as our knowledge of f_1, i.e. it is limited by Δf. But because we know that the nth harmonic equals the true $f_1 \cdot n \pm \Delta f/2$, we can use the frequency information of the harmonic to increase the accuracy of our estimate of f_1 from Δf to $\Delta f/n$. The update of f_1 is stopped as soon as an predicted harmonic is missing to prevent bad updates of f_1.

The process of finding a conclusive harmonic structure for a given f_1 is separated over several steps. First, to improve our knowledge of the true f_1 we create a harmonic structure from the ht-list only and update the value of f_1 utilizing the harmonics as described above. Second, using the updated f_1 we create a harmonic structure from the lt-list. Harmonics, which were predicted, but not found in the lt-list, are marked as missing. A group is discarded, if either too many harmonics are missing or frequencies of the lt-list are attributed to harmonic structures too often. Third, the new harmonic structure is compared to the previously accepted structure and preferred if (i) the amplitude sum of its frequency peaks is larger and (ii) if the number of missing harmonics is lower, taking into account the possibly differing length of the harmonic structures.

The frequencies contained in the resulting group are removed from the ht-list, but not from the lt-list. If no conclusive harmonic structure can be found for f_{max}, it is considered to be noise and is removed from the ht-list. The search for harmonic structures is continued with the next strongest frequency in the ht-list. This procedure is repeated until all frequencies in the ht-list are either distributed to harmonic structures or discarded. When all frequencies of the ht-list are distributed, unwanted harmonic structures can be removed, e.g., those with fundamentals outside a meaningful frequency range ($40 \leq f < 1500$ Hz, see Fig. 1.2) and those representing the mains hum and other sources of electrical noise.

A profound challenge is posed by frequencies missed by the frequency detector. No matter how the detection threshold is set, there will always be frequency peaks related to EODs, which are just below the

threshold and will therefore be missed and, eventually, not be accounted for. Allowing for a small number of non-detected frequency peaks when constructing the harmonic structures, including the fundamental itself, we improve the robustness of EOD detection. At the same time we reduce the tracking system's susceptibility to noise and, thereby, provide a more reliable base for further analysis steps.

At the stage of single electrode analysis some ambiguities remain unsolved: if a high-frequency EOD (e.g., $f_0 = 600\,\text{Hz}$) perfectly overlaps with a low-frequency EOD's harmonic (e.g., $f_0 = 300\,\text{Hz}$, $f_1 = 600\,\text{Hz}$ etc.), a distinction between the harmonic structures of these EODs is impossible without integrating information of multiple electrodes.

EOD tracking over electrodes and time

Consistency over electrodes

So far, we detected and organized EODs in harmonic structures separately for each electrode. In order to create consistency over multiple electrodes, we search for and join those harmonic structures, which represent the EODs of the same fish, starting with those structures that share the same fundamental frequency. Some events can cause harmonic structures referring to the same EOD to show differing fundamental frequencies, e.g., fast rises or dips of rapidly moving fish. Therefore, harmonic structures showing a small difference to the sought after frequency are selected, if no harmonic structure with this fundamental frequency is present on that specific electrode.

Consistency over time

In order to create temporal consistency, we match newly detected fish from the current analysis window to fish detected in recent analysis windows. If a fish with identical EOD*f* is found in the previous detections, the new data will be added, otherwise the fish will be treated as a new candidate. If this candidate is detected robustly in the following analysis windows, typically over several seconds, it is marked as a confirmed fish detection. Otherwise, it will be discarded as a false detection. Matching of fish EOD*f*s is performed based on the closest-neighbor principle, but limited by allowing for a small frequency tolerance between previous and current EOD*f* only ($<10\,\text{Hz}$).

Overlaps of frequency traces are not well handled, yet. This phenomenon is very common in some datasets, e.g., during short rises in data from Peru and in the data generated during the long-term breeding experiment, yet we did not observe it in the data obtained in Panamá. One possible solution for the correct and robust frequency tracking would be to take advantage of the multi-channel recordings. First, when tracking an EOD priority should be given to the electrode with the strongest signal for this particular EOD. Second, if ambiguities arise, EODs could be tracked not only based on last known EOD*f*, but also on their respective EOD amplitudes in the sequential time steps, which are most likely correlated. Short time steps between sequential analysis windows would further facilitate this approach.

At the end of each analysis cycle, we need to perform a set of organizational tasks. (i) We discard candidate fish detections, which are not detected continuously over several analysis windows. (ii) The activity status of confirmed fish detections is checked and set to inactive, if it is not detected for a certain period of time, typically minutes. In this case, it is not used for the matching of new fish detections. (iii) Rises are detected and handled. Some wave-type electric fish generate frequency rises and drops characterized by a sharp frequency increase or decrease and a slow return to the previous baseline after several seconds or minutes. During the fast frequency changes the tracked EOD might be lost because of the large frequency difference between previous and current detection. These events are taken care of by searching for a newly appeared fish whose EOD*f* returns to the baseline of a previously lost fish and subsequent merging of the datasets. This process could be improved in future versions by checking if the positions of the lost and the new fish are close to each other. (iv) Data management. The amount of data about detected fish stored in the computer's memory can grow immensely over time, especially when analyzing long recordings and datasets with many electrodes. Therefore, data on inactive fish has to be saved to hard disk and removed from memory continuously.

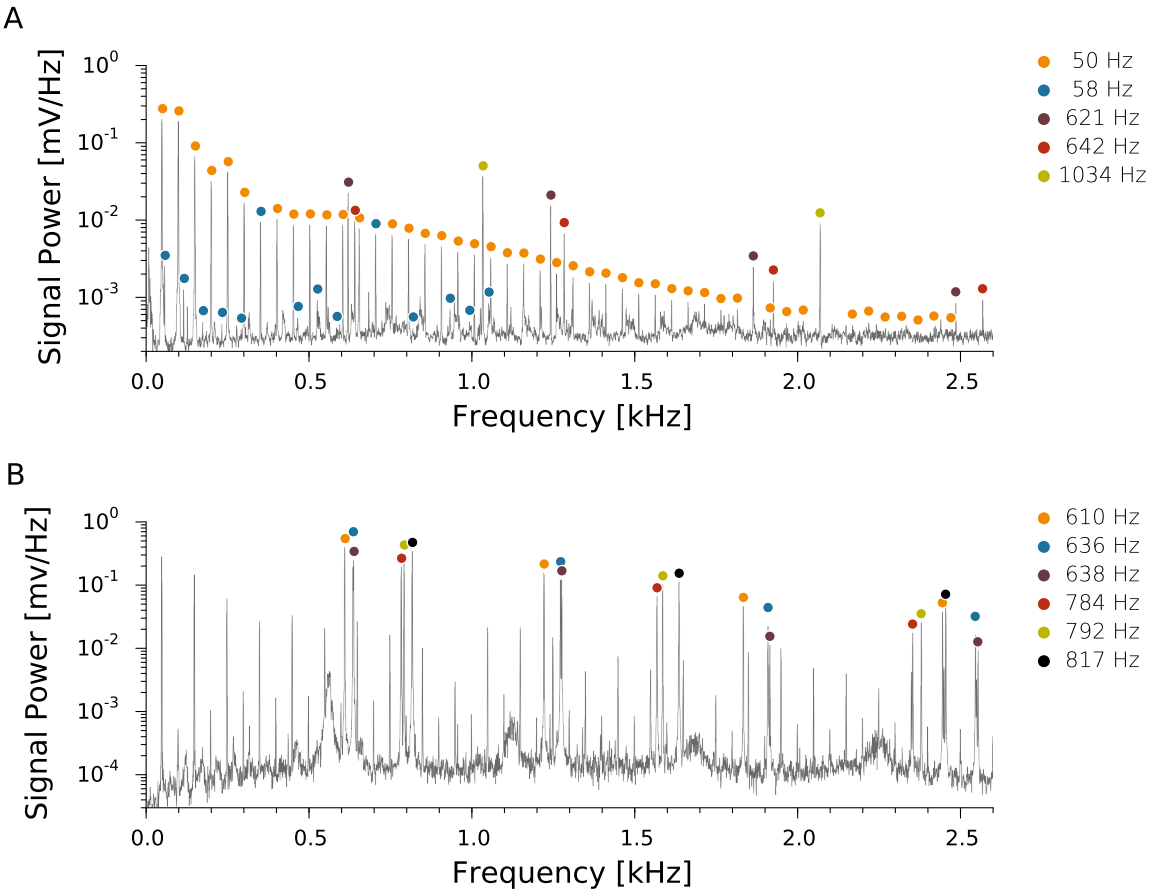

Figure 2.7: EOD DETECTION: EXAMPLES. **A**) Spectrum of field data recorded in Darién, Panamá, representing the EODs of five concurrently present electric fish belonging to two species. The colored markers refer to frequency peaks related to the same EOD, with double markings possible. The EODs of the low frequency species, *Sternopygus dariénsis*, cover a fundamental frequency range between 50 – 200 Hz. Its EODs are characterized by strong amplitudes and prominent harmonics up to 2 kHz. The EODs of the high frequency species, *Apteronotus rostratus*, cover a range between 500 – 1100 Hz, are generally weaker in amplitude and have only few harmonics. Although the harmonic frequencies of *Sternopygus* strongly overlap with the fundamental frequency range of *Apteronotus* our sorting algorithm successfully identifies frequencies related to the same EOD and groups them in the same harmonic structure. Successfully identified EODs are displayed on the right. **B**) Spectrum of data recorded in the laboratory in a breeding tank with six *Apteronotus leptorhynchus*. Again, frequency peaks related to the same EOD are marked with the same color. The electric fish's EOD fundamental frequencies cover a frequency range between 600 – 820 Hz. However, numerous additional frequency peaks caused by the mains (multiples of 50 Hz) and other electric devices are prominent over the whole spectrum. Our sorting algorithm successfully groups related frequencies and returns only those harmonic structures with fundamentals in the previously defined frequency range, in this case 500 – 1000 Hz. Successfully identified EODs are displayed on the right.

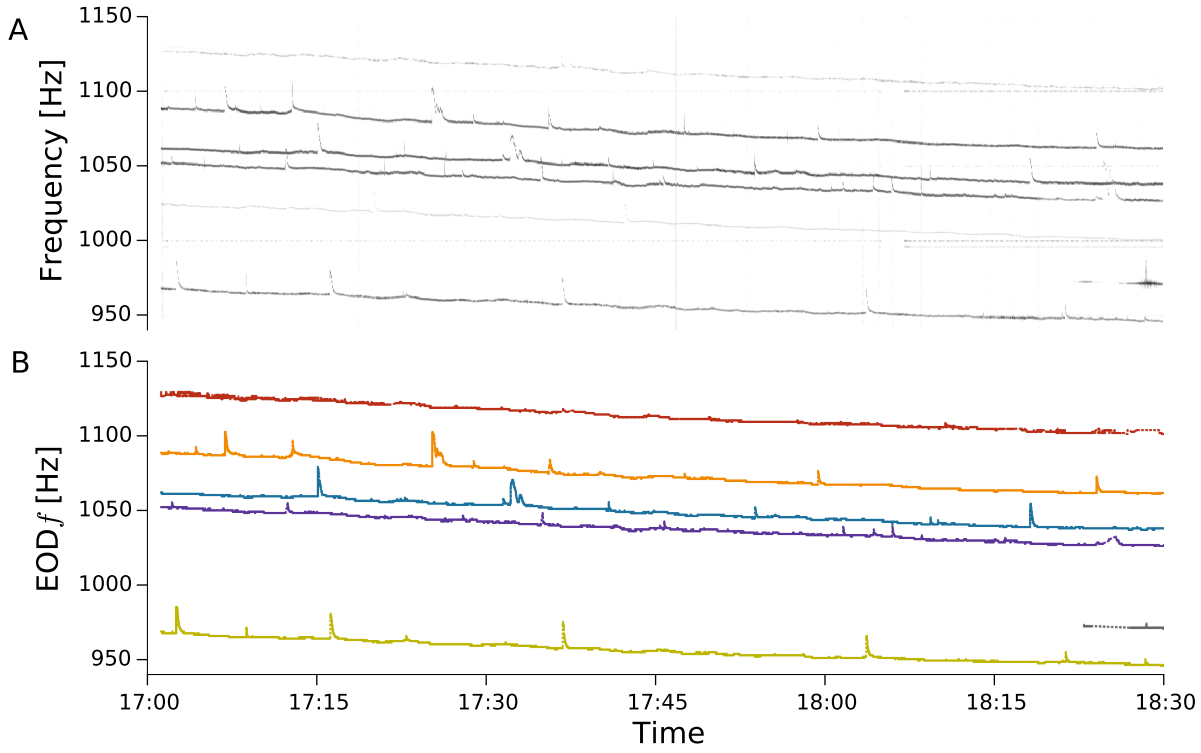

Figure 2.8: FREQUENCY TRACKING. **A**) Spectrogram of the EODs of several *Sternarchorhynchus* sp. (wave-type; Gymnotiformes: Apteronotidae) recorded with a 16-channel array in a fast flowing stream in the Ucayali region of Peru during dry season. The EODs show a slow temperature related frequency decrease and many rises. Most fish remain at their hideouts, with the exception of a single fish appearing around 18:22. Horizontal traces in the spectrogram are caused by constant electrical noise of the recording system. **B**) The EODs of the present fish are tracked accurately despite the numerous occurrences of rises and the continuous frequency decrease of the EODs. Occasionally, when the EOD frequency traces of two fish overlap during a rise, tracking of the rising fish might be interrupted temporarily, but is continued after the EODf of the rising fish drops below the second fish's EODf. Note that the spectrogram in A contains the weak EOD trace of another fish starting at about 1030 Hz, which is not tracked because its amplitude is lower than the detection threshold of the analysis.

2.4 Tracking electro-communication

Transient modulations of EOD frequency are commonly observed during social interactions, e.g., agonistic behavior and courtship, and are therefore believed to serve as communication signals in various gymnotiform species (Hopkins, 1974a,b; Hagedorn and Heiligenberg, 1985; Smith, 2013). Here, we focus on the detection and analysis of chirps and rises.

Rises in apteronotid species are frequency modulations with durations between a few hundred milliseconds to several minutes and frequency excursion of not more than a few tens of Hertz. Rises are readily detected as deviations from the baseline frequency of a fish (Fig. 2.9). The baseline frequency is estimated in large running analysis windows (30 minutes width) by fitting a straight line to the frequency trace. This approach allows to compare the actual frequency to the estimated baseline frequency, even if EODf changes over time because of temperature changes. Deviations from baseline of more than 3 Hz over more than 600 ms are considered to be rises.

Chirp detection for all types, e.g., small or long chirps, is based on the same principle (Fig. 2.10). For each fish the electrode's voltage traces are bandpass-filtered (Butterworth filter, 3rd order, 5$\times$ multi-pass, $\pm$7 Hz width) at the fish's EODf and 10 Hz above the EODf. For each passband the signal envelope is estimated each 40 ms using a root-mean-square filter over 10 EOD cycles multiplied by $\sqrt{2}$. Rapid EOD frequency excursions, both positive and negative, will cause the signal envelope to drop at the fish's baseline frequency. At the same time, the signal envelope of the passband above the fish's EODf increases transiently and in synchrony with the frequency excursion or interruption. Because of the narrow frequency range of the passband, 14 Hz, even envelope amplitude modulations caused by rapid frequency excursions are broadened in the time domain. Therefore, even very short frequency modulations, e.g., the few cycles long EOD interruptions of *Eigenmannia*, cause a broad and substantial decrease in envelope amplitude. If events are detected in both passbands and exceed a preset amplitude threshold, they are accepted as communication signals, and timestamps for the beginnings and endings of the signals are extracted. Communication signals with a single peak in the upper passband were detected as small chirps. Signals of up to 600 ms duration and two peaks in the upper passband, marking the begin and the end of the longer frequency modulation, were detected as long chirps. Using the bandpass parameters described above, chirps with a duration greater 50 ms are detected as long chirps.

All thresholds have been set such that the number of false detections are negligible. This comes at the price of an increased rate of missed detections. Manual reevaluation of 86 episodes containing small chirps, each with a duration of 25 seconds, showed that on average 56 % of present small chirps (1693 of 3029) are successfully detected. However, no evidence for missed long chirps has been found.

2.5 Spatial tracking of electric fish

A crucial aspect for the understanding of electric fish behavior and their interactions are the fish's locations and movements over time. Further, we want to understand the context of the fish interactions, e.g., distances and signal amplitudes between fish at the time at which specific behaviors occur, e.g., communication and the initiation of agonistic behavior, in order to learn about the limits of electro-behavior and the underlying sensory processing.

Estimation of electric fish location and orientation

The electric organ generates a non-uniform, approximately dipolar shaped electric field (Knudsen, 1975; Fig 1.3 A). Our electrode array can pick up the spatial amplitude distribution of this field continuously. The EOD amplitude is attenuated dependent on orientation of and distance from the electric fish and is well approximated by the ideal dipole model at distances greater than the fish's body lengths (Eq. 2.2; Knudsen, 1975). This aspect of the EOD's electric field enabled us to employ the ideal dipole model to extract information on the approximate fish location and orientation from the recorded EOD amplitudes and also to create new datasets for testing the performance of position estimation. A similar, lookup-

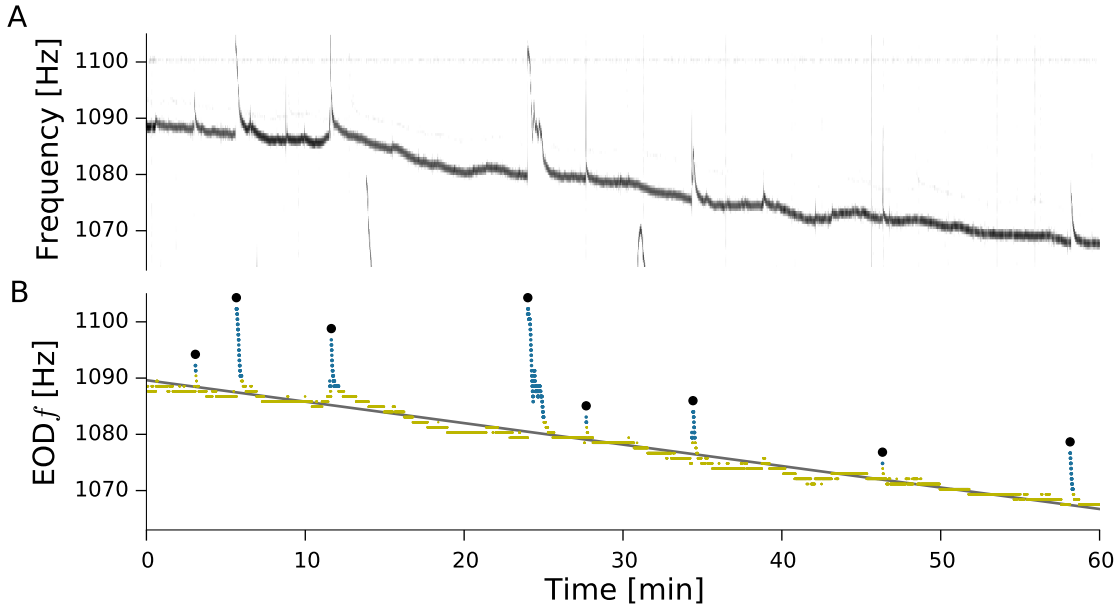

Figure 2.9: DETECTION OF RISES. **A**) Spectrogram of a section of the data from Fig. 2.8. The shown EOD trace descends over time and contains several long frequency rises. **B**) Illustration of rise detection. The baseline EODf within a large rolling analysis window is estimated by a linear regression fit, illustrated by the black line. Frequency excursions with a difference to baseline of more than 3 Hz (blue dots) are considered to be rises and key parameters, e.g., the peak time (black dots), are extracted.

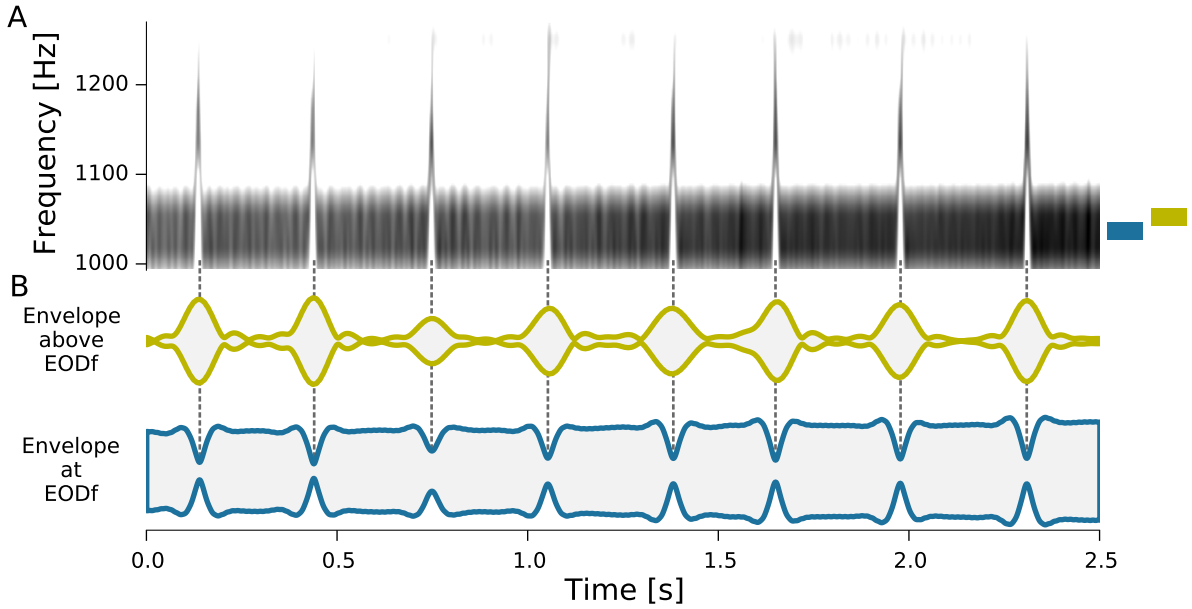

Figure 2.10: DETECTION OF CHIRPS. **A**) Spectrogram of a series of small chirps emitted by a male fish. In *Apteronotus*, chirps are rapid and transient, positive frequency modulations of the EOD. For chirp detection, the recorded voltage traces are filtered at and 10 Hz above a fish's EODf using a narrow passband (indicated by the colored rectangles) and the filtered signal's envelope is calculated. During a chirp, the amplitude at the EODf decreases (but note the surrounding halo) and increases in the frequency range above. **B**) The filtered signal's envelopes in the respective passbands. Chirps are detected on the envelopes as synchronous amplitude decreases in the passband at the EODf (blue) and amplitude increases in the passband above (green). In synchrony with the spectral chirp traces (emphasized by the dotted lines), the envelope's amplitude at the EODf decreases and increases in the passband above.

table-based approach, adapted to a laboratory-based setup with shallow water, has been described by Jun et al. (2013).

The estimated location of a fish always refers to a fish's electric center. The center's relative position within the fish depends on the type and location of the fish's electric organ (Caputi et al., 2005), which in some species is distributed along the body axis and in others concentrated in a small area, and which is never located in the fish's front. We have to keep this information in mind, when judging the estimated distance between two fish. In infrared video footage of courtship interactions (Fig. 4.4) we can see that the fishs heads can be very close, although the electric organs located in the caudal parts, and thereby the fish's electric centers, are quite far away from each other.

Generally, the EOD amplitude data used for the estimation of fish location and orientation is extracted from the envelopes of the bandpass-filtered voltage traces at the EOD*f* as described for the detection of chirps. To simplify the notation in this section, we will often use the term *electrode* to refer to the fish specific EOD amplitude as measured at a specific electrode location.

Weighted spatial average

A first estimate of 2D fish location and orientation is based on a weighted spatial average (WSA). In the following, we will differ between the WSA_{all}, which uses all available electrodes to compute the fish location, and the $\mathrm{WSA}_{largest}$, which uses only a selection of electrodes with the largest amplitudes. The fish position $\vec{x}$ is estimated from the electrodes i with the largest envelope amplitudes A_i at position e_i as a weighted spatial average, given by

$$\vec{x} = \sum_{i=1}^{n=z} \sqrt{A_i} \cdot \vec{e}_i. \tag{2.1}$$

The position was computed only, if at least 2 electrodes with amplitudes greater than 15 µV were available. If at least 4 electrodes with amplitudes greater 1 µV were available, $z = 4$, otherwise $z = 2$. Although this estimate does not relate to the underlying physics of the electric field, it proved to be the most robust against interference by electrical noise (Hopkins, 1973) and fish moving close to the edges of the electrode array (see Fig. 2.13).

The EOD of a fish can cause a very large amplitude on nearby electrodes, because of the electric field's reciprocal dependence on distance. This effect results in a relatively large localization error, if a simple weighted spatial average is used, because the position estimate is pulled towards the strongest electrode. The localization error is reduced by using the square-root of the EOD amplitude as a weight, $\sqrt{A_i}$, which reduces the impact of electrodes with large EOD amplitudes.

Similar to an electric dipole, the fish's EOD is of opposite polarity at the head and at the tail of the fish. To approximate fish orientation, we divide the electrodes into two subgroups of opposite polarity and calculate the direction vector between the estimated centers of these two groups. Because the EOD amplitudes are extracted as absolute values, polarity information of the EOD on the respective electrodes is missing and has to be estimated. The polarity of the electrodes is determined by calculating the correlations of the electrodes' bandpass filtered voltage traces (40 ms window width) to that of the electrode with the largest amplitude. Electrodes with correlations larger than $+0.9$ are assigned to one group and correlations smaller than -0.9 to the other. If both groups contained at least 4 electrodes, each group's center was estimated by calculating the weighted spatial average as described above (Eq. 2.1) and determining the direction vector between them. Because the requirements of the correlation coefficients are set close to the extremes of $+1$ and -1, respectively, electrodes with small amplitudes, which are more likely affected by noise, are implicitly discarded by this procedure.

The ideal dipole model

A second approach was pursued for fish location estimation, based on the ideal dipole function. The electric far-field of free swimming electric fish in a large body of water is well approximated by the three-dimensional ideal dipole model (Knudsen, 1975 and see below). In the following equations, $\vec{\cdot}$

denotes a 3D vector, $\langle .,. \rangle$ the dot product, $\|.\|$ the Euclidean norm of a vector and $|.|$ the absolute value of a scalar. The potential at location $\vec{e}$ of an ideal dipole in vacuum located at $\vec{x}$ is given by

$$f(\vec{e};\vec{p},\vec{x}) = \frac{1}{4\pi\varepsilon_0} \frac{\langle \vec{p}, \vec{e}-\vec{x} \rangle}{\|\vec{e}-\vec{x}\|^3}, \tag{2.2}$$

where ε_0 is the permittivity of vacuum and $\vec{p}$ is the dipole moment. This model yields the typical potential distribution of an electric dipole with positive and negative amplitudes separated by a zero potential equator orthogonal to the dipole moment. To simplify notation, the constant $1/4\pi\varepsilon_0$ will be absorbed into the dipole moment.

To clarify the orientation dependence of the electric field's amplitude, we rewrite Eq. 2.2 as

$$\frac{\langle \vec{p}, \vec{e}-\vec{x} \rangle}{\|\vec{e}-\vec{x}\|^3} = \frac{\|\vec{p}\| \, \|\vec{e}-\vec{x}\| \cos\phi}{\|\vec{e}-\vec{x}\|^3} = \frac{\|\vec{p}\| \cos\phi}{\|\vec{e}-\vec{x}\|^2}, \tag{2.3}$$

where ϕ is the angle between the dipole moment $\vec{p}$ and the vector $\vec{e}-\vec{x}$. This notation also clarifies that the effective value of the power law decay of the electric field in the three-dimensional vacuum is 2.

Because the amplitude data fitted with this model are absolute values, we used the absolute value of Eq. (2.2). The localization of a 3D dipole by means of an electrode array and a gradient descent is a difficult minimization problem, because of the large number of local minima in the loss function. We introduced a regularizer α in the denominator, to remove the singularity at the position of the electrodes and make the problem numerically more stable. The search for a robust solution was improved by introducing an additional offset parameter β. Finally, the exponent of the power law determined for the ideal dipole in three-dimensional free space, 2, might not hold true for the conditions occurring during EOD measurements because the water body is limited by the water surface and the stream bed or tank walls, which are known to introduce boundary effects that could change the effective exponent of the power law (Fotowat et al., 2013; Jun et al., 2013). Therefore, we made the power law parameter q a free parameter to account for this effect.

Together, these modifications yield the regularized dipole function, given by

$$f_\alpha(\vec{e};\vec{p},\vec{x},q) = \left| \frac{\langle \vec{p}, \vec{e}-\vec{x} \rangle}{\|\vec{e}-\vec{x}\|^q + \alpha} + \beta \right| = |g_\alpha(\vec{e};\vec{p},\vec{x},q)|. \tag{2.4}$$

The estimation of the dipole location from measured potentials has no direct analytical solution. Therefore, we minimized the mean squared loss, χ^2, between the measurements and the regularized dipole of Eq. (2.4) using gradient descent optimizer (BFGS; Wright and Nocedal, 1999):

$$\chi^2 = \frac{1}{m} \sum_{i=1}^{m} \left(A_i - f(\vec{e}_i;\xi)\right)^2 \quad \text{, with} \quad \xi = (\vec{p},\vec{x},q) \tag{2.5}$$

by descending along its gradient towards the minimum of χ^2, where $\frac{\partial \chi^2}{\partial \xi} = 0$. The gradient of the loss function can be written in terms of the partial derivatives of Eq. (2.4)

$$\frac{\partial \chi^2}{\partial \xi} = -\frac{2}{m} \sum_{i=1}^{m} \left(A_i - f(\vec{e}_i,\xi)\right) \cdot \operatorname{sgn}\left(g(\vec{e}_i,\xi)\right) \cdot \frac{\partial}{\partial \xi} g(\vec{e}_i,\xi) \tag{2.6}$$

The partial derivatives of (2.4) are given by

$$\frac{\partial}{\partial \vec{p}} g(\vec{e},\vec{p},\vec{x},q) = \frac{\vec{e}-\vec{x}}{\|\vec{e}-\vec{x}\|^q+\alpha} \tag{2.7}$$

$$\begin{aligned}
\frac{\partial}{\partial \vec{x}} g(\vec{e},\vec{p},\vec{x},q) &= \frac{(\|\vec{e}-\vec{x}\|^q+\alpha)\cdot\frac{\partial}{\partial\vec{x}}\langle\vec{p},\vec{e}-\vec{x}\rangle - \langle\vec{p},\vec{e}-\vec{x}\rangle\cdot\frac{\partial}{\partial\vec{x}}(\|\vec{e}-\vec{x}\|^q+\alpha)}{(\|\vec{e}-\vec{x}\|^q+\alpha)^2} \\
&= \frac{-(\|\vec{e}-\vec{x}\|^q+\alpha)\cdot\vec{p} - \langle\vec{p},\vec{e}-\vec{x}\rangle\cdot\frac{\partial}{\partial\vec{x}}\langle\vec{e}-\vec{x},\vec{e}-\vec{x}\rangle^{\frac{q}{2}}}{(\|\vec{e}-\vec{x}\|^q+\alpha)^2} \\
&= \frac{-(\|\vec{e}-\vec{x}\|^q+\alpha)\cdot\vec{p} - \langle\vec{p},\vec{e}-\vec{x}\rangle\cdot\frac{q}{2}\langle\vec{e}-\vec{x},\vec{e}-\vec{x}\rangle^{\frac{q-2}{2}}\cdot(-2\vec{e}+2\vec{x})}{(\|\vec{e}-\vec{x}\|^q+\alpha)^2} \\
&= \frac{-(\|\vec{e}-\vec{x}\|^q+\alpha)\cdot\vec{p} - \langle\vec{p},\vec{e}-\vec{x}\rangle\cdot q\langle\vec{e}-\vec{x},\vec{e}-\vec{x}\rangle^{\frac{q-2}{2}}\cdot(\vec{x}-\vec{e})}{(\|\vec{e}-\vec{x}\|^q+\alpha)^2} \\
&= \frac{-\vec{p}}{(\|\vec{e}-\vec{x}\|^q+\alpha)} - \frac{\langle\vec{p},\vec{e}-\vec{x}\rangle\cdot q\|\vec{e}-\vec{x}\|^{q-2}\cdot(\vec{x}-\vec{e})}{(\|\vec{e}-\vec{x}\|^q+\alpha)^2}
\end{aligned} \tag{2.8}$$

$$\begin{aligned}
\frac{\partial}{\partial q} g(\vec{e},\vec{p},\vec{x},q) &= -\frac{\langle\vec{p},\vec{e}-\vec{x}\rangle}{(\|\vec{e}-\vec{x}\|^q+\alpha)^2}\cdot\frac{\partial}{\partial q}\|\vec{e}-\vec{x}\|^q \\
&= -\frac{\langle\vec{p},\vec{e}-\vec{x}\rangle}{(\|\vec{e}-\vec{x}\|^q+\alpha)^2}\cdot\frac{\partial}{\partial q}\exp(q\log\|\vec{e}-\vec{x}\|) \\
&= -\frac{\langle\vec{p},\vec{e}-\vec{x}\rangle}{(\|\vec{e}-\vec{x}\|^q+\alpha)^2}\cdot\|\vec{e}-\vec{x}\|^q\log\|\vec{e}-\vec{x}\|
\end{aligned} \tag{2.9}$$

$$\frac{\partial}{\partial \beta} g(\vec{e},\vec{p},\vec{x},q,\beta) = 1 \tag{2.10}$$

A weighted spatial average over all available electrodes was used to compute initial values for the optimization. The optimization is performed over two iterations using stepwise decreasing values for α (10^{-2} and 10^{-3}) and using the result of the first iteration as initial values for the last. The successful optimization directly yields the dipole's location, orientation, its moment's magnitude, and the potential distribution's effective power law. Since we are optimizing a function with 8 parameters, at least 8 data points are necessary for a successful optimization. For a comparison of methods for fish localization, see below.

Data-based evaluation of localization methods

The errors of three methods for fish localization were evaluated using data of the EOD's spatial distribution (Fig. 2.16). First, a weighted spatial average using all available, but at least 5 electrodes (WSA_{all}). Second, the weighted spatial average as described in Section 2.5, using the 4 electrodes with the largest EOD amplitudes ($WSA_{largest}$). And third, the dipole model fit described in Section 2.5, requiring at least 8 electrodes (dipole model). The dataset (1728 data points) was divided into subgroups representing electrode arrays with spacings ranging from 18 – 108 cm. For each spacing, 18 – 420 datasets were available, each with 4 – 72 electrodes. If a method required more electrodes than were available in a dataset, the evaluation was omitted. For each spacing, the errors are convolved with a Gaussian kernel ($\sigma = 1$ cm) and displayed as violin plots in Fig. 2.11 A. All three methods yielded similar error distributions for small spacings, i.e. 18 and 36 cm, with means and medians smaller than 6 cm (Table 2.1) and thereby much smaller than the length of the fish (18 cm). Larger spacings, i.e. 72 and 108 cm, could be evaluated only using $WSA_{largest}$. The error distribution for 72 cm has a longer tail than the error distributions computed for different spacings using the same method, but the distribution's median is similar (6.1 cm). The extended tail might be a consequence of the large number of locations (n = 420), which were sampled for this spacing.

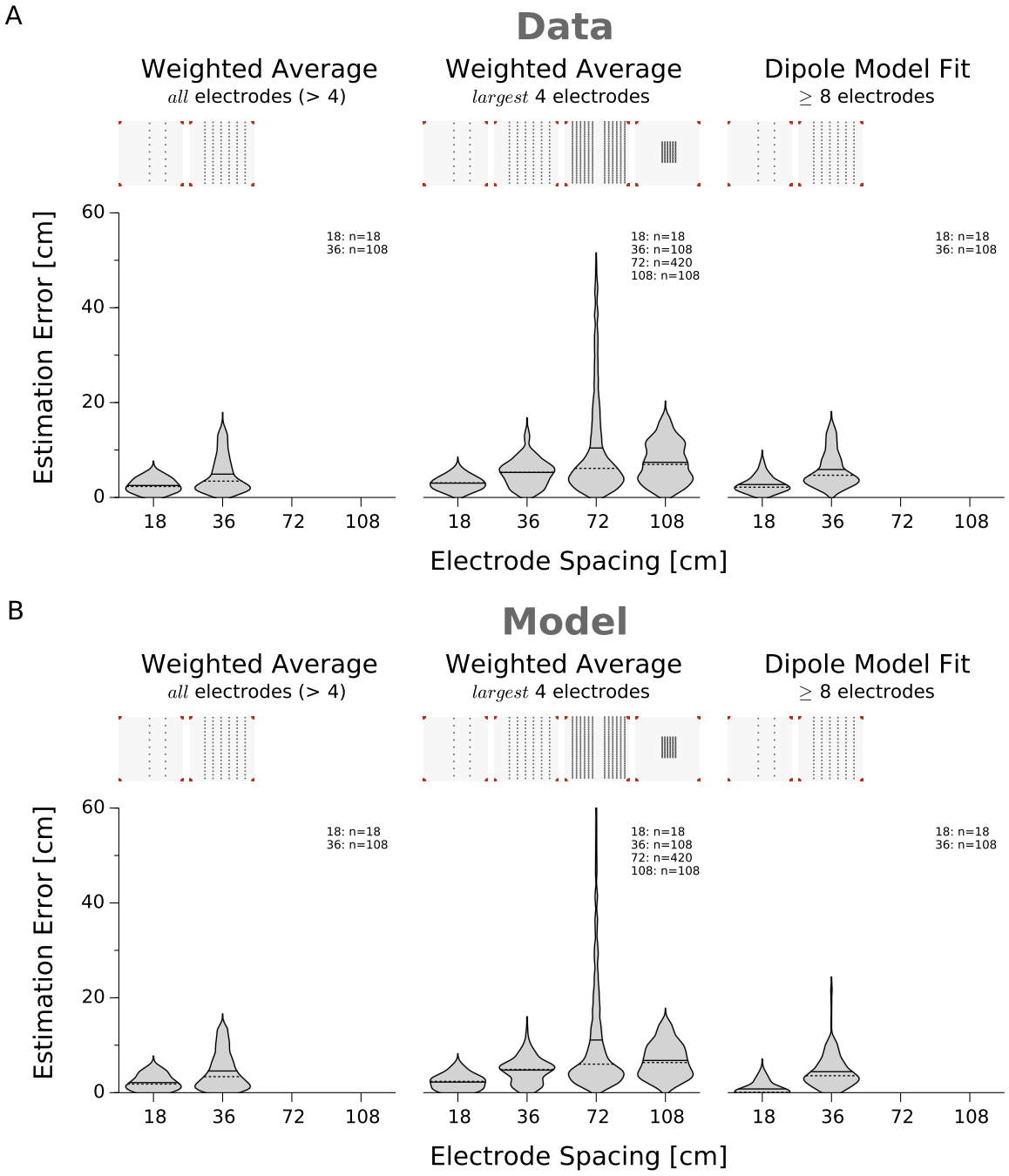

Figure 2.11: EVALUATION OF METHODS FOR POSITION ESTIMATION BASED ON EOD MEASUREMENTS. **A**) Errors of fish localization based on EOD amplitudes recorded in a large outdoor tank (Fig. 2.16). **B**) Errors of fish localization based on a dataset simulated with a dipole model using the electrode configurations of A. The model parameters were extracted from the model fit to the EOD amplitude measurements as shown in Fig. 2.16 E. Above each distribution of errors, we display the sampled fish locations (black dots) in relation to the four surrounding electrodes (red dots) in the center of the electrode array. The distributions' means and medians are denoted by solid and dashed lines, respectively.

DATA	WSA_{all}				$WSA_{largest}$				Dipole model			
Spacing	18	36	72	108	18	36	72	108	18	36	72	108
Mean	2.5	4.9			3.0	5.3	10.4	7.4	2.7	5.9		
Median	2.3	3.4			3.1	5.3	6.1	7.0	2.2	4.7		
Std. Dev.	1.3	3.8			1.3	2.8	10.7	4.2	1.5	3.6		
MODEL	WSA_{all}				$WSA_{largest}$				Dipole model			
Spacing	18	36	72	108	18	36	72	108	18	36	72	108
Mean	2.1	4.6			2.2	4.8	11.1	6.8	0.8	4.4		
Median	1.8	3.4			2.4	4.9	6.0	6.3	0.1	3.6		
Std. Dev.	1.5	3.9			1.5	2.6	12.4	3.6	1.2	3.2		

Table 2.1: SUMMARY OF THE EXPERIMENTAL AND MODEL UNCERTAINCIES OCCURRING IN POSITION ESTIMATION SHOWN IN FIG. 2.11. All values are given in cm. WSA: weighted spatial average. SD: standard deviation.

The numbers and arrangements of the locations that could be sampled for each spacing and method varied greatly and the results must be generalized with care. We therefore tested, if the measurement-based evaluations could be replaced by simulations to allow for a more comprehensive evaluation of fish localization. For the model, we used the parameters extracted in Section 2.6. The error distributions resulting from the simulations (Fig. 2.11 B, Table 2.1 B) matched closely those derived from the measurement-based evaluation. The main differences were the slightly smaller errors extracted from the simulations, an effect that might be attributed to the fact that the simulations were free of any noise. This difference is particularly strong for the dipole fit and could suggest that the dipole model fit is more susceptible to noise than the WSA. In summary, these results demonstrate that simulations based on the dipole model are suited to generate feasible datasets for further evaluations of position estimation.

Simulation-based evaluation of localization methods

To study the performance of the three proposed localization methods under ideal conditions, we simulated large electrode arrays (40×40) with spacings of $15-90$ cm and sampled many fish locations and orientations at the array's center quadrant (20×20 steps xy-resolution; 3 elevations; orientations between $0-180°$ with $4.5°$ resolution; 16400 samples/spacing, total). This configuration allowed for neglecting effects caused by the limits of the electrode array. Data were simulated with a dipole model using parameters extracted for *A. albifrons* and a power law with exponent -1.64 (see Section 2.6).

The means and medians of the WSA_{all} and the dipole model fit for all spacings and elevations were smaller than 6 cm with standard deviations smaller than 4 cm and generally increased with the size of the spacing (Fig. 2.12 A, Table 2.2). In comparison, the localization errors obtained for the $WSA_{largest}$ were greater, ranging from 2.1 cm for a spacing of 15 cm to 14.8 cm for a spacing of 90 cm, showing an almost linear dependence between mean error and the size of the spacing.

Do the three localization methods have inherent biases? To answer this question, we computed the estimates' locations relative to the surrounding electrode locations using the samples for a spacing of 30 cm and $z = 0$ cm only. The relative locations were transformed into a density distribution by convolution with a two-dimensional Gaussian kernel ($\sigma = 0.05$ cm for both dimensions) and were plotted as a heat map (Fig. 2.12 B). Because the true positions of the simulated fish were uniformly distributed, a position estimator without a systematic bias should also extract uniformly distributed estimates. The WSA_{all} and the dipole model fit yield almost uniform distributions of estimates. However, the $WSA_{largest}$ yields

WSA_{all}	$z = 0$ cm				$z = 15$ cm				$z = 30$ cm			
Spacing	15	30	60	90	15	30	60	90	15	30	60	90
Mean	3.1	1.0	2.9	5.6	3.2	1.0	2.9	5.7	3.3	1.1	3.1	5.8
Median	3.0	1.0	2.6	5.2	3.1	1.0	2.7	5.3	3.2	1.0	2.8	5.4
SD	1.5	0.5	1.7	3.0	1.5	0.5	1.7	3.1	1.6	0.6	1.7	3.2
$WSA_{largest}$	$z = 0$ cm				$z = 15$ cm				$z = 30$ cm			
Spacing	15	30	60	90	15	30	60	90	15	30	60	90
Mean	2.1	4.2	8.3	12.4	3.1	5.2	9.4	13.4	4.0	6.1	10.5	14.8
Median	1.9	3.8	7.7	11.5	2.7	4.7	8.9	12.5	2.8	5.4	9.5	13.8
SD	1.2	2.4	4.8	7.2	1.9	3.0	5.1	7.3	3.8	3.9	6.1	8.2
DIPOLE	$z = 0$ cm				$z = 15$ cm				$z = 30$ cm			
Spacing	15	30	60	90	15	30	60	90	15	30	60	90
Mean	1.8	1.6	2.8	4.9	1.6	0.5	1.8	3.9	1.9	0.6	1.7	3.5
Median	1.6	1.1	2.4	4.6	1.5	0.5	1.7	3.7	1.8	0.5	1.6	3.3
SD	1.4	1.3	1.7	2.6	0.8	0.3	1.0	2.1	0.9	0.3	1.0	1.9

Table 2.2: SUMMARY OF THE ERRORS OCCURRING IN POSITION ESTIMATION SHOWN IN FIG. 2.12. All values are given in cm. WSA: weighted spatial average. SD: standard deviation

a distinct non-uniform distribution with estimates clustered in a regular pattern, and thereby displays an inherent estimation bias.

As a byproduct we gain information on how many electrodes with EOD amplitudes above a given value we can expect when using different spacings (Table 2.3). This information should become valuable in the future when planning new electrode array configurations. These results should be considered an ideal case, because only samples vertically on level with the electrode array have been included and the dipole moment was oriented exclusively in parallel to the plane of the electrode array.

To understand which method is suited most for the analysis of field data, we performed simulations using a realistic configuration of electrodes as it was used during a field recording in Panamá (10×6 electrodes, Fig. 3.1). In the field, we used a fixed spacing of 30 cm, however, here we simulated a range of spacings between 15 – 90 cm and sampled the full area of the electrode array (20 steps per spacing, 3 elevations; orientations between 0 – 180° with 4.5° resolution; 749 521 samples/spacing, total).

Compared to the large-array setting, the errors from by the WSA_{all} (mean error > 20 cm) and the dipole model fit (mean error > 30 cm, with two exceptions) increased strongly, while the errors of the $WSA_{largest}$ remained almost the same (Fig. 2.13, Table 2.4). Consequently, the $WSA_{largest}$ performed at least $2.7\times$ better than the other methods. The enlarged errors were a consequence of the fact that the full area of the array was sampled, including locations close to the array's borders. The WSA_{all} has an inherent bias towards the center of the electrode array, where the spatial average of all electrodes is located. Therefore, the WSA_{all} results in larger errors towards the borders of the electrode array. The worsening of the performance of the dipole model is likely related to the enlarged errors of the WSA_{all}. Because the dipole model fit uses the results of the WSA_{all} as initial values, its performance is directly influenced by the increased errors resulting from the WSA_{all}.

In conclusion, the $WSA_{largest}$ is the most robust solution at hand and is therefore used for the analysis of

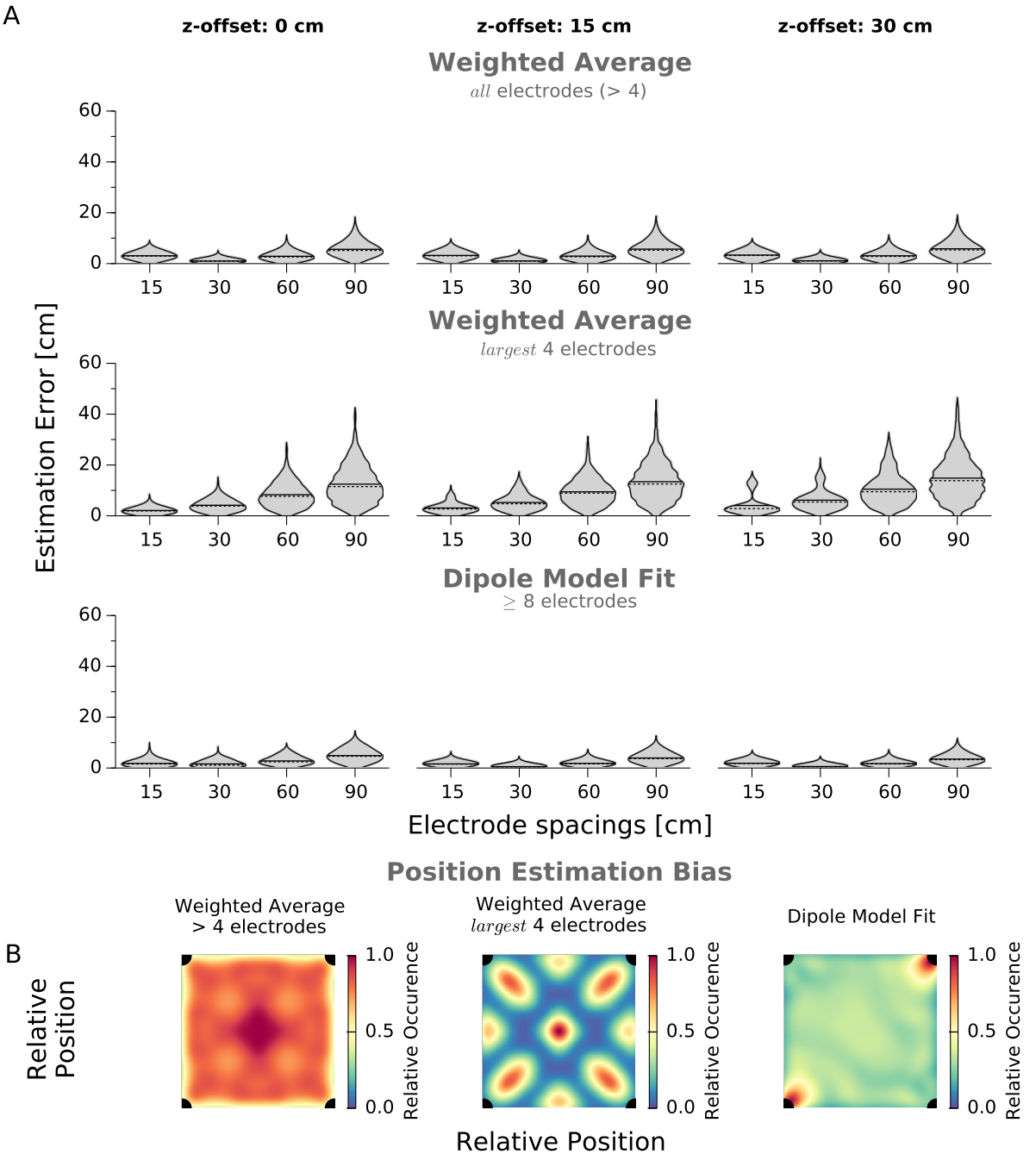

Figure 2.12: SIMULATION-BASED EVALUATION OF METHODS FOR POSITION ESTIMATION. **A**) We systematically tested the performance of three methods for position estimation (see text) for four different electrode spacings (15 – 90 cm) and for fish positioned at three different vertical elevations (0, +15, +30 cm) relative to the electrode array. To eliminate border effects, we simulated a large electrode array (40 × 40 electrodes) and only evaluated positions (n = 400) and orientations (0 – 180°, n = 40) within the central quadrant. To increase the practical relevance of the results, we used model parameters derived from the model fit shown in Fig. 2.16 E and excluded EOD amplitudes below 1 µV, the amplitude level at which interferences caused by naturally occurring electrical noise become noticeable under field conditions. Results are shown as density distributions and were calculated using a Gaussian kernel with $\sigma = 1.0$ cm. Solid line: mean, dashed line: median. **B**) To analyze inherent biases of the estimation methods, we calculated for each estimate its position relative to the surrounding electrodes and calculated the density distribution of the results using a Gaussian kernel with $\sigma = 0.05$ for both dimensions. All samples were computed vertically on level with the array (z = 0) and for a spacing of 30 cm.

Spacing [cm]	15	30	60	90
$A_i > 1$ mV	0.5 ± 0.5	0.1 ± 0.3	0 ± 0.2	0 ± 0.1
$A_i > 0.5$ mV	1.3 ± 0.6	0.3 ± 0.5	0 ± 0.3	0 ± 0.2
$A_i > 0.2$ mV	3.8 ± 0.9	1.0 ± 0.6	0.2 ± 0.4	0.1 ± 0.3
$A_i > 0.1$ mV	9.0 ± 0.9	2.2 ± 0.6	0.6 ± 0.5	0.2 ± 0.4
$A_i > 50$ µV	20.9 ± 1.3	5.2 ± 0.9	1.3 ± 0.6	0.6 ± 0.5
$A_i > 10$ µV	150.1 ± 2.1	37.5 ± 1.4	9.4 ± 1.0	4.2 ± 0.9
$A_i > 1$ µV	1333.0 ± 47.2	628.7 ± 3.2	157.2 ± 2.1	69.8 ± 1.7

Table 2.3: DATA AVAILABILITY. How many electrodes with large EOD amplitudes can we expect for a given electrode spacing? Each row shows the number of electrodes that measured amplitudes larger than a given value (left column) for electrode spacings between 15 – 90 cm. The numbers are extracted from simulations of a large array (40×40, see Fig. 2.12) using realistic values for the dipole moment of *A. albifrons* and each value is computed from 16359 samples. All values are given as mean ± std. dev.

field data.

Detection of moving fish

We tested the performance of the complete analysis chain with simulations of moving fish ($v = 10$ cm/s) generated with a horizontally oriented dipole model using parameters extracted from EOD measurements (Fig. 2.16). Electrodes were configured in a large array with 10×10 electrodes with a spacing of 30 cm, i.e. with the same spacing as used in our field studies. Data were generated for a sample rate of 20 kHz and for each sample we calculated the EOD's potential on each electrode and multiplied it with the current value of the EOD. For movement, we simulated a full circumference of a circular trajectory (103.3 cm radius), always with the circle positioned off-center in relation to the electrode array's grid in order to sample many different fish-to-electrode configurations. The trajectories were both on and above the vertical level of the electrode array (0 – 30 cm) and some were partially proceeding outside of the array's borders. Data were analyzed with the same analysis chain as applied to field data (see sections 2.3 and 2.5) and the locations and orientations of fish were estimated using the $\mathrm{WSA}_{largest}$ as described above. In order to obtain results that can be compared plausibly to results obtained from field data, minute EOD amplitudes below 1 µV were excluded. Representative examples are shown in Fig. 2.14. The mean errors and the modes of the error distributions for the localization of fish for all examples were clearly below 10 cm, which is a common length of a small-sized, mature *A. leptorhynchus* (Dunlap, 2002; Triefenbach and Zakon, 2003). Likewise, the errors for orientation estimation were small and the mean orientation error and the mode of the error distribution were clearly below 15°. The simulations demonstrated that our analysis is able to track fish moving outside the electrode array's borders and to correctly determine this fact by placing the location estimate at the borders of the array. For elevated trajectories the mean error and its spread of the localization error increased, while the orientation error remains almost unchanged. Because of the jitter present in fish localization, smoothing of the location trace using a running average (200 ms window width) further reduces the localization error.

Fig. 2.15 shows field data examples of fish, which were tracked while traversing the electrode array at night. Fish of three species were selected and demonstrate that spatial tracking with a high temporal resolution is possible independent of the fish's EOD*f*. While it is not possible to verify the validity of the shown trajectories by means of synchronously recorded videos, the overall movement patterns appear plausible in comparison to the simulations shown in Fig 2.14.

2.6 Spatial amplitude distribution of the EOD's electric field

Detailed knowledge of the spatial amplitude distribution of the EOD's electric field under realistic conditions is crucial both for the parametrization of the dipole model for simulations and for defining a feasible configuration of the electrodes of the array. We therefore extended the study of Knudsen (1975) and measured the electric field's amplitude distribution over larger distances. Non-conducting tank walls

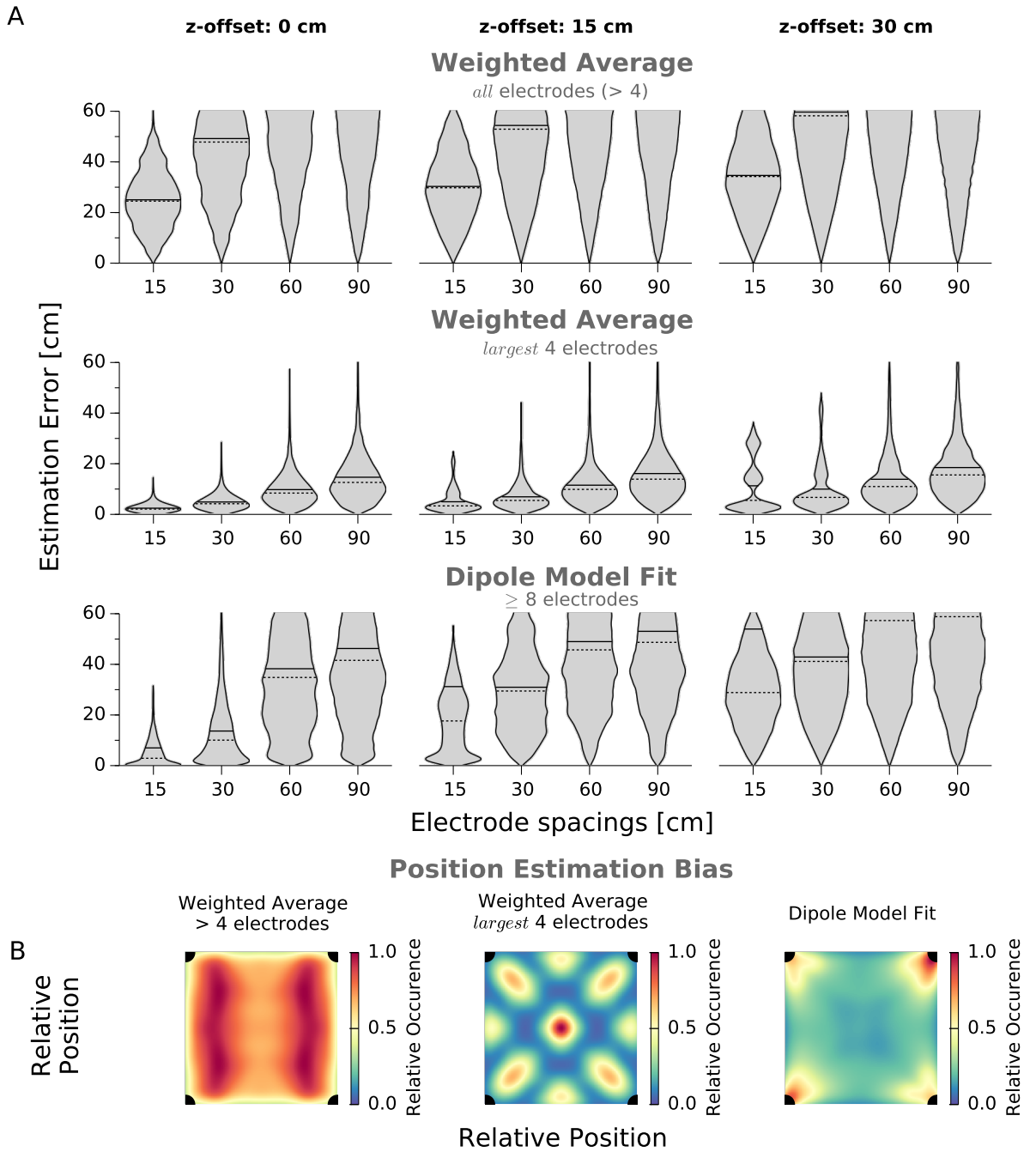

Figure 2.13: SIMULATION-BASED EVALUATION OF METHODS FOR POSITION ESTIMATION FOR A REALISTIC ELECTRODE CONFIGURATION. **A**) We repeated the evaluation shown in Fig. 2.12 for an electrode configuration used in the field (6×10) and for the whole area of the electrode array in order to expose possible border effects. Solid line: mean, dashed line: median. **B**) To analyze inherent biases of the estimation methods, we calculated for each estimate its position relative to the surrounding electrodes and calculated the density distribution of the results using a Gaussian kernel with $\sigma = 0.05$ for both dimensions.

WSA_{all}	$z = 0$ cm				$z = 15$ cm				$z = 30$ cm			
Spacing	15	30	60	90	15	30	60	90	15	30	60	90
Mean	25.0	49.2	87.7	96.9	30.3	54.4	92.1	N/A	34.6	59.7	97.3	N/A
Median	24.5	47.8	83.8	93.6	29.8	52.9	88.4	97.5	34.2	58.2	93.6	N/A
SD	11.2	22.5	42.1	45.4	13.4	24.7	43.8	46.7	14.9	26.8	46.2	48.8
$WSA_{largest}$	$z = 0$ cm				$z = 15$ cm				$z = 30$ cm			
Spacing	15	30	60	90	15	30	60	90	15	30	60	90
Mean	2.4	4.9	9.8	14.7	5.0	6.9	11.5	16.1	11.3	10.0	13.9	18.5
Median	2.1	4.2	8.4	12.6	3.4	5.5	9.9	13.9	5.5	6.7	11.0	15.6
SD	1.7	3.5	7.0	10.5	4.5	5.5	8.3	11.4	10.2	9.1	11.1	13.7
DIPOLE	$z = 0$ cm				$z = 15$ cm				$z = 30$ cm			
Spacing	15	30	60	90	15	30	60	90	15	30	60	90
Mean	7.0	13.7	38.3	46.3	31.2	31.0	49.0	53.0	53.9	42.9	60.8	63.2
Median	2.9	10.1	34.8	41.6	17.6	29.5	45.7	48.7	28.8	41.2	57.3	58.8
SD	N/A	25.4	24.5	28.5	N/A	17.3	26.0	29.1	N/A	21.3	31.6	33.6

Table 2.4: SUMMARY OF THE ERRORS OCCURRING IN POSITION ESTIMATION SHOWN IN FIG. 2.13. All values are given in cm. WSA: weighted spatial average. SD: standard deviation. N/A: value ≥ 100 cm.

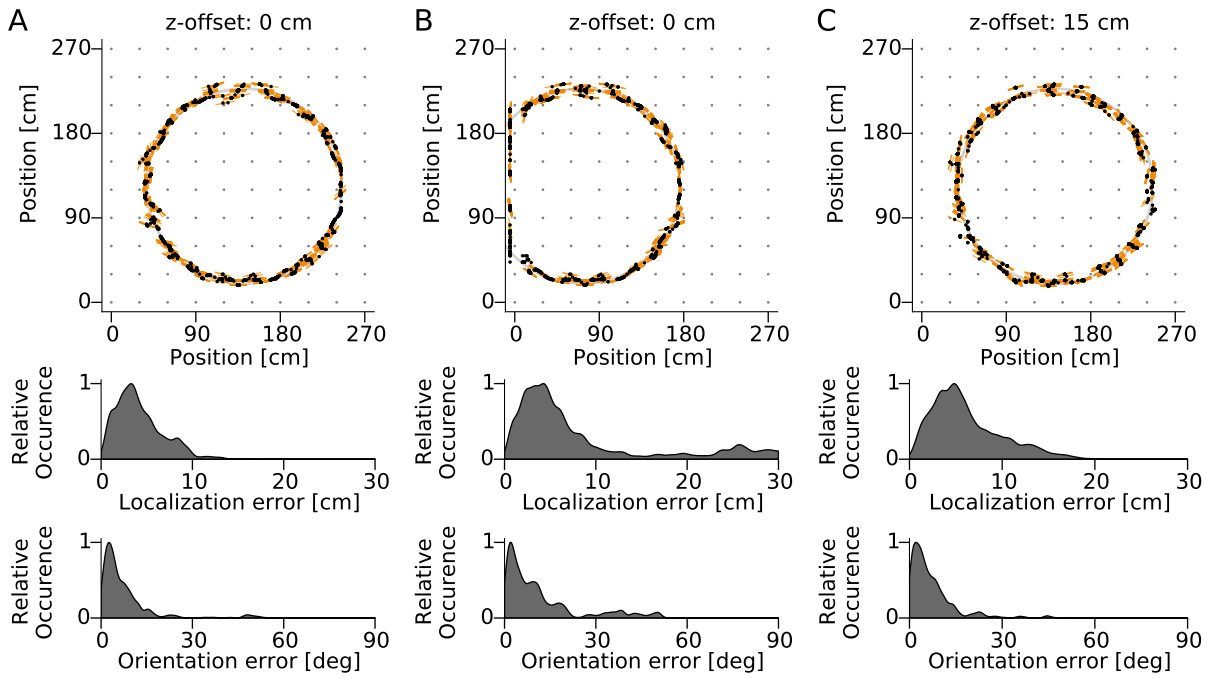

Figure 2.14: EVALUATION OF POSITION AND ORIENTATION ESTIMATES OF A SIMULATED MOVING FISH. We simulated the EOD of a fish moving ($v = 10$ cm/s) on a circle with tangential orientation under various conditions and treated the data with the standard EOD analysis chain as it is applied to recorded EOD voltage traces. Top: The estimated, non-smoothed 2D-locations (black dots) and orientations (orange lines) were then compared to the simulated fish locations (gray line) and orientations. Center and bottom: Error distributions of localization and orientation estimation. Estimation errors are expressed as means $\pm$ standard deviation. **A**) A moving fish vertically on level with the electrode array. Estimation errors for location are 4.2 ± 2.6 cm, and for orientation $7.2 \pm 7.2°$. **B**) A moving fish in level of the electrode array, but partially outside the recording array. Accurate location is lost when the fish leaves the electrode array, but is reestablished after reentry. Estimation errors for location are 8.6 ± 8.4 cm, and for orientation $11.4 \pm 12.4°$. Errors include the difference to the known fish location and orientation for the time period the fish moves outside the array. **C**) A moving fish 15 cm above the electrode array. The error of location estimation increases slightly, compared to A. Estimation errors for location are 6.2 ± 3.8 cm, and for orientation $6.9 \pm 7.3°$.

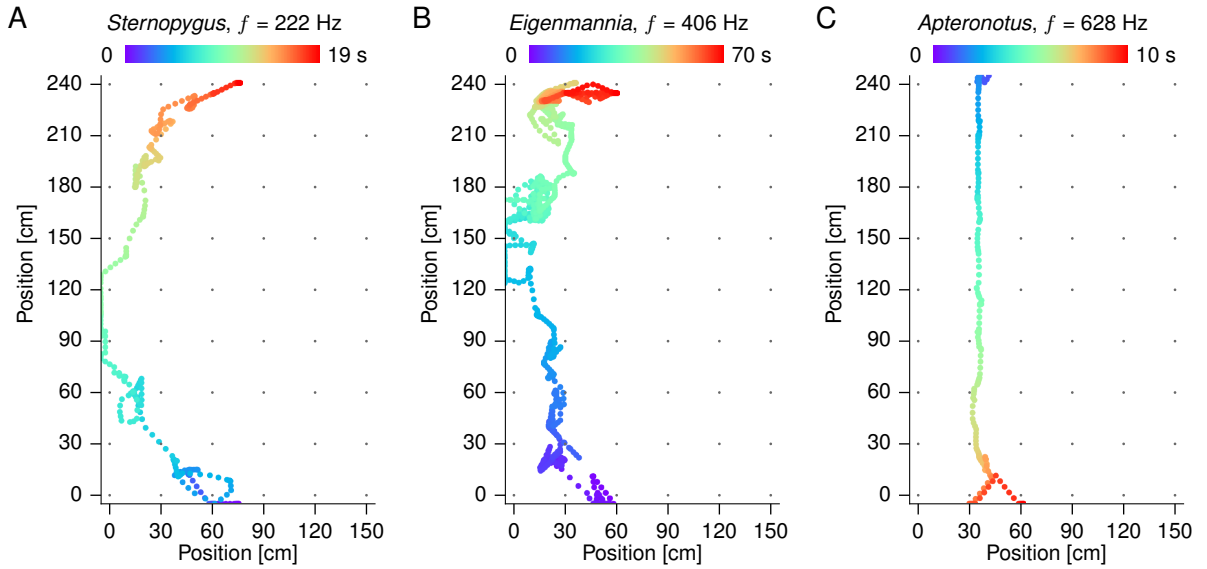

Figure 2.15: FIELD DATA EXAMPLES FOR LOCATION ESTIMATION PERFORMED ON MOVING FISH OF THREE SPECIES. Location traces have been smoothed with a running average filter (width=0.2 s). Some trajectories show jitter at entry and/or exit of the recording area. **A**) A *Sternopygus dariensis* female (recognizable by the relatively high EOD*f*) traversing the array upstream. **B**) An *Eigenmannia humboldtii* individual slowly moving upstream. **C**) An *Apteronotus rostratus* female rapidly traversing the array downstream in a straight line, possibly navigating along the electrode array's rigid frame (see Fig. 2.4 D).

and the water surface induce boundary effects in the electric field. In order to limit the influence of the boundary effects on our measurements, the measurements were performed at the center of a large outdoor tank ($3.5 \times 7.5 \times 1.5$ m, $w \times l \times h$).

First, to generate a preliminary dataset, water depth was adjusted to 60 cm and a 4×4 array of recording electrodes mounted on round PVC profiles (108×108 cm; 36 cm spacing; 3 cm diameter; Georg Fischer GmbH, Albershausen, Germany) was submerged in the central area of the tank at a depth of 30 cm. The water conductivity was 150 µS and temperature was adjusted to 23.5° C. A weakly electric fish (*A. albifrons*, 18 cm) was carefully placed in a fish holder made of fine nylon mesh, which was then fixed horizontally in a frame made of PVC (18×8 cm, inner dimensions). While the fish movement was restricted by the frame, care was taken to allow for sufficient room for gill movement. During the measurement the fish did not change posture. The fish holder was placed on a xy-slider made of PVC within the center of the electrode array. This setup allowed to adjust the fish to the same depths as the electrodes and to set the xy-position manually in reference to preset marks on the slider. In order to systematically measure the spatial distribution of the electric field, we kept the position of the electrodes constant and instead adjusted the fish's location. We sampled a grid with a total of 108 locations in 18×6 steps using a resolution of 2×4.5 cm.

For each measurement the electrode signals were amplified by the 16-channel amplifier described in Section 2.2, digitized at a sample rate of 10 kHz and EOD waveforms were recorded for two seconds. We tested various locations for the reference electrode and eventually placed it at the far end corner of the tank at a distance of 300 – 335 cm from the fish. For each channel, we calculated the FFT spectrum (16384 data points, i.e. a resolution of 0.3 Hz) and extracted the EOD amplitude by summing over the frequency range containing the spectral peak representing the fish's EODf (1005 – 1045 Hz), thereby carefully omitting the frequency peaks caused by the mains). The resulting distribution of EOD amplitudes (Fig. 2.16) had a distinct dipolar shape and was fitted with the regularized dipole model described in Section 2.5. The fit yielded the estimated location of the dipole's center ($x = 73.5$, $y = 67.1$ cm), the dipole moment's amplitude (29 mV m^2), and the distribution's power law (-1.63). The latter is clearly smaller than the exponent of -2 determined for an ideal dipole in three-dimensional free space. This may be attributed to near-field deviations from a dipole (Knudsen, 1975; Chen et al., 2005) and to boundary effects induced by the shallow water surface and the tank walls (Fotowat et al., 2013; Jun et al., 2013).

Estimation of electric field parameters

Tuberous electro-receptors, so-called P-units, distributed over the fish's skin encode amplitude modulations (AMs) of the fish's own EOD (Benda et al., 2006; Nelson et al., 1997; Walz et al., 2014). Superposition of a fish's EOD with that of a nearby fish results in a beat, a periodic amplitude modulation with frequency given by the difference between the two fish's EODfs. The amplitude of the beat AM equals the EOD amplitude of the nearby fish at the position of the receiving fish. Therefore, in order to estimate stimulus amplitudes occurring during electric fish interactions it is crucial to estimate the interacting fishes' EOD amplitudes. Measurements of the transdermal potentials occurring during dyadic interactions of *A. leptorhynchus* in shallow water showed that AMs drop below 20% at distances beyond 23 cm (Fotowat et al., 2013).

Here, we present a novel method for the estimation of a fish's EOD amplitude and the effective exponent of the power law governing the EOD's amplitude decrease over distance under natural conditions. These values can be used to estimate the largest possible AMs occurring in dyadic interactions of electric fish.

The method relates the measured EOD amplitudes to the distance between the estimated fish location and the recording electrodes. The basic assumption is that the EOD amplitude decreases over distance following a power law. The latter determines the largest possible EOD amplitude at a given distance, but only those electrodes in line with the electric fish's body axis will be exposed to the maximum EOD amplitudes. Because of the anisotropic, dipole-shaped electric field, smaller EOD amplitudes are always possible, even very close to the fish, and only a small fraction of electrodes will be exposed to maximum EOD amplitudes (Fig. 2.17 A)).

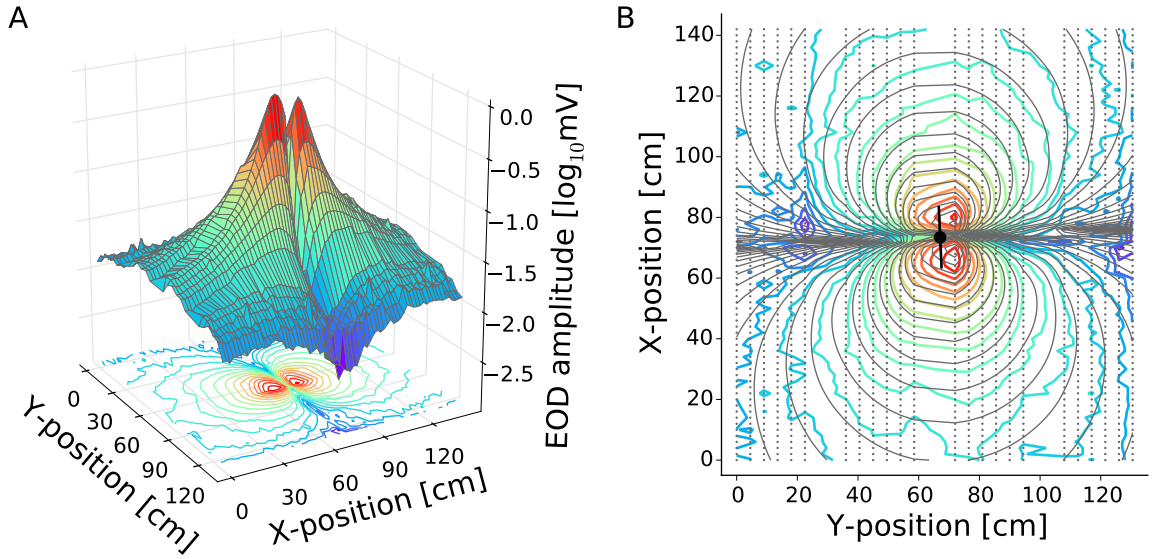

Figure 2.16: SPATIAL AMPLITUDE DISTRIBUTION OF THE EOD'S ELECTRIC FIELD POTENTIAL. **A**) Spatial distribution of an electric fish's EOD amplitude (absolute values), recorded at a depth of 30 cm (60 cm total) on level with the electric fish. By varying the position of the fish within the recording array, we obtained fine grained measurements of the EOD field amplitude with a resolution of $4.5x2$ cm and a total of 1728 data points. Warm colors indicate the highest and cold colors the lowest potential. **B**) A dipole model was used to fit the measurements and is able to reproduce orientation and and amplitude distribution of the electric fish's electric field well. Estimated position and orientation of the electric fish are shown in black. The estimate yielded a power law of -1.63 and an EOD amplitude of 29 mV m^2.

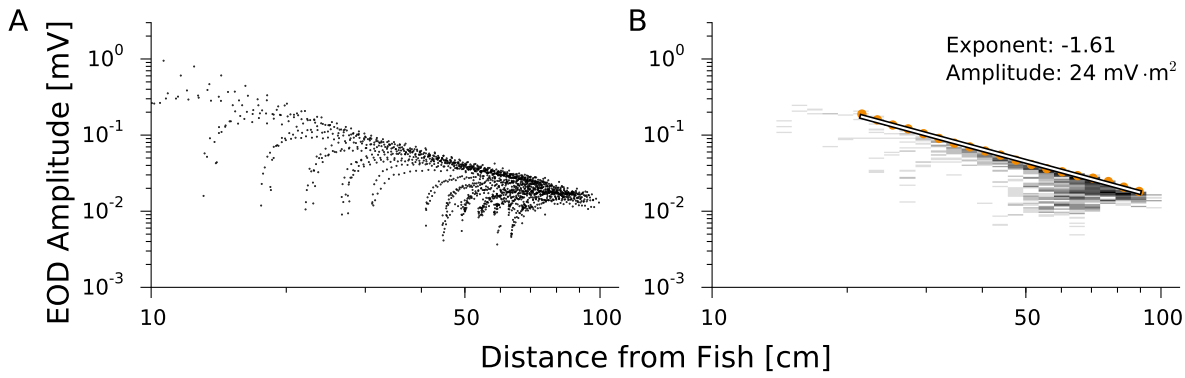

Figure 2.17: ESTIMATION OF EOD CHARACTERISTICS. **A**) Measurements of EOD amplitude against distance from the estimated fish position in a log-log representation, showing the same data as in Fig. 2.16. Generally, the maximum EOD amplitude decreases over distance with a power law exponent of -1.61, a similar value as extracted in Fig 2.16. Because of the anisotropic shape of the dipole's electric field, lower EOD amplitude measurements are always possible, even at very small distances. **B**) Estimation of the electric field's characteristics from the measurements. Two-dimensional histogram of the data shown in A. The intensity of the shading codes for the number of data points present in each bin (light to dark). For each distance-bin the largest 20% of EOD amplitudes are extracted, averaged (orange markers), and fitted with a power law function. This process directly yields the amplitude of the electric field and the exponent of the power law of the EOD's amplitude decay over distance.

The parameters governing the electric field's spatial distribution can be estimated from the EOD's maximum amplitudes at a given distance. To extract the maximum amplitudes, data were binned logarithmically over distance and for each bin the 20% largest amplitudes were extracted, averaged, and fitted with a power law function. Because of the two dimensional arrangement of the electrodes, the available data increases with r^2, such that more data is available for large than for small distances. Also, because of the non-linear amplitude decrease over distance, the inaccuracy of location estimation is particularly noticeable at small distances. We therefore limit the fit to the distance range $> 20\,\mathrm{cm}$.

The example shown in Fig. 2.17 B demonstrates that the fraction representing the maximum intensities is reliably extracted and the fit yields values similar to those estimated with the ideal dipole model (Fig. 2.16). However, because the largest amplitudes are extracted as a substantial fraction of the data in each bin, 20%, the method has an implicit bias to underestimate the EOD amplitude in comparison to the dipole model fit. As to environmental conditions, water conductivity influences the effective EOD amplitude, but not the exponent of the power law governing the decrease of EOD amplitude over distance.

We tested this method on data from simulations of moving fish (see Section 2.5). For fish moving on the same vertical level as the electrode array, both power law exponent and EOD amplitudes are extracted accurately (Fig. 2.18 A – D), even if the fish was moving partially outside the array. In contrast, for fish moving vertically elevated (E – H), the proposed method profoundly underestimates both exponent and EOD amplitude. The cause of this effect can easily be determined from the amplitude distributions over distance (Fig. 2.18 E, G). For small distances, the largest amplitudes of elevated fish saturate on a low level and deviate greatly from those of fish on level with the electrodes. The distribution of the largest amplitudes could not be reproduced well by a simple power law function. This effect could be compensated by fitting the amplitude distribution over larger distances only. In case of the fish moving 15 cm above the electrode array, a fit to distances $> 50\,\mathrm{cm}$ yielded the exponent -1.62 and an EOD amplitude of $28\,\mathrm{mV\,m^2}$, values that are close to the parameters used in the dipole model.

2.7 Discussion

We presented a comprehensive set of tools allowing for the tracking of movement and communication of multiple individual wave-type electric fish. The multi-channel electrode and amplifier system we developed permits the recording of the EODs of spatially distributed electric fish. Our system is highly portable and was successfully deployed in Peru and Panamá (see Chapter 3) to record many different species of electric fish in their natural habitats. The analysis presented here reliably detects EODs independently of the EOD waveform and based only on the EOD's spectral structure. Fish are tracked continuously by following their individual-specific EOD*f*. The spatial amplitude distribution of the EOD then allows to estimate the location of tracked fish and enables us to analyze the relative positions and interactions of multiple fish. Electro-communication signals embedded in the EOD are extracted using spectral analysis and are linked to the time and location of their generation.

Two aspects of the method presented hold particular promise for future studies. First, our method enables us to acquire data on the behavior of unrestrained fish in their natural habitat in unprecedented detail, thereby providing knowledge of naturally occurring signals and their context, i.e. the nature of relevant interactions between electric fish, intra- and interspecifically. Embedded in the fish's natural behavior are the sensory scene analysis problems, which the animals face and solve in a natural environment (Lewicki et al., 2014), e.g., the detection of communication signals on various signal backgrounds. Learning about the extent to which the fish are able to successfully perform scene analysis will shed light on the underlying computations and, eventually, the involved neural structures. This will prove valuable for physiological studies researching the processing of information between sensation and behavior (i) as guidance and inspiration for new research questions and designs and (ii) by providing a repertoire of the parameters of natural signals and their contexts.

Second, automated analysis enables us to analyze much larger amounts of data on electric fish behavior than ever before, allowing for a high throughput and more complete statistical descriptions of

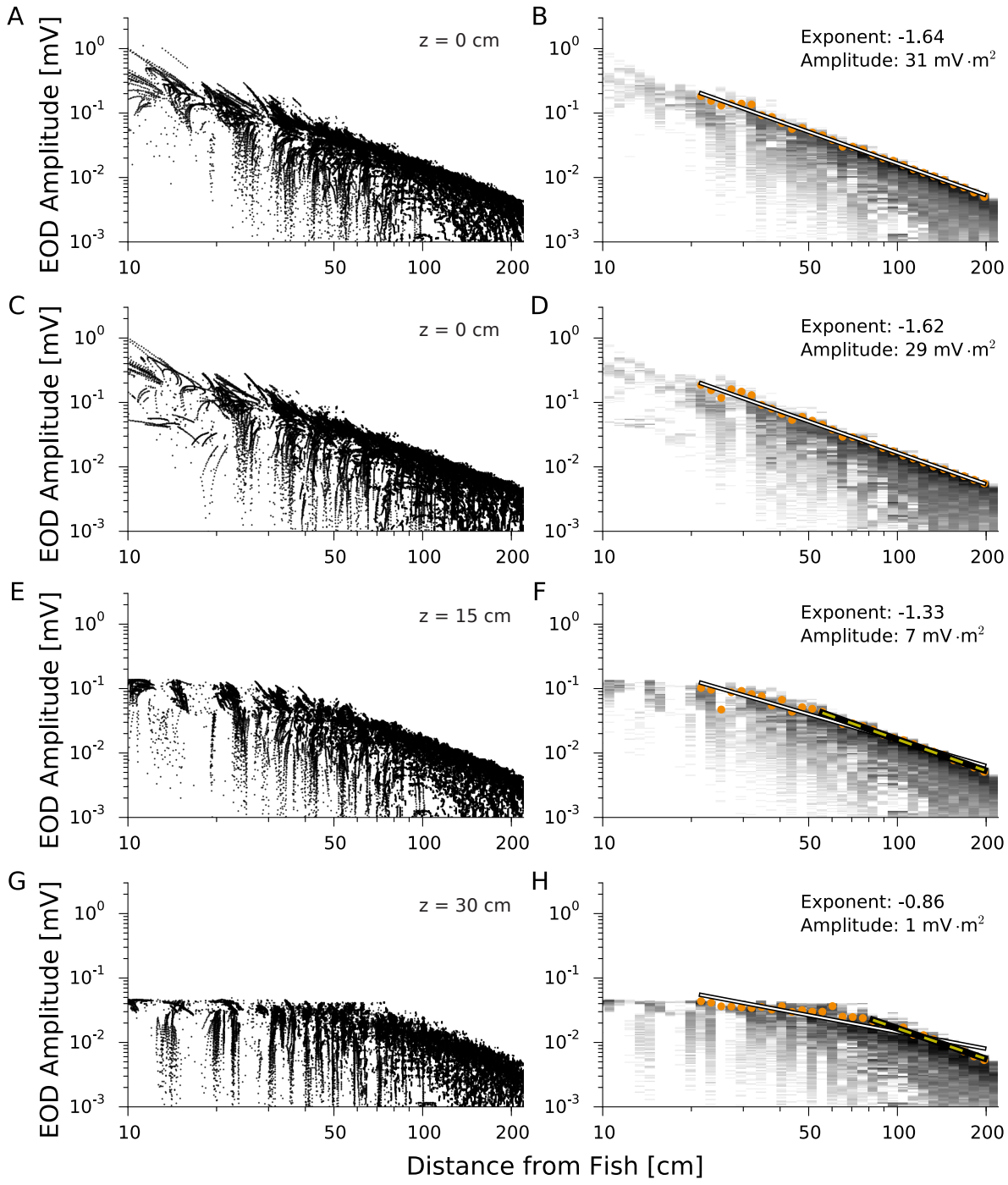

Figure 2.18: EOD AMPLITUDE ESTIMATION ON MOVING FISH. We evaluated the applicability of the EOD amplitude estimation using the simulations of moving fish shown in 2.14. We show EOD amplitudes (left column) versus estimated distance from fish and the respective power law fits (right column) over various conditions. **A, B**) Data and fit from a fish moving vertically on level with and within the area of the electrode array (2.14 A). **C, D**) Data and fit from a fish moving vertically on level with, but partially outside the electrode array (2.14 B). **E, F**) Data and fit from a fish moving 15 cm above and with the area of the electrode array (2.14 C). The estimation restricted to larger distances yields a power law of -1.62 and an amplitude of 28 mV m^2. **G, H**) Data and fit from a fish moving 30 cm above and with the area of the electrode array. The estimation restricted to larger distances yields a power law with exponent -1.58 and an amplitude of 23 mV m^2.

behaviour and the associated sensory scenes. For field studies, our method offers the opportunity to acquire biologically relevant data of a statistical rigor similar to laboratory data. For the laboratory, automated processing allows for new experiment designs, e.g., long term playback experiments with multiple unrestrained fish. In Chapter 4, we present some of the opportunities our tracking system offers in a laboratory setting.

In the following, some technical aspects and suggestions for future improvements on hardware and software of the tracking system are discussed.

Hardware

We recorded large and irregular discharges resulting in broadband noise exclusively in the field (see Fig. 2.1 C, 3). It is possible that these discharges were caused by environmental factors, e.g., lightning (Hopkins, 1973), and thus were authentic signals recorded by the electrodes. However, we can not exclude yet that these discharges are a consequence of the high humidity and/or the design of the amplifier system. A new amplifier version should therefore be better protected against high humidity.

The cables of the electrodes proved to be too sensitive. Damage of the cables' isolation was frequent and could expose the shielding, which in the worst case caused channel crosstalk, since the shielding and the reference were connected. These damages were simple to repair, however, future versions should use a more robust cable.

One of the bigger drawbacks of the current system is the complex and time consuming handling of a large number of electrodes. A future system could improve handling by using electrodes arranged in a row using a fixed spacing on a single ribbon cable, thereby greatly reducing the number of cables and thus cable entanglement.

Software

The detection of electric fish based on harmonic groups proved highly effective and very robust to electrical noise as it tends to be present both in the field (large, irregular discharges) and in the lab (many devices act as strong and permanent noise sources, additionally to the ubiquitous main hum). Some noise sources can be excluded directly on the level of harmonic groups (e.g., mains hum), while others are identified as potential fish and have to be removed later based on higher-level criteria.

Of course, suggestions for further improvement of the analysis software exist, too. Chirps are generally detected well, but on weak signals too many chirps remain undetected. For future implementations the reliability of the chirp detection algorithm might be improved by two measures. (i) Up to now, chirps are detected as frequency modulations of the EOD's fundamental frequency. However, ideally chirps would be detected additionally on the EOD's harmonics. By only accepting events detected synchronously on the fundamental and the harmonic frequencies as valid chirps, we should be able to lower the detection thresholds without increasing the amount of false-positive detections. This enhancement would also allow for better distinguishing the chirps of fish with very similar EODfs, because the frequency difference between the EODfs increases with the order of the harmonics. (ii) The current approach to chirp detection is functional, but very costly in respect to computing power, because for each fish the EODs have to be separately bandpass-filtered and evaluated. A different approach could be based on temporally fine-grained spectrograms, e.g., with time shifts between analysis windows of only 2 ms (2.10 A). Although these spectrograms are costly to generate, they have to be generated only once for all electric fish present on the channel. Using the information on the fish's precise EODf, chirps would be then detected as described above in separate frequency bands. The next logical step would then be to extend chirp detection to allow for the automated extraction of chirp parameters, e.g., duration, amplitude modulation, and extend and maybe even time course of the frequency excursion.

For the spatial tracking of individual fish under ideal conditions, the WSA_{all} and the dipole model fit yield the best results (Fig. 2.12). However, for realistic configurations the $\mathrm{WSA}_{largest}$ appears to be the most robust solution to the localization problem (Fig. 2.13). This is particularly true for small electrode spacings, such as 30 cm, where the median error is below 6 cm and thereby clearly smaller than an adult

fish's length. The localization yielded by the $WSA_{largest}$ is strongly biased (Fig. 2.12 B and Fig. 2.13 B), but the bias and the errors can reliably be reduced by smoothing of the resulting position traces using a running window of 200 ms width. Still, it might be worth to invest more time to improve the dipole model fit or to consider an implementation based on the fast look-up-table approach proposed by Jun et al., 2013, which might improve localization in three-dimensional space. In short, this approach is based on a list of normalized, pre-calculated values for the spatial EOD amplitude distribution for many fish positions and orientations. Fish position is estimated by computing the Euclidean distance between the normalized electrode measurements and all entries in the list, and then choosing the entry with the smallest distance. This process is computationally cheap and fast compared to optimization processes as the dipole model fit.

Finally, our method can be extended for the detection and tracking of pulse-type electric fish. The approach for detecting pulse-type fish proposed by Jun et al., 2013 can be combined with our tracking system, thereby extending our approach to South American and African mormyrid pulse-type fish.

In conclusion, in its current version the tracking system we presented here is highly effective for the automated tracking of many wave-type electric fish and their communication and promises fascinating insights into the private life of these previously almost 'invisible' fish.

CHAPTER 3

COMMUNICATION SCENES RECORDED IN NATURAL HABITATS CHALLENGE SENSORY PROCESSING

> *Neuroscience is part of biology, more specifically of zoology, and it suffers tunnel vision unless continuous with ethology, ecology, and evolution.*
>
> *From* Bullock, 1984

The quantification of behaviorally relevant natural stimuli provides a powerful tool to probe the function of complex sensory systems (Olshausen and Field, 1996; Lewicki et al., 2014). Weakly electric fish offer a unique opportunity for continuous monitoring of movements and communication signals in the natural habitat, which permits the reconstruction of natural social interactions and the associated sensory scenes. We developed a novel type of electrode array (Fig. 3.3 A) allowing, for the first time, to track movements and social interactions of multiple individual electric fish in their natural habitat continuously over extended periods of time without the need to implant transmitters. Our data provide unprecedented quantitative insight into courtship and electro-communication behavior and reveal tight constraints on sensory processing imposed by natural social interactions.

3.1 Methods

Field site

The field site is located in the Tuira River basin, Province of Darién, Republic of Panamá (Fig. 3.1 A), at Quebrada La Hoya, a narrow and slow-flowing creek supplying the *Chucunaque River*. Data was recorded about 2 km from the Emberá community of Peña Bijagual and about 5 km upstream of the stream's mouth (8° 15'13.50"N, 77° 42'49.40"W). The water of the creek is clear, but becomes turbid for several hours after heavy rainfall. The creek flows through a moist secondary tropical lowland forest, which, according to local residents, gets partially flooded on a regular basis during the wet season (May–November). The water levels of the creek range from 20–130 cm, but can rise temporarily to over 200 cm after heavy rainfall. At our recording site (Fig. 3.1 B), the water level ranged from 20–70 cm. The banks of the creek are typically steep and excavated, consisting mostly of root masses of large trees. The water temperature fluctuated between 25 and 27 ° C on a daily basis and water conductivity was stable at 150–160 μS cm^{-1}.

Field monitoring system

Our recording system (Fig. 3.3 A, Fig. 3.1 B) consists of a custom-built 64-channel electrode and amplifier system (npi electronics GmbH, Tamm, Germany) running on 12 V car batteries. Electrodes are

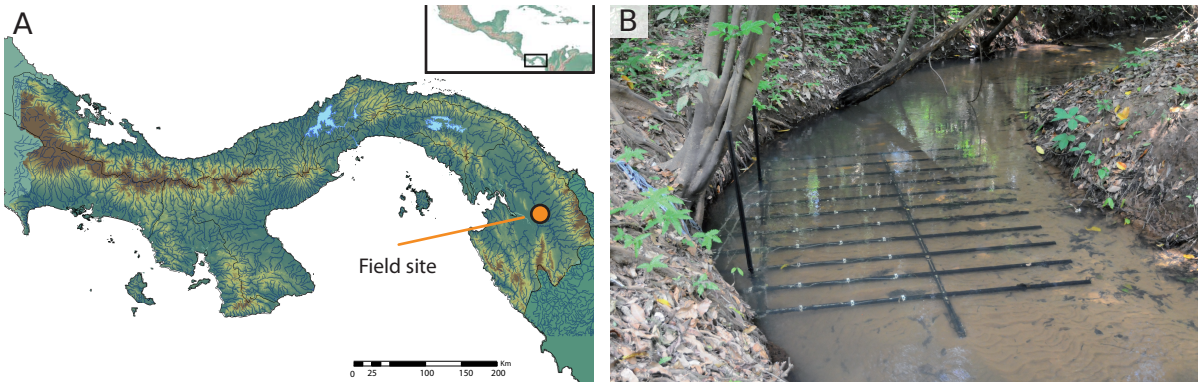

Figure 3.1: FIELD SITE AND POSITION OF ELECTRODE ARRAY. **A)** The field data were recorded in the Darién province in Eastern Panamá. **B)** The electrode array covered $2.4 \times 1.5\,m^2$ of our recording site in a small quebrada of the Chucunaque River system. Electrodes (on white electrode holders) were positioned partly beneath the excavated banks, allowing to record electric fish hiding deeply in the root masses.

low-noise headstages encased in epoxy resin ($1\times$ gain, $10 \times 5 \times 5$ mm). Signals detected by the headstages are fed into the main amplifier ($100\times$ gain, 1st order high-pass filter 100 Hz, low-pass 10 kHz) and digitized with 20 kHz per channel with 16-bit using a custom-built low-power-consumption computer with two digital-analog converter-cards (PCI-6259, National Instruments, Austin, Texas, USA). Recordings were controlled with custom software written in C++ that also saved data to hard disk for offline analysis (exceeding 400 GB of uncompressed data per day). Raw signals and power spectra were monitored online to ensure the quality of the recordings. We used a minimum of 54 electrodes, arranged in an 9×6 array covering an area of 240×150 cm (30 cm spacing). The electrodes were mounted on a rigid frame (thermoplast 4×4 cm profiles, 60 % polyamid, 40% fiberglass; Technoform Kunststoff-profile GmbH, Lohfelden, Germany), which was submerged into the stream and fixed in height 30 cm below the water surface. Care was taken to position part of the electrode array below the undercut banks of the stream in order to capture the EODs of fish hiding in the root masses. The recording area covered about half of the width of the stream and the hiding places of several electric fish. The maximum uninterrupted recording time was limited to 14 hours, determined by the capacity of the car batteries (2×70 Ah) and the power consumption of the computer (22 W) and amplifier system (25 W). Facilities for charging the batteries were a bottleneck (solar power and gasoline-powered generators), therefore we focused on nighttime recordings. Gymnotiform species feature a cyclic reproduction controlled by environmental factors. In the tropics these factors are related to the transition from dry to wet season and include an increase in water level and a decrease in water conductivity (Kirschbaum and Schugardt, 2002). We therefore recorded EODs during the transition from dry to wet season in February, March, and May 2012 and acquired a total of 162 hours of data.

Data analysis

All data analysis was performed in Python 2.7 (www.python.org). Summary data are expressed as means $\pm$ standard deviation, unless indicated otherwise. Our EOD tracking system is optimized for identifying and tracking individual wave-type electric fish, to estimate the fish's positions, and to detect communication signals. The signals of pulse-type electric fish are detected, but remain unprocessed for now.

Fish identification and tracking

First, information about electric fish presence, EOD frequency, and approximate position is extracted as described in Section 2.3. Slow EOD frequency modulations, so-called frequency rises (Zakon et al., 2002), are already detected at this stage, but we observed only a single rise emitted by a retreating intruder fish. Once the presence of an electric fish is established, the fish's position is estimated and chirps are detected as described in Sections 2.4 and 2.5.

Spectrograms and instantaneous frequencies

Spectrograms in Fig. 3.3 D and Fig. 3.6 B were calculated on data sampled at 20 kHz in windows of 4096 data points size, corresponding to 204.8 ms, applying a Blackman window function. Sequential windows were shifted by 50 data points (2.5 ms).

Instantaneous frequencies in Fig. 3.3 E were calculated on data of single electrodes. The recorded voltage trace was bandpass filtered (forward-backward Butterworth filter, 3rd order, 5× multi-pass, frequency bands at 500–900 Hz and 880–1200 Hz for the low-frequency and the high frequency fish, respectively) and the time of the EOD's zero-crossings was estimated by interpolating between the negative and positive data points closest to each zero-crossing. Instantaneous frequency was then computed as the inverse of the time interval between successive zero-crossings.

Chirp detection and analysis

Chirps were detected as described in Section 2.10. In short, for each fish the electrode voltage traces were bandpass-filtered (forward-backward Butterworth filter, 3rd order, 5× multi-pass, ±7 Hz width) at the fish's EODf as well as at 10 Hz above the EODf. For each passband the signal envelope was estimated using a root-mean-square filter over 10 EOD cycles and subsequent multiplication with $\sqrt{2}$. Rapid positive EOD frequency excursions cause the signal envelope at the fish's baseline frequency to drop and in the passband above the fish's EODf to increase in synchrony with the frequency excursion. If events were detected synchronously in both passbands on more than two electrodes, and exceeded a preset amplitude threshold, they were accepted as communication signals. All chirps in this study were verified visually using a custom-written software. E.g., over the course of approximately 25 hours with 23461 small chirps total, 387 false-positive chirps have been excluded. However, it is likely that some chirps were missed, since detection thresholds were set such that the number of false positives was very low.

Interchirp interval probability densities, auto correlation, and return maps were generated for pairs of fish and only for the time period in which both fish were producing chirps. Kernel density histograms of interchirp intervals (Fig. 3.5 A–D) were computed with a Gaussian kernel with a standard deviation of 20 ms.

Autocorrelograms of n chirp times t_i (Fig. 3.4 A–D) convolved with a Gaussian kernel $g(t)$ (σ=200 ms) were computed according to

$$r(\tau) = \frac{1}{n} \sum_{j=1}^{n} \sum_{i \neq j}^{n} g(\tau - (t_i - t_j)) \, .$$

This is the average chirp rate as a function of time τ relative to each chirp t_j. To estimate its confidence intervals, we repeatedly resampled the original dataset (1000 times bootstrapping, i.e. random sampling with replacement), calculated the autocorrelograms as described above and determined the 2.5 and 97.5 percentiles. To create the autocorrelograms of independent chirp intervals, we repeatedly (1000 times) shuffled the interchirp intervals, calculated the cumulative sum to create a new time series of chirps, calculated the autocorrelograms as described above and determined the mean and the 2.5 and 97.5 percentiles.

2D histograms of interchirp-interval return maps (Fig. 3.4 E–H) were generated with logarithmic hexagonal bins (function *hexbin* of the *matplotlib* library, www.matplotlib.org, v1.3.1).

For quantifying the echo response (Fig. 3.5 E–H) we computed the crosscorrelogram

$$r(\tau) = \frac{1}{n_a} \sum_{j=1}^{n_a} \sum_{i=1}^{n_b} g(\tau - (t_{b,i} - t_{a,j}))$$

with the n_a chirp times $t_{a,j}$ of fish a and the n_b chirp times $t_{b,i}$ of fish b. To estimate its confidence intervals, we repeatedly resampled the original dataset (2000 times jackknife bootstrapping; random sampling with replacement), calculated the crosscorrelogram as described above and determined the 2.5 and 97.5 percentiles. To create the crosscorrelograms of independent chirps, we repeatedly (2000 times)

calculated the crosscorrelograms on chirps jittered in time by adding a random number drawn from a Gaussian distribution with a standard deviation of 500 ms and determined the mean and the 2.5 and 97.5 percentiles.

Rates of small chirps before and after female long chirps (Fig. 3.6 A and Fig. 3.7) were calculated by convolving the chirp times with a Gaussian kernel ($\sigma = 0.5$ s) separately for each episode and subsequently calculating the means and standard deviations. The chirp times in Fig. 3.6 B depict chirp onsets.

Electric fields

The EOD amplitude of individual fish and its decrease over distance was estimated as described in Section 2.6. In short, histograms of envelope amplitudes from all electrodes of the array were computed as a function of the estimated distance between the electrodes and the fish (Fig. 3.8 A). For each distance bin at 20–100 cm the upper 95 percentile of the histogram was determined and a power law was fitted to these data points (orange line). This method of EOD amplitude estimation yields very reliable results for fish vertically close to the electrode array.

Gymnotiform electro-receptors measure the electric field (3.9 A), i.e. the first spatial derivative of the electric potentials shown in Fig. 3.8.

Electrophysiology

For *in vivo* recordings fish were anesthetized with MS-222 (120 mg/l; PharmaQ, Fordingbridge, UK; buffered to pH 7 with sodium bicarbonate) and a small part of the skin was removed to expose the posterior branch of the anterior lateral line nerve that contains only electro-receptor afferent fibers innervating electro-receptors on the fish's trunk (Maler et al., 1974). The margin of the wound was treated with the local anesthetic Lidocaine (2%; bela-pharm, Vechta, Germany). Then the fish were immobilized by intramuscular injection of Tubocurarine (Sigma-Aldrich, Steinheim, Germany; 25–50 µl of 5 mg/ml solution), placed in a tank, and respired by a constant flow of water through their mouth. The water in the experimental tank ($47 \times 42 \times 12$ cm) was from the fish's home tank with a conductivity of 300 S/cm and kept at 28 ° C. All experimental protocols were approved by the local district animal care committee and complied with federal and state laws of Germany (file no. ZP 1/13) and Canada.

Population activity in whole-nerve recordings was measured using a pair of hook electrodes of chlorided silver wire. Signals were differentially amplified (gain 10 000) and band-pass filtered (3 to 3 000 Hz passband, DPA2-FX; npi electronics), digitized (20 kHz sampling rate, 16-bit, NI PCI-6229; National Instruments), and recorded with RELACS (www.relacs.net) using *efield* and *efish* plugins. The strong EOD artifact in this kind of recording was eliminated before further analysis by applying a running average of the size of one EOD period (Benda et al., 2006). The resulting signal roughly followed the amplitude modulation of the EOD and we quantified its amplitude by taking its standard deviation. The nerve recordings closely resemble the properties of P-unit responses obtained from single-unit recordings (Benda et al., 2006; Walz et al., 2014). Note, however, that P-units might still respond in subtle ways to a stimulus even though the nerve recording is already down at baseline level, because of additional noise sources in this kind of recording.

Electric sine-wave stimuli with frequencies ranging from -460 to $+460$ Hz in steps of 2 Hz ($|\Delta f| \leq 20$ Hz), 10 Hz ($20 < |\Delta f| \leq 200$ Hz), and 20 Hz ($|\Delta f| > 200$ Hz) relative to the fish's EODf were applied through a pair of stimulation electrodes (carbon rods, 30 cm long, 8 mm diameter) placed on either side of the fish. Stimuli were computer-generated and passed to the stimulation electrodes after being attenuated to the right amplitude (0.05, 0.1, 0.2, 0.5, 1.0, 2.5, 5.0, 10.0, 20.0, 40.0 % of the fish's EOD amplitude estimated with a pair of electrodes separated 1 cm perpendicular to the side of the fish) and isolated from ground (Attenuator: ATN-01M; Isolator: ISO-02V; npi electronics). For more details, see Benda et al., 2006; Walz et al., 2014.

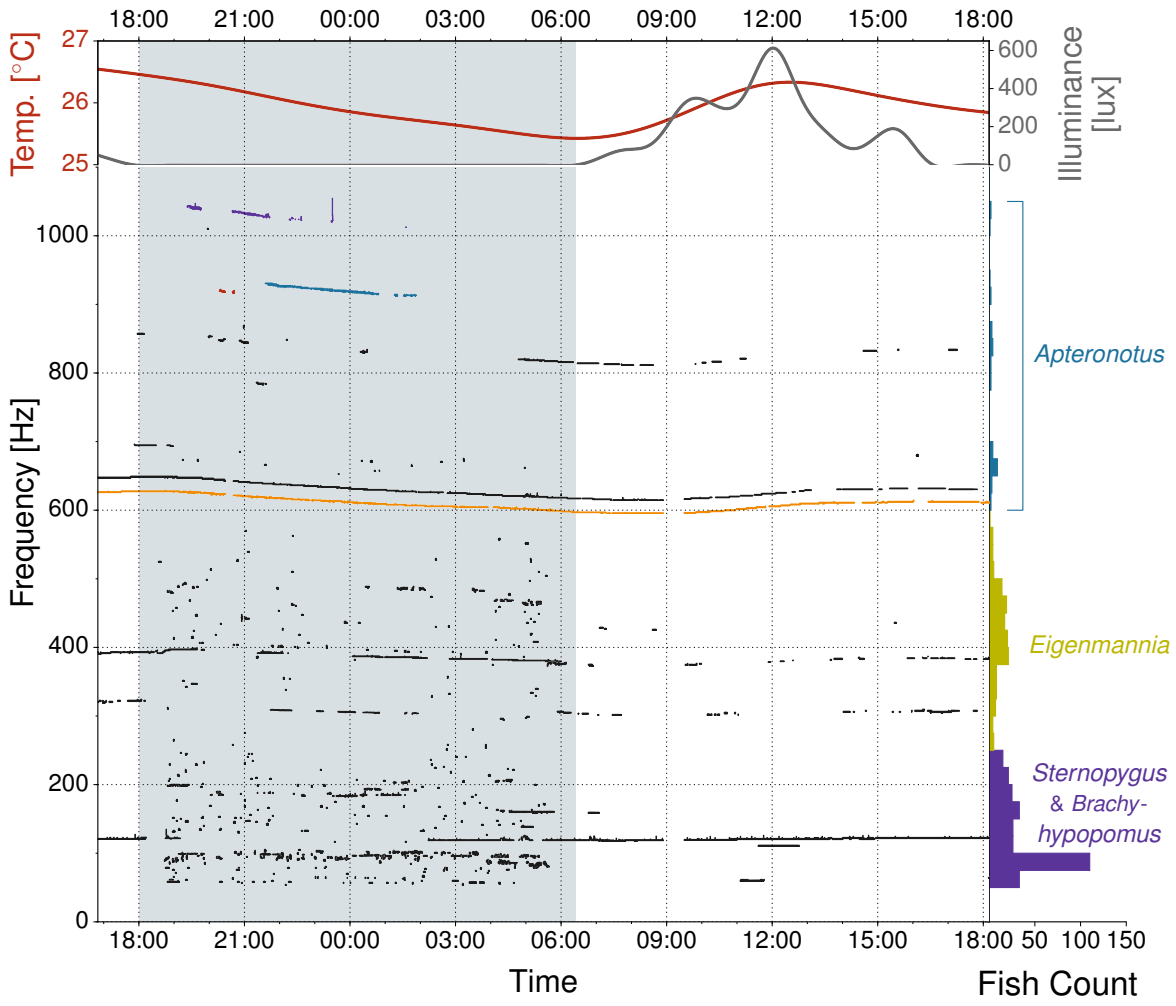

Figure 3.2: OVERVIEW OF WEAKLY ELECTRIC FISH TRACKED OVER 25 HOURS. **Top:** Water temperature drops at night and increases during the day (red line). The gray line indicates the time course of light levels. **Center:** Each dot and horizontal line represents the fundamental frequency of a single detected electric fish. Colored lines refer to the individuals shown in the same colors in all the other figures. The number of fish detections increased at night (gray band). **Right:** Histograms of EODfs allow to separate the wave-type fish *Eigenmannia humboldtii* and *Apteronotus rostratus* from *Sternopygus dariensis* and the pulse-type *Brachyhypopomus occidentalis*. The frequency ranges of *S. dariensis* and *E. humboltii* are likely to overlap partially. For a spectrogram of the raw data underlying this analysis, see Fig. 2.1 B.

Difference frequencies and spatial distances

The distance between two fish (Fig. 3.9 C) at the time of each chirp was determined from the estimated positions of the fish. Because position estimates were not always available for each time point, we allowed for a tolerance of maximally two seconds around the chirp for retrieving the position estimate. The positions were compiled into kernel density histograms that were normalized to their maximal value. The Gaussian kernel had a standard deviation of 1 cm for courtship small chirps, and 2 cm for courtship big chirps as well as intruder small chirps.

Males ($n = 8$) intruding on a courting dyad initially lingered at some distance from the dyad before either approaching the dyad further or being chased away by the courting resident male. Distances between the intruding male and the courting male during this assessment behavior (Fig. 3.9 D, top) were measured every 40 ms beginning with the appearance of the intruding fish until the eventual approach or attack. These distances, collected from a total assessment time of 923 s, were summarized in a kernel density histogram with Gaussian kernels with a standard deviation of 2 cm.

When a male intruded on a courting dyad it was directly approached by the resident male. In that

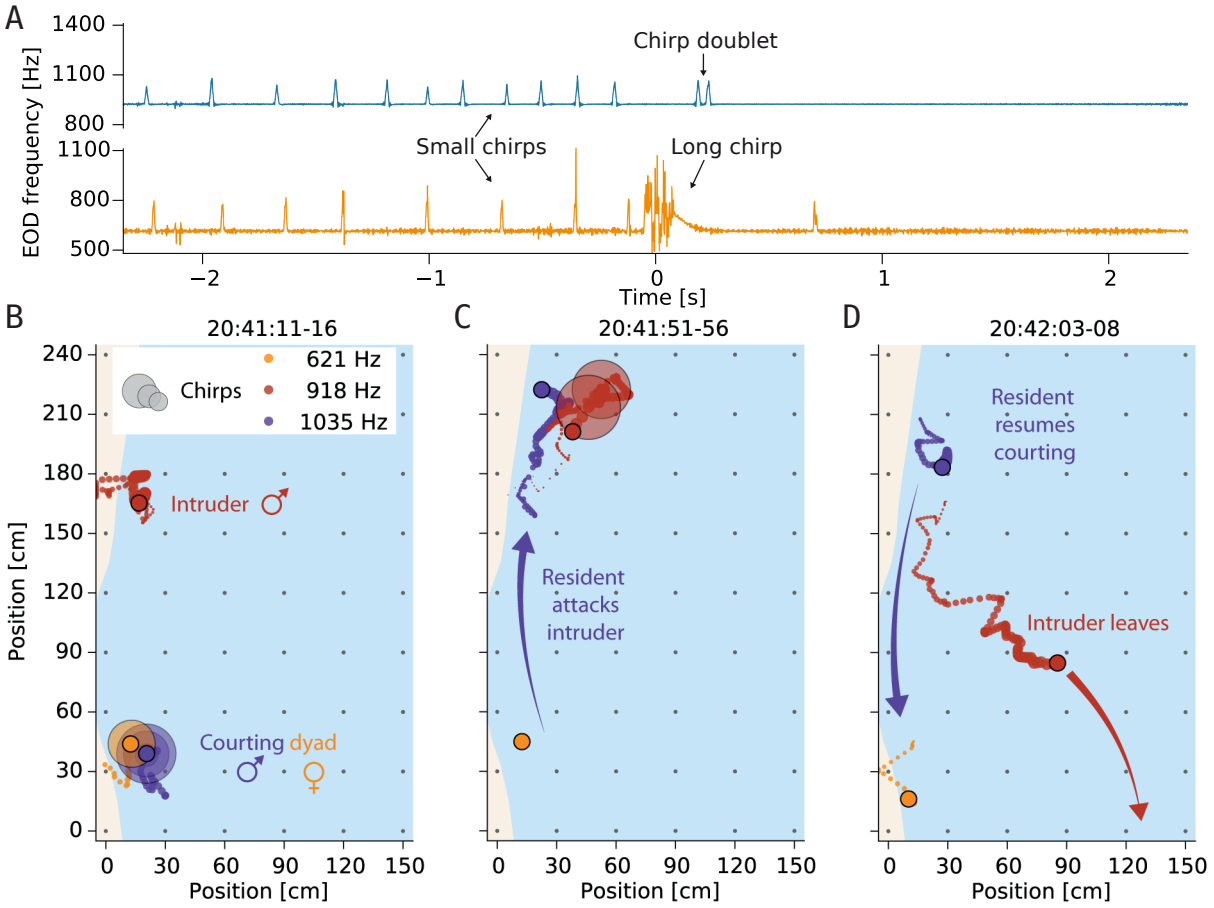

Figure 3.3: MONITORING ELECTRO-COMMUNICATION BEHAVIOR IN THE NATURAL HABITAT. **A)** Instantaneous frequencies of each fish. The two fish concurrently produce a series of small chirps before the female (orange) generates a long chirp and the male (blue) responds with a chirp-doublet. See S 1 for the corresponding audio trace. **B, C, D)** Interruption of courtship by an intruder. The current position of each fish is marked by the black circle and the tail indicates the positions of the last 5 s. Large transparent circles denote the location of emitted chirps. Gray dots indicate electrode positions. See movie S 3 for an animation. **B)** A courting female (orange) and male (purple) are engaged in intense chirp activity. An intruder male (red) lingers at a distance of about one meter. **C)** The courting male attacks the intruder (purple arrow) who emits a series of chirps and, **D)** leaves the recording area (red arrow). Colors label individual fish consistently throughout the manuscript.

process courtship was always interrupted and eventually one of the males withdrew. In some cases a few chirps were emitted by the retreating male. The winning male always (re-)approached and courted the female. The attack distances between two males (Fig. 3.9 D, bottom) were determined at the moment a resident male initiated its movement toward an intruding male. This moment was clearly identifiable as the onset of a linear movement of the resident male towards the intruder from plots showing the position of the fish as a function of time.

The distribution of EOD frequency differences of fish concurrently present in the recording area (Fig. 3.9 F) was calculated from all available recordings during the breeding season. The average frequency differences of each pair of fish simultaneously detected in the recordings were compiled into a kernel density histogram with a Gaussian kernel with a standard deviation of 10 Hz. Similarly, for courtship and agonistic interactions (Fig. 3.9 G,H) the mean frequency differences were extracted for the duration of these interactions.

3.2 Results

We recorded four species of weakly electric fish, the pulse-type fish *Brachyhypopomus occidentalis*, and the wave-type fish *Sternopygus dariensis, Eigenmannia humboldtii*, and *Apteronotus rostratus* (Fig. 3.2). During the day only a small number of fish hiding in the root masses were detected. At night many more

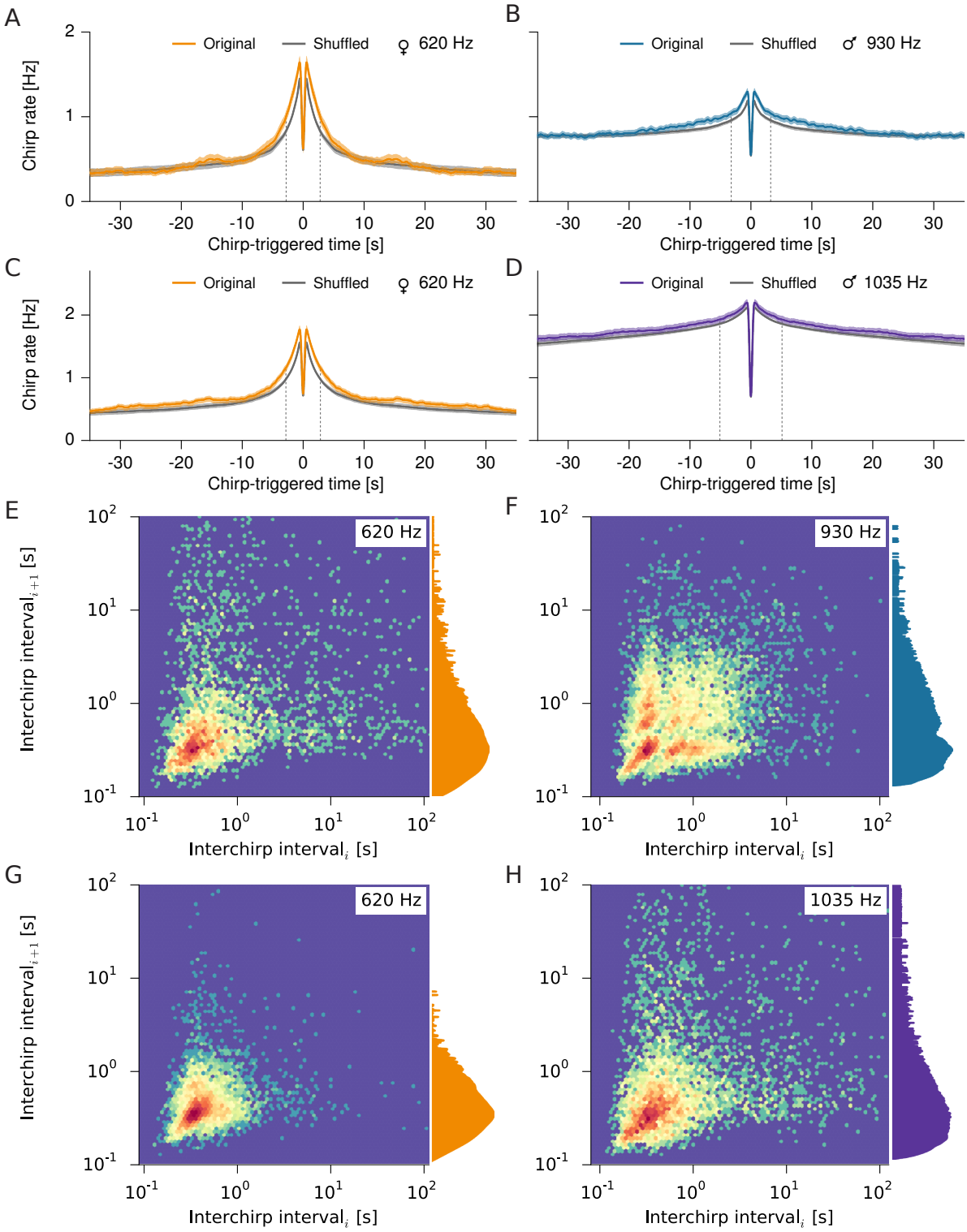

Figure 3.4: CORRELATION STRUCTURE OF SMALL CHIRP ACTIVITY FROM TWO COURTING DYADS (SAME FEMALE WITH TWO DIFFERENT MALES). Same layout and fish as in Fig. 3.5. **A–D)** Auto-correlograms of chirp timing show a single peak of 5.6 s (A, C, female), 6.5 s (B, first male), and 10.2 s (D, second male) width at half amplitude. The auto-correlograms obtained by shuffling interchirp interval sequences (gray) are slightly narrower in comparison to the original data. **E–H)** Return maps of interchirp intervals show a weak positive correlation between successive intervals for the female (E: $r = 0.04$, $p = 0.02$; G: $r = 0.12$, $p \ll 0.01$) and the males (F: $r = 0.14$, $p \ll 0.01$; H: $r = 0.06$, $p \ll 0.01$). Double-logarithmic interval distributions to the right emphasize the heavy tails of the distributions shown in Fig. 3.5 A–D.

fish were detected, demonstrating the nocturnal activity of these fish. Since EOD frequency changes with water temperature (Dunlap et al., 2000) EODfs of single fish vary considerably during the course of a day. Our data include interspecies interactions. However, we here focus exclusively on *A. rostratus*, a member of the *A. leptorhynchus* species group (brown ghost knifefish, de Santana and Vari, 2013) and its intra-species interactions.

The Neotropical gymnotiform fish *Apteronotus rostratus* generates a periodic, high-frequency (600–1200 Hz) electric organ discharge (EOD, Fig. 3.3 B, Meyer et al., 1987) and uses its active electric sense for localization and communication (Heiligenberg, 1991b; Nelson and MacIver, 1999). At our main study site in the Panamanian rain forest (Fig. 3.1), we observed in total 54 sequences of short-distance courtship interactions between low-frequency females (EOD frequency EODf < 750 Hz) and high-frequency males (EODf > 750 Hz) exclusively at night (Fig. 3.2). Courting was characterized by extensive production of chirps (brief frequency modulations, Fig. 3.3 C–F) by both males and females — with up to 8 400 chirps per fish and night. This contrasts with previous studies on restrained fish, in which chirps were generated preferentially by males in response to male-like EODfs (Zakon et al., 2002; Hupé and Lewis, 2008). Most chirps were so called "small chirps", characterized by short duration (<20 ms) and EODf excursions of less than 150 Hz (Fig. 3.3 C–E), similar to type-2 chirps described for *A. leptorhynchus* (Engler et al., 2000). Occasionally, courting was interrupted by intruding males. See Fig. 3.3 F–H and movies S 3 and S 5 for examples of courtship and aggression interactions. The large numbers of recorded chirps allowed for a detailed statistical analysis of electro-communication (Fig. 3.4). Chirping activity appears to be structured into episodes of elevated activity. This is demonstrated by the autocorrelation functions of small chirp times that show a single peak of 5.1 ± 2.5 s width at half height for both males and females (Fig. 3.4 A–D). The peaks were less pronounced in males because of their higher baseline activity. The duration of successive interchirp intervals was weakly positively correlated in 6 of 10 fish ($r = 0.10 \pm 0.06$, $p < 0.02$, Fig. 3.4 E–H), reflecting extended episodes of high frequency chirping (see also difference between shuffled and original autocorrelation in Fig. 3.4 A–D). In addition to the overall positive correlation, the return maps in Fig. 3.4 E–H show more structure in the timing of small chirps. In particular, the lobes extending in parallel to the axes arise from short interchirp intervals that are followed by long ones and *vice versa*.

Courting fish chirped with a preferred interval of about 325 ± 94 ms (mode of distribution, $n = 10$ fish from 5 pairings) interspersed randomly by longer intervals, resulting in a heavily left-skewed distribution of interchirp-intervals (skewness $= 19 \pm 11$, Fig. 3.5 A–D). Male chirping was structured by the timing of female chirps (Fig. 3.5 F,H). It was first inhibited at 84 ± 13 ms after the female emitted a chirp (t-test $p \ll 0.001$, effect size Cohen's $d = 1.4 \pm 0.4$, $n = 5$ pairs). Then the male's chirp probability increased significantly and peaked at 169 ± 9 ms (t-test $p \ll 0.001$, $d = 1.6 \pm 0.6$). The precise timing of this echo response demonstrates the functional relevance of chirping as a communication signal. In contrast to this finding and to previously described male-male echo responses (Hupé and Lewis, 2008; Walz et al., 2013; Salgado and Zupanc, 2011), females did not show any echo response — they timed their chirps independently of the males' chirps ($d < 0.6 \pm 0.2$ within 0–250 ms, Fig. 3.5 E,G).

Only females emitted an additional type of chirp of 162 ± 39 ms duration ($n = 54$) with a pronounced decrease in EOD amplitude, similar to type-4 chirps described for male *A. leptorhynchus* (Engler et al., 2000). These "long chirps" are the central element of a specific, highly stereotyped motive of chirping during courtship interactions (Fig. 3.3 D,E). Males consistently acknowledged the occurrence of a long chirp with a doublet of small chirps 229 ± 31 ms after the onset of the long chirp. The two chirps of the doublet were separated by only 46 ± 6 ms, more than seven-fold shorter than the preferred chirp intervals (Fig. 3.5 A–D).

The pivotal role of the female long chirp was also evident on a larger timescale (Fig. 3.6 A and Fig. 3.7). Long chirps were preceded by persistent chirping of the male with rates up to 3 Hz, clearly exceeding maximum chirp rates reported from laboratory observations (Engler and Zupanc, 2001; Hupé and Lewis, 2008). The last phase before the long chirp was initiated by a strong increase in female chirp rate from below 1 Hz to about 3 Hz within a few seconds. This concurrent high-frequency chirping of both fish was terminated by the long chirp emitted by the female and followed by the chirp doublet

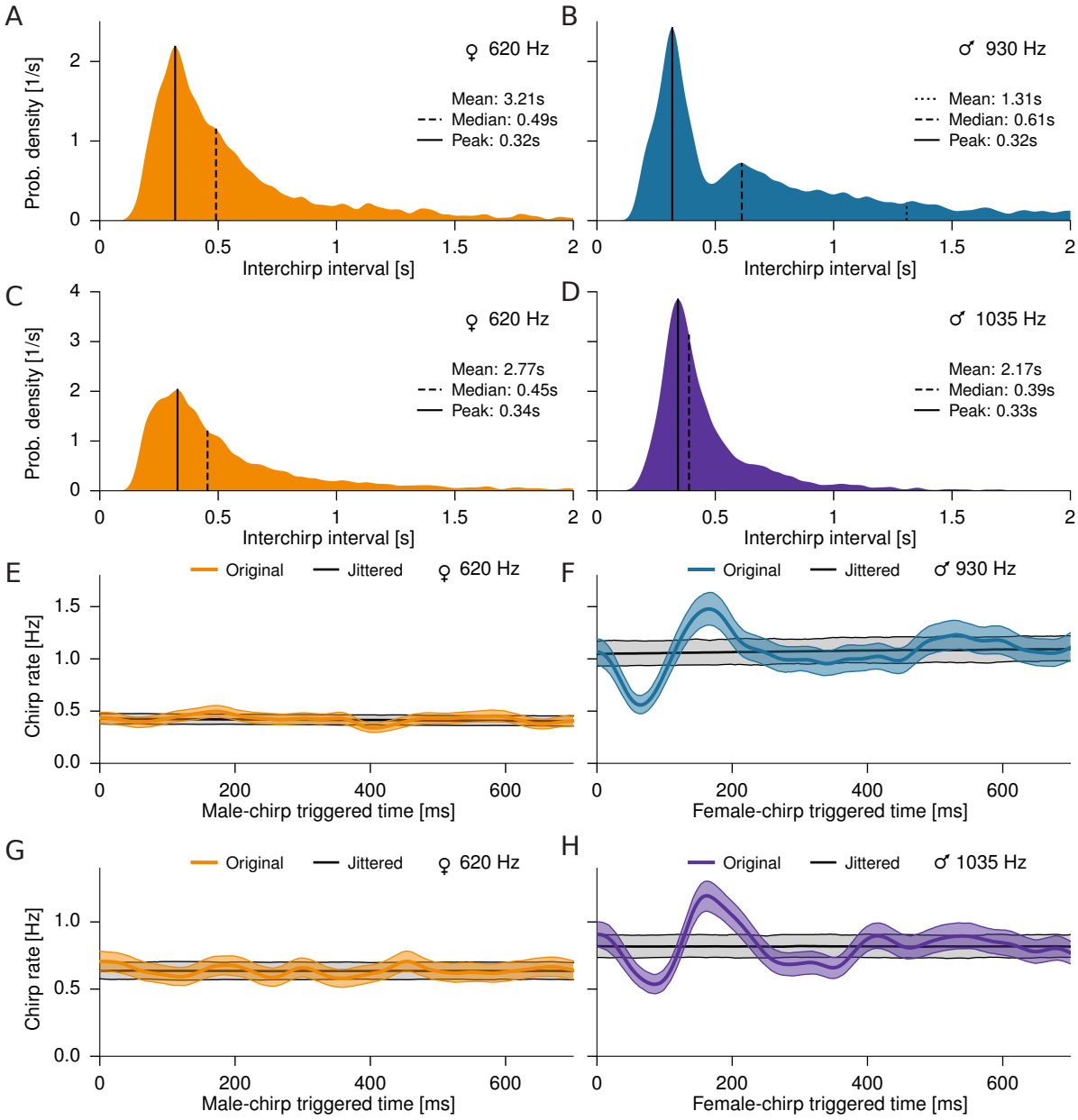

Figure 3.5: TEMPORAL STRUCTURE OF COURTSHIP CHIRPING. A–D) Interchirp interval distributions of small chirps of an example female (left column, EODf= 620 Hz; A: $n = 3431$, C: $n = 5336$ chirps) interacting with two males (right column; B: EODf= 930 Hz, $n = 8439$; D: EODf= 1035 Hz, $n = 6857$ chirps) peak at 318 ms (A,B), 328 ms (C) and 342 ms (D). E–H) Chirp rate of one fish relative to each chirp of the other fish (cross-correlogram, median with 95 inter-percentile range in color). Corresponding chirp rates from randomly jittered, independent chirp times are displayed in gray. Female chirps are timed independently of the male chirps (E: Cohen's $d < 0.73$ SD; G: $d < 0.47$). Male chirping is first inhibited right after a female chirp (F: at 64 ms, $d = 1.93$ SD; H: at 85 ms, $d = 1.49$) and then transiently increased (F: 166 ms after a chirp, $d = 1.60$ SD; H: at 162 ms, $d = 1.96$).

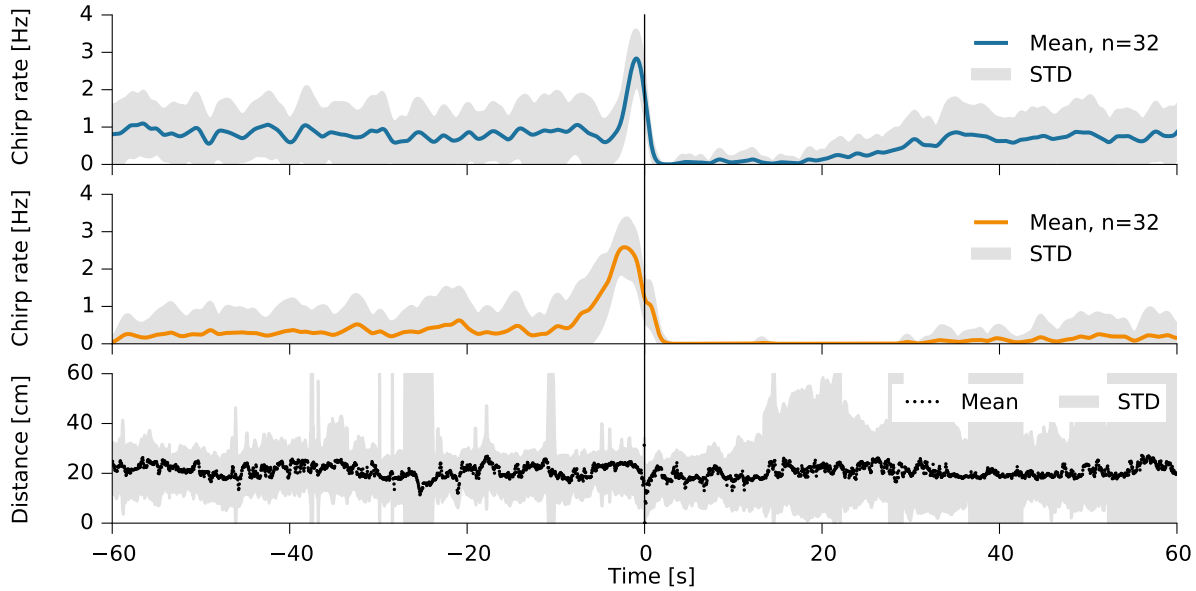

Figure 3.6: SYNCHRONIZING ROLE OF THE LONG CHIRP IN SPAWNING. The average rate of small chirps and the distance between two courting fish before and after a female long chirp at time zero. Gray bands mark SD. See Fig. 3.7 for another example.

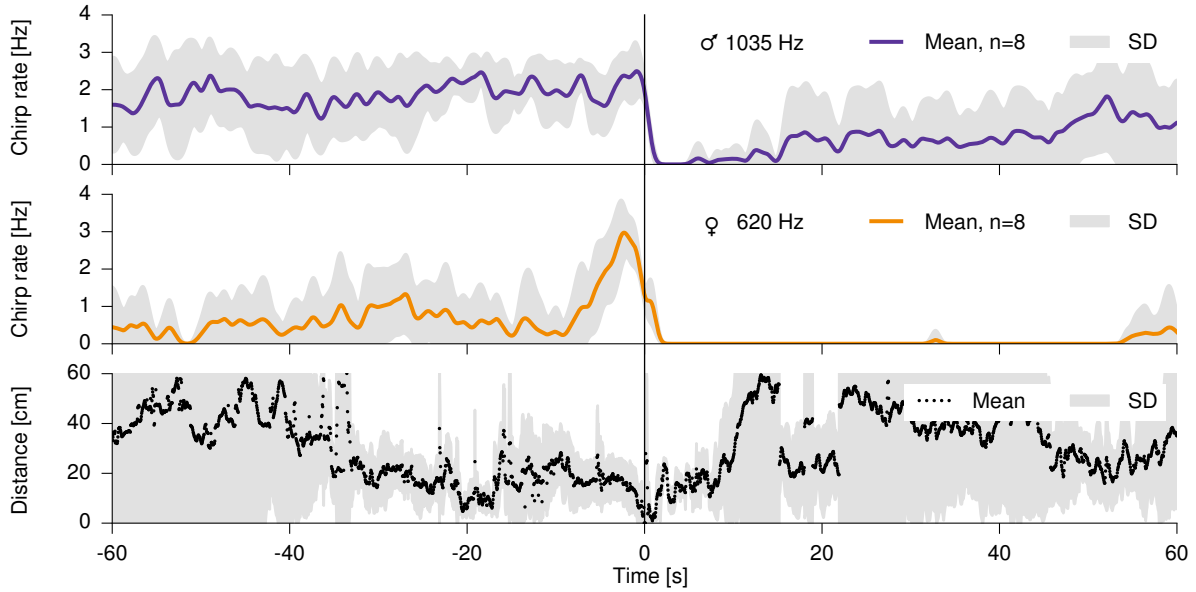

Figure 3.7: CHIRP RATE OF THE SECOND PAIR OF FISH SHOWN IN FIG. 3.5 C,D,G,H AND FIG. 3.4 C,D,G,H. Here the male (top) is chirping continuously with an elevated rate before the long chirp is emitted by the female (gray vertical line at time zero). Note the reduction in distance and the reduced standard deviation of distance around time zero, the presumed time of spawning.

as described above. These episodes were characterized by close proximity (< 30 cm, bottom panel in Fig. 3.6 A and Fig. 3.7) of the two fish. The distance was further reduced at the time of the long chirp. Per night and female we observed 9 to 45 long chirps generated every 3 to 9 minutes (1st and 3rd quartile) exclusively between 7 pm and 1 am (Fig. 3.10).

The only major difference we found in the chirping statistics between individual fish was in the time course of the chirp rate of the male right before the female long chirp. Whereas the male shown in Fig. 3.6 transiently increased its chirp rate for a few seconds, the male shown in Fig. 3.7 chirped along at a constant high rate.

The sequence of chirping and movement suggests a synchronizing function in spawning (Hagedorn and Heiligenberg, 1985; Murray, 1995; Dulka and Nickla, 2001). We tested and confirmed this hypothesis in a breeding experiment in the laboratory (Kirschbaum and Schugardt, 2002) by continuously recording and videotaping a group of 3 males and 3 females of the closely related species *A. leptorhynchus* over more than 5 month (see Chapter 4).

In addition to courtship chirping, we observed small chirps in the field during agonistic male-male interactions (Fig. 3.3 G,H, movie S 3). Occasionally, courting residents were approached by intruding males. The resident males then usually attacked the intruder. In 5 out of 12 such situations a few small chirps indistinguishable from those produced during courtship were elicited exclusively by the retreating fish (Fig. 3.10), suggesting an additional, possibly submissive function of small chirps in agonistic contexts (Hupé and Lewis, 2008; Smith, 2013).

What are the implications of the observed behavioral interactions for sensory processing of electrocommunication signals? Tuberous electro-receptors (P-units) distributed over the fish's skin encode amplitude modulations (AMs) of the fish's own EOD (Nelson et al., 1997; Benda et al., 2006; Walz et al., 2014). Superposition of a fish's EOD with the one of a nearby fish results in a beat, a periodic amplitude modulation with frequency given by the difference between the two EODfs. The amplitude of the AM equals the EOD amplitude of the nearby fish at the position of the receiving fish.

Since the electric field generated by the EOD approximates that of a dipole, the amplitude is expected to decay with the squared distance and to strongly depend on the relative orientation of the fish (Knudsen, 1975; Chen et al., 2005; Kelly et al., 2008). We estimated the dependence of EOD amplitude on distance directly from our field data (Fig. 3.8 A). The maximum EOD amplitude declined with distance with a power law in the relevant range of about 20 to 100 cm. Smaller amplitudes are always possible because of the dependence of the dipolar electric field on orientation. The average exponent of -1.25 ± 0.08 ($n = 8$) is, however, smaller than the -2 for a dipole in infinite vacuum. This may be attributed to near-field deviations from a dipole (Knudsen, 1975; Chen et al., 2005) and to boundary effects induced by the shallow water surface and the bottom of the stream (Fotowat et al., 2013; Jun et al., 2013). The EOD amplitudes of the two females estimated at 10 cm distance (0.44 and 0.66 mV) are considerably lower than the ones of the males (0.76 – 1.94 mV, $n = 8$, Fig. 3.8 B). Among males EOD amplitude did not correlate with EODf (Pearson $r = -0.35$, $p = 0.40$). Males with smaller EOD amplitudes seemed to receive more long chirps from females (Pearson $r = -0.62$, $p = 0.10$, Fig. 3.10). This is surprising since EOD amplitude increased with body size in a population of *A. leptorhynchus* recorded in the lab (Pearson $r = 0.76$, $p < 0.0001$, $n = 40$ (O. Bargelletti and R. Krahe, personal communication; Knudsen, 1975).

We estimated the population activity of electrosensory afferents in *A. leptorhynchus* from the standard deviation of the summed nerve activity, which is known to closely match the tuning properties of single nerve fibers (Benda et al., 2006; Walz et al., 2014). Driven by the electric field the P-unit population response quickly drops down to non-detectable levels at about 50 cm for beats with optimal frequencies (Fig. 3.9 A, Fig. 3.8). For higher beat frequencies the P-unit response is further scaled down (Fig. 3.9 B). All courtship chirping (small and long chirps) and submissive chirping occurred at distances below 32 cm and therefore is potentially well encoded by the electro-receptor population (Fig. 3.9 C, Walz et al., 2014). In contrast, two behaviors involving intruding males occurred at much larger distances (Fig. 3.9 D): (i) Intruding males initially often lingered at some distance from the interacting dyad (8 of 16 scenes, median duration 58.5 s; Fig. 3.3 F), consistent with assessment behavior (Arnott and Elwood, 2008). These

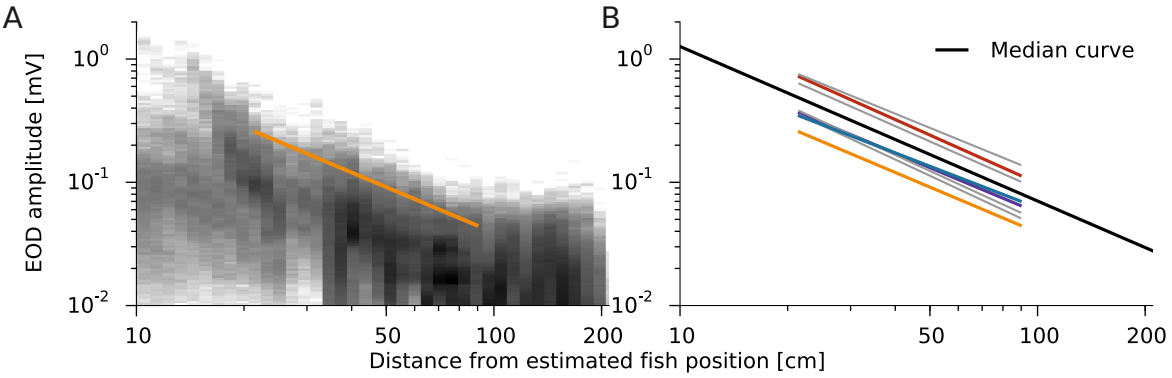

Figure 3.8: RELATIONSHIP OF EOD AMPLITUDE AND DISTANCE FROM THE FISH. **A)** Histograms (gray scale) of EOD amplitudes of the 620 Hz female recorded from all electrodes of the array as a function of distance between the electrodes and the estimated fish position. A power law was fitted to the upper 95 percentile of the histograms in each distance bin (orange line). **B)** Power-law fits to EOD amplitudes of eight fish (gray and colored lines) and the power-law with median amplitude and exponent (black line).

assessment distances were larger than 70 cm. (ii) The distances at the initiation of attacks by resident males ranged from 20 cm to 177 cm (81 ± 44 cm, $n = 10$). At the largest observed attack distance of 177 cm the electric field strength was maximally 0.34 μV/cm, close to minimum threshold values of about 0.1 μV/cm measured in the laboratory (Knudsen, 1974; Bullock et al., 1972). This demonstrates the high sensitivity of the electrosensory system for the detection of same-sex conspecifics even over large distances.

P-unit afferents are most sensitive to beat frequencies from about 20 and 130 Hz (Fig. 3.9 E, Nelson et al., 1997; Benda et al., 2006; Walz et al., 2014), which only covers the lower range of frequency differences observed in the field (Fig. 3.9 F). Indeed, the vast majority of chirp interactions occurred among courting dyads with much higher beat frequencies (205–415 Hz, Fig. 3.9 G), resulting in minute P-unit activity despite the small distances. Same-sex interactions, on the other hand, resulted in lower beat frequencies up to 245 Hz (median 86 Hz) that matched the P-unit's preferred range of beat frequencies (Fig. 3.9 H). These interactions, however, were often associated with much larger distances and thus considerably reduced P-unit responses.

3.3 Discussion

The richness of our behavioral data of weakly electric fish interacting freely in their natural habitat revealed several unexpected insights into their communication behavior and the corresponding electrosensory scenes. Electro-communication signals often result in minute activation of electro-receptors, either because of a frequency mismatch in courtship contexts or because of large interaction distances in agonistic contexts. Our field data demonstrate a striking ability of weakly electric fish to detect, categorize, and respond to these weak signals reliably within a few tens of milliseconds as demonstrated by echo responses (Fig. 3.5 E–H), chirp doublets (Fig. 3.3 E), and attacks (Fig. 3.9 D). We therefore expect adaptations of the electrosensory system for processing signals at the limit of sensitivity (Sharafi et al., 2013; Lewicki et al., 2014). In addition, the frequency mismatch between courting signals and receptor tuning should be an important selective constraint on the evolution of the sexual dimorphism in EODf that causes this unusual mismatch (Dunlap et al., 1998; Smith, 2013).

We studied electro-communication and courtship behaviors in the weakly lectric fish *A. rostratus* and *A. leptorhynchus*. Here we discuss the evidence our data provides for these two basic behaviors. Animal communication can be defined as the transfer of information by a signal generated by the sender that affects the behavior of the receiving animal (Wilson, 1975) [1]. Our data directly demonstrate the function

[1] '*Biological communication is the action on the part of one organism (or cell) that alters the probability pattern of behavior in another organism (or cell). ... Communication is neither the signal by itself nor the response; it is instead the relation*

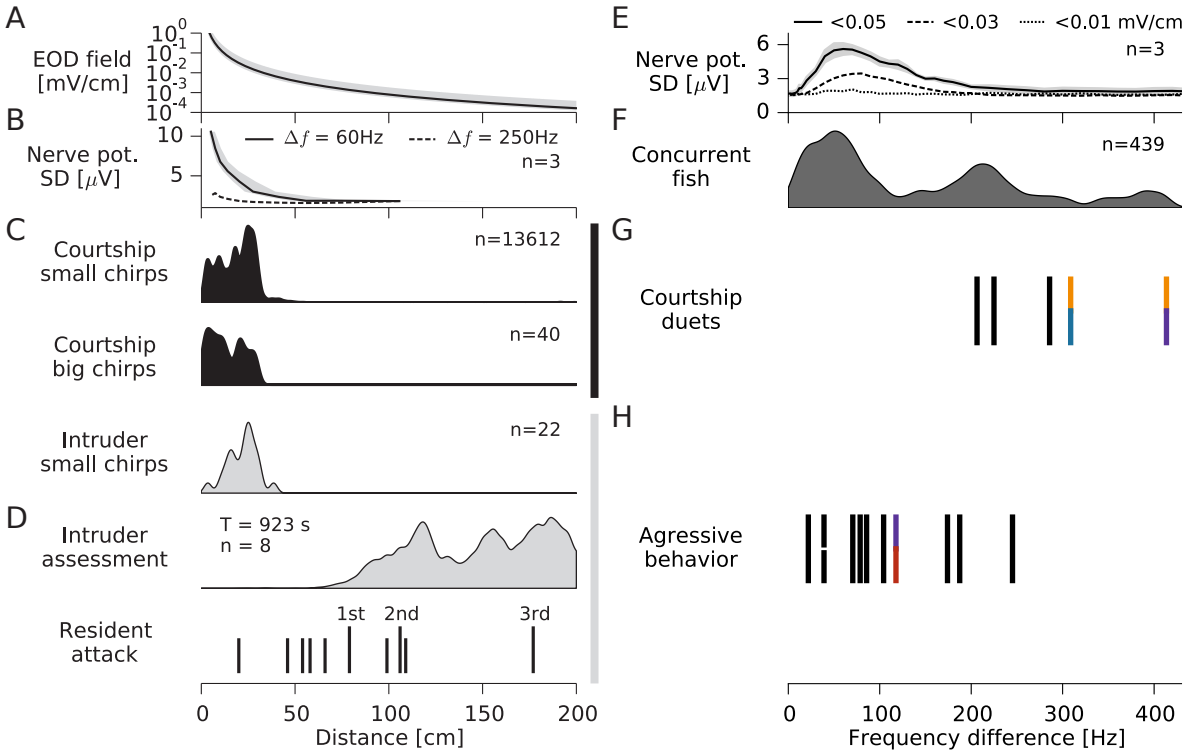

Figure 3.9: INTER-FISH DISTANCES AND FREQUENCY DIFFERENCES AND THEIR ENCODING. **A)** Maximum electric field strength as a function of distance from the emitting fish (median fish in black with total range of all fish in gray). **B)** Activity of the electro-receptor afferent population rapidly decays with fish distance and depends on the difference Δf between the EODfs of the two fish. **C)** Small and long chirps in both courtship and agonistic contexts are emitted consistently at short distances below 32 cm. **D)** In contrast, intruder assessment and initiation of attacks on intruders occur at much larger distances. The distance at which the resident male started to approach a repeatedly intruding male grew larger with each intrusion (numbered and extended lines). **E)** Tuning of electro-receptor activity to Δf. Smaller electric field strengths resulting from larger distances between the fish scale the tuning curve down. **F)** Distribution of Δfs of all *A. rostratus* appearing simultaneously in the electrode array ($n = 439$ pairings, peaks at 51, 213, and 393 Hz). **G)** Courtship behaviors occurred at Δfs in the range of 205–415 Hz, far from the receptors' best frequency. **H)** In contrast, agonistic interactions occurred at Δfs below 245 Hz, better matching the tuning of the electro-receptors.

of the EOD and its frequency modulations as communication signals in natural conditions. Courting male fish respond with great temporal precision to female chirps. First, there is the stereotyped emission of a doublet of small chirps in response to the female big chirp (Fig. 3.3 E). Second, males show a temporally precise echo response in reaction to female small chirps (Fig. 3.5 F,H). Laboratory studies found slower echo responses between males (Zupanc et al., 2006; Hupé and Lewis, 2008; Salgado and Zupanc, 2011) and inhibiting effects of small chirps on attack behavior (Walz et al., 2013). A submissive function of male-to-male chirping is supported by our observation that in resident-intruder interactions only the intruder, who then left the area, produced chirps. Females, on the other hand, respond to male chirping on a slower time scale by raising their chirp rate (Fig. 3.6 A and Fig. 3.7). Our field data also suggests additional functions of the EOD in agonistic male-male interactions, in particular the ability of males to recognize individual fish (Fig. 3.9 D, numbered attacks). However, more extensive studies in the field and the laboratory are necessary to confirm these hypotheses. Previous studies already suggested a function of the EOD and its modulations in courtship of *A. rostratus* (Hagedorn and Heiligenberg, 1985; Hagedorn, 1988) and in the synchronization of spawning and external fertilization in the pulse-type Gymnotiform *Brachyhypopomus pinnicaudatus* (Silva et al., 2008). Results from both our field data on *A. rostratus* and from our breeding experiments with *A. leptorhynchus* provide strong evidence that female long chirps are an exclusive communication signal for the synchronization of egg spawning and sperm release: (i) The female long chirp was the central part of a highly stereotyped duet-like

between the two.' Wilson, 1975, 6th edition, p. 176.

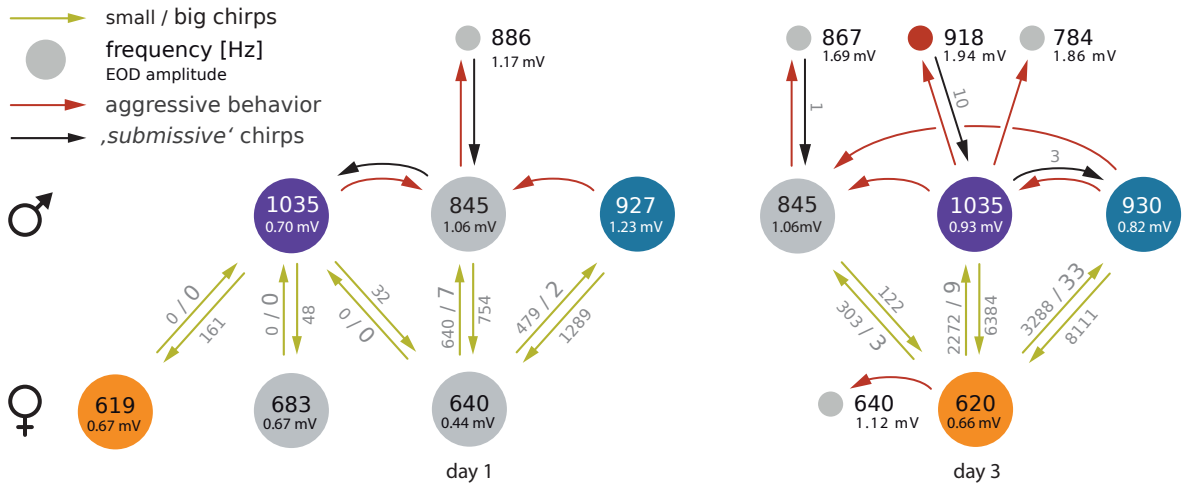

Figure 3.10: SOCIOGRAM OF A SELECTION OF INTERACTING *A. rostratus* INDIVIDUALS DISPLAYING THEIR SOCIAL RELATIONSHIPS FROM TWO NIGHTS. The numbers within shaded circles refer to the EODf (top, in Hz) and the EOD amplitude at 10 cm distance (bottom). Similar EODfs on day 1 and day 3 might indicate the same fish. Females were identified based on their low EOD frequency (Meyer et al., 1987). Green arrows and associated numbers indicate the numbers of small chirps and long chirps emitted in close proximity (< 50 cm). Red arrows indicate agonistic interactions, and black arrows the number of small chirps emitted during agonistic interactions. Day 1: 2012-05-10, day 3: 2012-05-12.

communication pattern between a male and female fish. Similar patterns have been observed in other aquatic animals (Dawkins and Guilford, 1994; Lobel, 1992; Ladich, 2007). (ii) Fertilized eggs were found at the locations of male-female interaction, and only when the female had produced long chirps in the preceding night (see Chapter 4). (iii) The period before the female long chirp was characterized by extensive chirp production by the male, consistent with a male courting behavior (Bradbury and Vehrencamp, 2011). We therefore refer to episodes around female long chirps in both species as courtship behavior.

A summary of the main courtship and agonistic interactions we observed is illustrated in Fig. 3.10. Females are approached by roaming males that extensively court the females by emitting large amounts of small chirps. Females appear to have good control over who they mate with, because their cooperation by means of the long chirp is crucial for synchronous gamete release and thus successful external fertilization. The males compete for access to females and females mate with several males over the course of a night. This suggests a scramble competition mating system as it is common for animals living in a three-dimensional environment, e.g., fish and birds (Bradbury and Vehrencamp, 2011).

With our novel method of long term data collection combined with automated analysis we extended the approaches of the newly emerging field of Computational Ethology (Anderson and Perona, 2014) from the lab to the field (Rodriguez-Munoz et al., 2010). The unprecedented amount of observational data on electro-communication behavior of weakly-electric fish in an unrestrained, natural setting allowed for detecting and quantifying patterns of behavior and the associated sensory scenes (Gomez-Marin et al., 2014). This constitutes a significant advance over laboratory studies conducted in tanks that necessarily limit the animals' choices of interaction partners and their ability to escape from each other. The combination with neurophysiological approaches provides deep insights into constraints on sensory processing and its evolution.

CHAPTER 4

LONG-TERM BREEDING EXPERIMENT

In our field study in Panamá (Chapter 3) we observed intensive, dyadic interactions during the reproductive period of *Apteronotus rostratus* revolving around an repeated, stereotyped communication pattern. Central element of this pattern was a conspicuous signal emitted exclusively by female fish, the long chirp. The whole, synchronized sequence of chirping and movement and the fact that the interactions were observed in the reproductive period suggested a function in spawning (Hagedorn and Heiligenberg, 1985; Murray, 1995; Dulka and Nickla, 2001). We tested this hypothesis in a breeding experiment in the laboratory with a group of 6 *A. leptorhynchus*, a species closely related to *A. rostratus* (de Santana and Vari, 2013). In collaboration with Prof. Frank Kirschbaum from the Humboldt-Universität zu Berlin, we set up a community tank allowing for inducing breeding conditions and for the continuous recording of fish behavior.

4.1 Methods

A tank ($100 \times 45 \times 60$ cm) was placed in a darkened room and equipped with bubble filters and PVC tubes provided for shelter. Water temperature was controlled via room temperature and varied between 21 and 30 ° C (Fig. 4.1). The light/dark cycle was set to 12/12 hours. Several rocks were placed in the center of the tank as spawning substrate.

EOD signals were recorded differentially using four pairs of graphite electrodes. Two electrode pairs were placed on each side of the spawning substrate. The signals were amplified and analog filtered using a custom-built amplifier (80× gain, 100 Hz high-pass, 10 kHz low-pass; npi electronics GmbH, Tamm, Germany), digitized at 20 kHz with 16 bit resolution (PCI-6229, National Instruments, Austin, Texas, USA), and saved to hard disk for offline analysis. The electrode pairs were positioned orthogonally to each other, thereby allowing for robust recordings of EODs independent of fish orientation. The tank was illuminated at night with infrared LED spotlights (850 nm, 6W, ABUS TV6700) and monitored continuously with two infrared-sensitive high-resolution video cameras (Logitech HD webcam C310, IR filter removed manually). The cameras were controlled with custom written software and a timestamp for each frame was saved for later synchronization of the cameras and EOD recordings. A recording session had a duration of exactly 24 hours and was started and stopped at 12 am.

Six individuals of *A. leptorhynchus* (three male, three female; imported from the Río Meta region, Columbia) were kept together in a tank for over a year before being transferred to the recording tank. At first, fish were monitored for about a month without external interference. We then induced breeding conditions (Kirschbaum and Schugardt, 2002) by slowly lowering water conductivity from $830\,\mu\mathrm{S\,cm^{-1}}$ to about $100\ \mu\mathrm{S\,cm^{-1}}$ over the course of three months. Conductivity was reduced by diluting the tank water with deionized water created with a reverse-osmosis system. The tank was monitored regularly for the occurrence of spawned eggs. We analyzed 134 days of EOD and video recordings.

Tracking of electric fish and electro-communication

Fish were tracked based on their EODf as described in Section 2.3. All analysis steps were performed on the separate, daily datasets and no efforts were made yet to track individual fish over several datasets. During the recordings external noise was constantly present. Noise sources were excluded by only accepting EODfs in the frequency range between 500–1100 Hz.

Chirps were detected as described in Section 2.4. Chirps with a single peak in the upper passband were detected as small chirps. Chirps of up to 600 ms duration and two peaks in the upper passband, marking the begin and the end of the longer frequency modulation, were detected as long chirps. Female fish emitted many long chirps with only small frequency excursions. Therefore, female long chirps with large frequency excursions, resembling those emitted during our field recordings in Panamá (Fig. 3.3), were selected manually from all detected female long chirps. Video sequences were extracted for time periods before and after the selected female long chirps ($\pm$15 s).

We manually confirmed the chirps in the period $\pm$60 s before and after the selected female long chirps for 17 out of 79 episodes, and chirps were added, where missing. Manual revision of chirp detection was necessary to ensure that the extracted chirp times of long chirps precisely mark the chirp's onsets. In the analyzed episodes, 318 female chirps and 1365 male chirps were emitted by the courting fish and were included in the analysis. Kernel density histograms of interchirp intervals, cross-correlograms (Fig. 4.6 A–D) and chirp rates before and after female long chirps (Fig. 4.5) were computed as described in Section 3.1.

4.2 Results

We continuously recorded EODs (Fig. 4.1) and video footage of a group of *A. leptorhynchus* for more than a year and recordings were interrupted only for short maintenance breaks. We analyzed the EODs of individual fish for communication signals and, specifically, for the occurence of female long chirps. More than 1.2 million chirps emitted by both male and female fish were found (Fig. 4.2, 4.3) and categorized into small and long chirps. After the onset of conductivity reduction (day 0), the chirp rate of males increased for several weeks, but decreased to a low level after about day 50. However, manual revision showed that many male chirps failed to be detected at that time. The female chirp rate increased gradually over the course of the recordings. Chirps were generated mostly at night, a pattern which was particularly distinct in males (Fig. 4.3). Overall, almost equal numbers of chirps were detected for males and females.

Four types of chirps could be distinguished. The large majority of chirps (96%) was similar to type-2, or small chirps described by Engler et al. (2000) and was emitted by males and females in agreement with previous reports (Zakon et al., 2002). Courting males also generated a substantial amount of a long chirp similar to type-4, which were characterized by large frequency excursions (>200 Hz) and durations from 50 up to about 500 ms. The observation is in agreement with previous reports on *A. leptorhynchus* (Zakon et al., 2002), but contrasts with field data from *A. rostratus*, where males emitted only small chirps. Another type of long chirp was emitted by males and females alike with small frequency excursions of about 20 Hz and durations of up to 600 ms. Finally, females emitted a small number (n=79) of long chirps with frequency excursions of up to 400 Hz and durations of about 250 ms. This type of long chirp showed strong similarity to the long chirps emitted by female fish recorded in the field in Panamá (see Chapter 3). This chirp was detected exclusively during the six nights in which eggs were spawned (Fig. 4.2) and has been emitted by multiple females. Spawned eggs were found at the sites of male-female interaction, often located at inaccessible parts of the substrate, e.g., in fissures between rocks and in filter material. Spawned eggs were collected in petri dishes filled with tank water and successful fertilization was confirmed when embryos developed and hatched after a few days.

We created video sequences triggered on these female long chirps (see movie S 6 for an example), and for each long chirp we found highly stereotyped courtship behavior as described before by Hagedorn and Heiligenberg (1985). Before spawning the female swam on her side close to a substrate, e.g., a rock or a filter, while the male hovered in the vicinity of the female and emitted chirps continuously (Fig. 4.4).

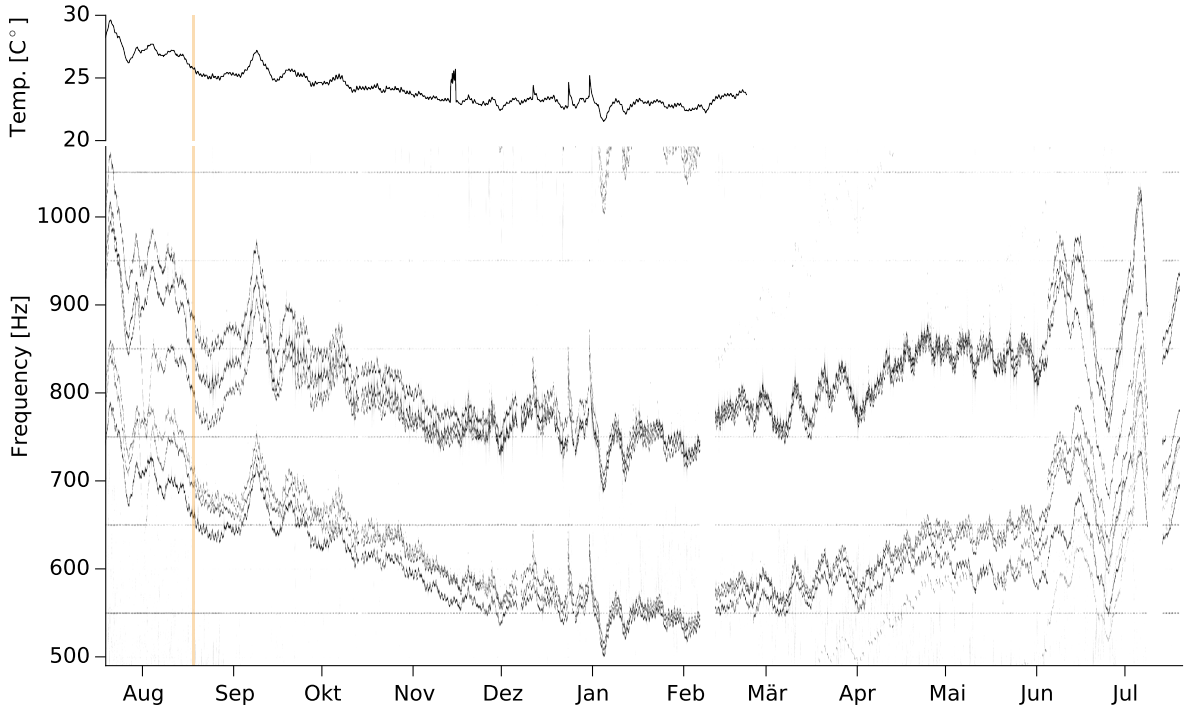

Figure 4.1: SPECTROGRAM OF EODS RECORDED IN THE BREEDING TANK. The EODs of 3 male and 3 female fish were recorded over the course of a year (bottom). The fish were monitored for a month before water conductivity was slowly reduced to stimulate breeding, starting on August 18th (orange marker). EODf is modulated by water temperature (top).

In the last seconds before spawning, the female started to emit a series of chirps, whereupon the male approached the female closely. Just before the female emitted its long chirp, the male pushed the female and retreated almost immediately afterwards. The female continued chirping, while it swam briskly around the substrate, possibly to attach the fertilized egg to the substrate.

We analyzed chirping in greater detail for 17 out of 79 episodes of spawnings, centered around the female long chirp (Fig. 4.5) and involving the same male and female. Similar to *A. rostratus*, spawning was always preceded by persistent chirping of the male at a rate of about 1 Hz and only few chirps by the female. The male emitted small and long chirps of varied duration before the spawning. The last phase before spawning was initiated at about 10 s before the female long chirp with a synchronous increase of female small chirp rate and male long chirp rate, the latter of which then composed almost 100% of all emitted male chirps. After spawning males ceased to generate long chirps, but emitted small chirps at a decreasing rate. Females emitted a single long chirp at the time of spawning and then continued to emit small chirps at a decreasing rate. This contrasts with *A. rostratus*, where females ceased to emit chirps almost immediately after spawning.

The 17 selected episodes of spawning were further analyzed for temporal structure and the occurrence of echo chirps (Fig. 4.6). The chirp interval distribution of females has a weakly pronounced peak at 750 ms and a long tail reflecting long pauses between chirps. In contrast, males chirped with a preferred interval of 567 ms (mode of the distribution), but also inserted longer pauses between chirps, resulting in a left-skewed distribution. Similar to our field observations in *A. rostratus* the onset of male chirping in *A. leptorhynchus* was structured by female chirps. The probability of male chirp generation decreased to almost zero at 66 ms after a female chirp (effect size, Cohen's $d = 2.1$), and increased strongly afterward, peaking at 215 ms ($d = 4.2$), an effect much more pronounced than in our field data. An effect of similar size is not observed for female fish, but note that female chirp probability shows a reduction between 70–350 ms and an increase between 400–600 ms after a male chirp ($-1.4 < d < 2.2$ within 0–600 ms). This could indicate a female echo response on a slower time scale than the male echo response.

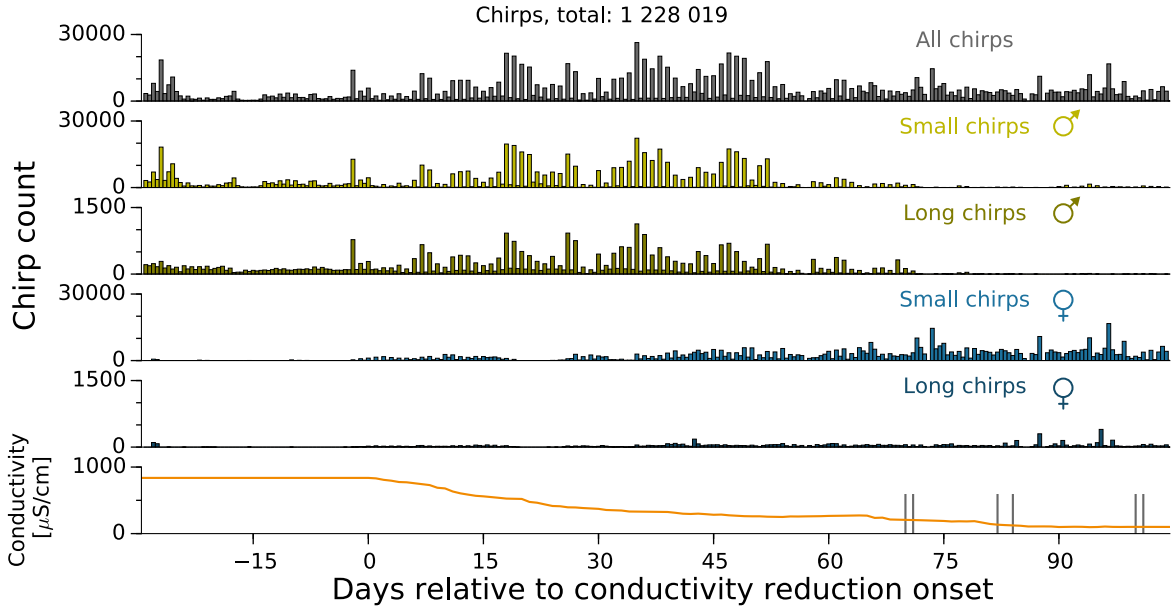

Figure 4.2: OVERVIEW OF EMITTED CHIRPS DURING THE BREEDING EXPERIMENT. Small and long chirps were detected for all individuals and attributed to the group of males (green) and females (blue), respectively, according to their EODf. The number of chirps emitted during the light and dark phases, each lasting 12 hours, was determined and plotted as histograms jointly (top) and separately for males and females, and small and long chirps (center). Note that the term 'long chirp' denotes all chirps with durations between 50–600 ms, independent of their frequency excursion. This is especially noteworthy in the case of females, which emitted many chirps with long durations and small frequency excursions. The bottom plot displays the course of the conductivity (orange) and the dates of the six spawning nights (gray lines).

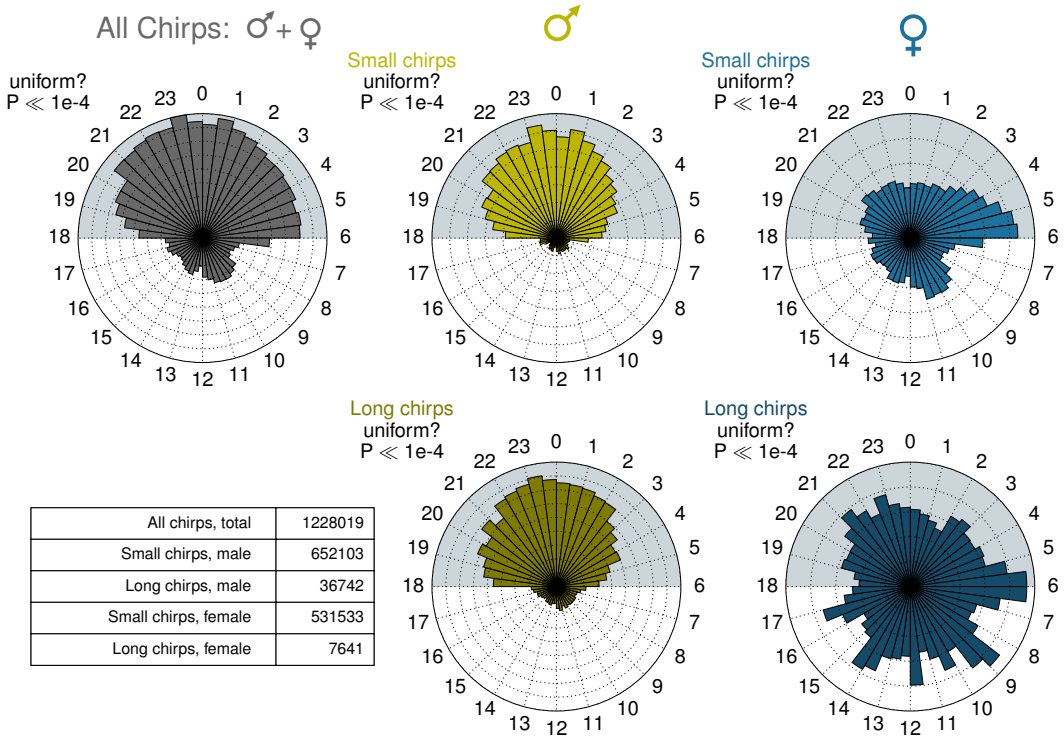

All chirps, total	1228019
Small chirps, male	652103
Long chirps, male	36742
Small chirps, female	531533
Long chirps, female	7641

Figure 4.3: DIURNAL CHIRPING PATTERNS. Histograms of the diurnal occurrences of small and long chirps for males (green) and females (blue) with bins of 30 minutes. Shaded areas mark the dark cycle of the experiment. P-values for the Rayleigh test of uniformity are shown for each histogram. Absolute numbers of detected chirps are denoted at the bottom left.

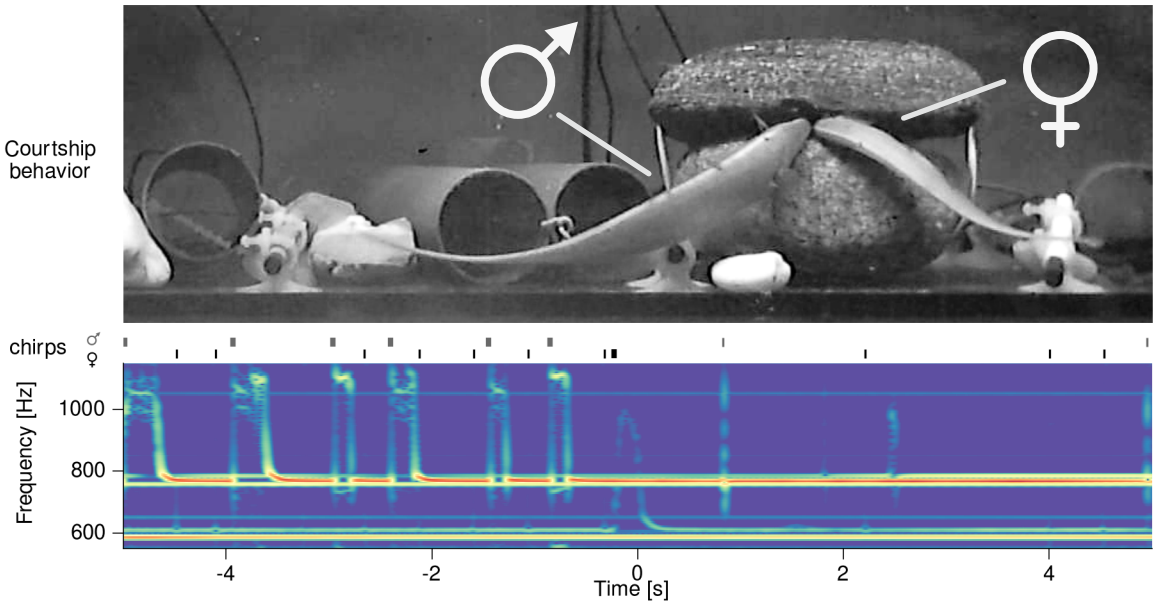

Figure 4.4: SYNCHRONIZING ROLE OF THE LONG CHIRP IN SPAWNING. Simultaneous video (top, see movie S 6) and voltage recordings (spectrogram, bottom) of six *A. leptorhynchus* in the lab demonstrate the synchronizing function of the female long chirp (at time zero; trace starting and ending with frequency at 608 Hz) in spawning. The spawning female swims on her side close to the chosen substrate and is approached by the chirping male. The chirp activity of the two fish is displayed in the spectrogram below. Additionally, chirp times of male (gray) and the female (black) are marked by vertical bars above the spectrogram. In contrast to *A. rostratus*, male *A. leptorhynchus* generate additional long chirps before spawning (trace with baseline at 768 Hz). Interestingly, the baseline EOD*f*s of the individuals of each sex, in the spectrogram recognizable as horizontal lines, are closely grouped in two narrow frequency bands around 600 and 770 Hz and the two sexes are separated by about 150 Hz.

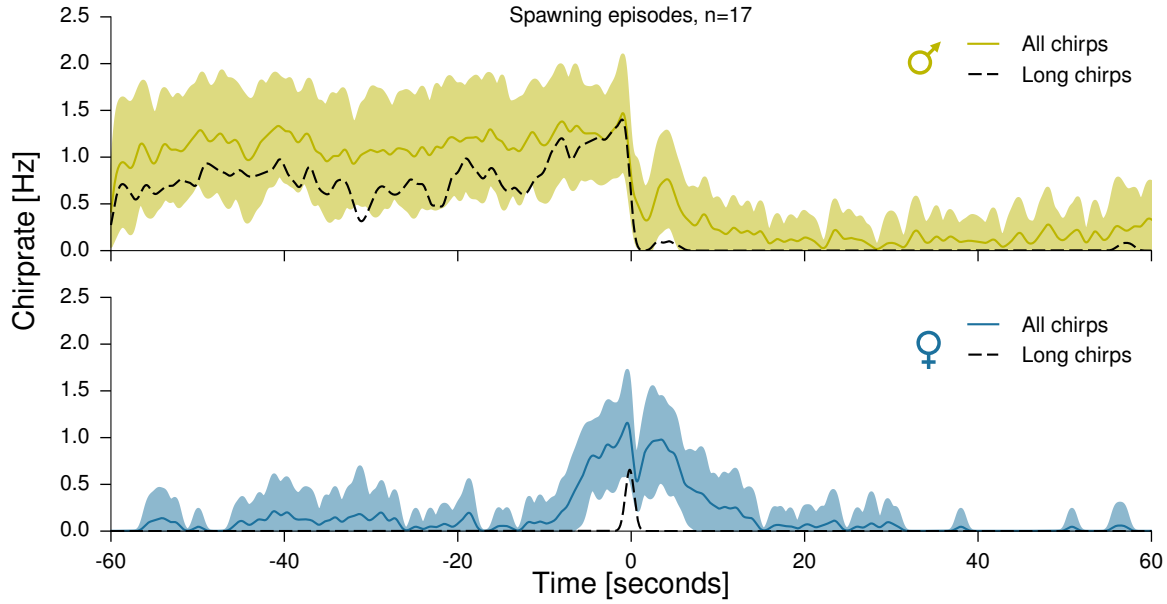

Figure 4.5: CHIRP RATES DURING SPAWNING EPISODES. Average chirp rates of a male (top, green) and a female (bottom, blue) fish before and after spawning (female long chirp at time zero; ±60 s). The same male and female were participating in all of the 17 analyzed episodes. Shaded bands mark standard deviation.

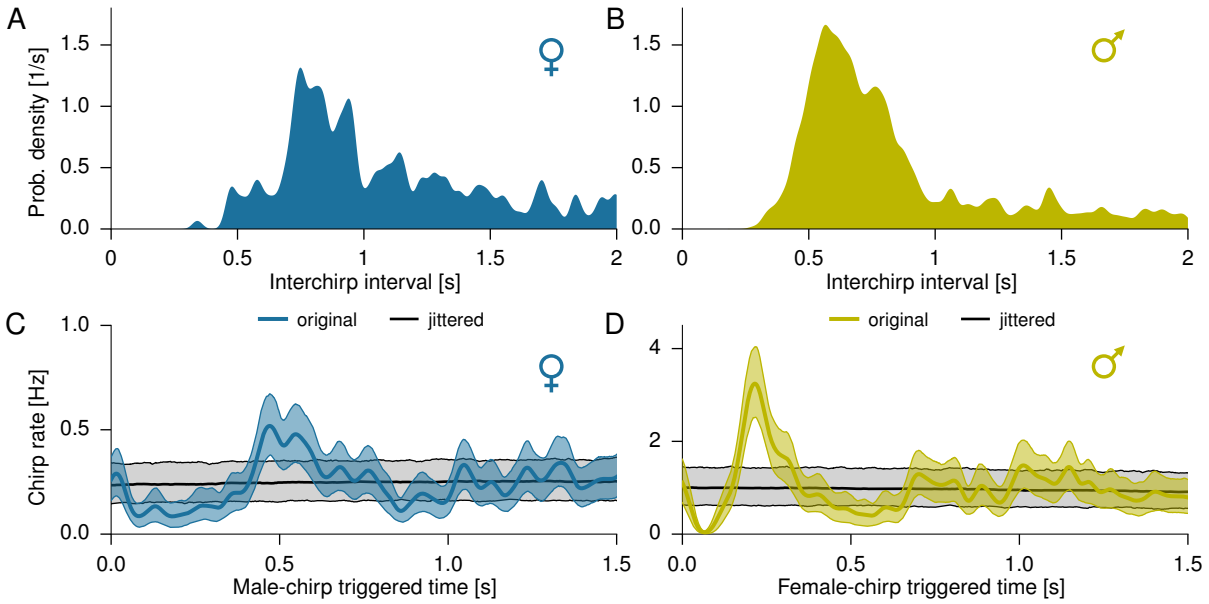

Figure 4.6: TEMPORAL STRUCTURE OF COURTSHIP CHIRPING. **A, B**) Pooled interchirp interval distributions of all chirps emitted by the same female (blue) and male (green) during 17 episodes of courtship. **C, D**) Chirp rate of one fish relative to each chirp of the other fish (cross-correlogram, median with 95 % inter-percentile range in color; female: blue, male: green). Corresponding chirp rates from randomly jittered, independent chirp times are displayed in gray. Note the differing scale on the y-axis. Female chirps: 318, male chirps: 1365.

4.3 Discussion

Our study demonstrated the large potential of the automated behavioral monitoring of electric fish. We successfully induced breeding in a group of 6 *A. leptorhynchus* and scanned the recorded EODs for communication signals over a period of 134 days using the same analysis as was applied for field data (Chapter 2). Among the large number of emitted chirps, we detected 79 female long chirps resembling those emitted by females during nocturnal dyadic interactions between male and female *A. rostratus* in their natural habitat (Fig. 3.3 A). Video footage triggered on these chirps demonstrated that they are elements of a stereotyped and precisely timed behavioral pattern among dyads of male and female fish. A similar behavior has been described earlier as courtship and spawning (Hagedorn and Heiligenberg, 1985; Zakon et al., 2002). This assessment is reaffirmed by our observation that this specific type of female long chirp occurred exclusively at nights after which spawned and fertilized eggs were found in the tank at the locations of male-female interaction. However, the total number of eggs found was often smaller than the number of detected courtship interactions. This could either indicate that not every courtship episode concluded in successful spawning of an egg or that some spawned eggs were cannibalized, as is common in other species of electric fish (Frank Kirschbaum, personal communication). Our data strongly suggest an exclusive function of the female long chirp in synchronizing spawning.

Before the reduction of conductivity and the simultaneous increase of male chirp rates (Fig. 4.2), females chirped only rarely. This observation is consistent with previous studies, which focused exclusively on male chirping, because females were presumed to generate only few chirps (e.g., Dye, 1987; Zupanc and Maler, 1993; Dulka and Maler, 1994). However, our data clearly demonstrate that while females produce fewer chirps than males, they still produce large numbers starting with the conductivity reduction and associated the transition to reproductive state, and especially in the context of courtship and spawning. In contrast to males, females generate substantial amounts of chirps likewise during light and dark periods. And in contrast to common view, females generate many chirps on days without courtship and spawning. These findings suggest that the functions of many female chirps are far from understood.

The stereotyped communication pattern observed in the breeding tank closely resembled that observed in the field (Fig. 3.3 A) in many key aspects. (i) The patterns revolve around the female long

chirp as the central element. (ii) The patterns are preceded by persistent chirping by males. (iii) The patterns are characterized by an increase in tempo concluding with the female long chirp, after which chirping activity is strongly reduced. (iv) The patterns occurred exclusively among males and females. We therefore propose that the observed patterns are two versions of a homologous, behavioral pattern conserved in the *A. leptorhynchus* species group. However, differences between the two patterns exist. (i) In *A. rostratus* only two types of chirps are emitted, i.e. small chirps by both sexes and long chirps by females, while in *A. leptorhynchus* males additionally emitted long chirps. (ii) *A. rostratus* females almost completely ceased chirp activity after the emission of the long chirp, in contrast to *A. leptorhynchus* females, where the chirp activity was distributed almost symmetrically. (iii) *A. rostratus* males always and exclusively emitted a small chirp doublet after the female long chirp. This signal has not been observed in *A. leptorhynchus*. It might be speculated that the small chirp doublet in *A. rostratus* has a function in synchronizing spawning that in *A. leptorhynchus* might be achieved by the male push. If that were the case, synchronization of spawning in *A. rostratus* might be achieved by electro-communication cues alone. A male pushing behavior before spawning and in synchrony with electric signaling can be found in the gymnotiform pulse-type fish *Brachyhypopomus pinnicaudatus* (Philip Stoddard, personal communication), providing yet another example of a conserved element in courtship behavior of gymnotiform species. The male push is interesting physiologically. The PPnC, the nucleus initiating chirp-like modulations, receives mechanosensory input, mostly from the lateral line, through at least 5 different pathways from the nucleus electrosensorius (Wong, 1997; Zupanc and Maler, 1997), which acts as an interface between the electrosensory and the electromotor system (Keller et al., 1990). These pathways could provide the basis for a rapid chirp response to a mechanical stimulus and also aid the detection of synchronous mechanical and electrical signals.

The video sequences of spawning demonstrate clearly that fertilization must occur at the time between the male pushing the female and a short time period after the female's long chirp, before the male retreats and the female swims around the substrate. However, it remains to be determined, if fertilization occurs before or after the female's long chirp, and therefore, if the function of the long chirp is one of signaling readiness-to-spawn or one of feedback for the male's actions. The video footage also showed that male and female fish move in close proximity in the time period preceding the female long chirp, similar to our results extracted from field data (Fig. 3.9 C), and even closer in the last 10 seconds. Hagedorn (1986) hypothesized that fertilization occurs just as the egg leaves the female's cloaca, because the egg is thrust out with a tremendous force and then sticks to the substrate. In this scenario, the male sperm must have been released before the egg is thrust out, such that it traverses the sperm cloud. Further high-resolution video and electric recordings are necessary to reveal the precise temporal sequence of the fertilization process.

We have not yet thoroughly analyzed the identity of the individuals participating in courtship, although the video footage suggests that only the largest of the three males took part. In contrast, we observed multiple females, each spawning several eggs, during the same night. Both observations match well those by Hagedorn and Heiligenberg (1985). The systematic analysis of dominance structures and their relationship to EODf and the generation of communication signals remains to be done. In any case, clear-cut dominance and monopolized reproductive success of a single male, if it were found, might be an artifact of this specific laboratory setting. In this setting, the fish had no opportunity to evade direct competition, and dominating a group of females concentrated at a single location is likely much easier than doing so in a spread out natural habitat with many roaming competitors. The latter argument is supported by our field observations, in which dyadic interactions similar to the courtship in the lab occurred among various pairs of males and females (Fig 3.10).

A typical feature of courtship displays is an increase in tempo as gamete release approaches (Bradbury and Vehrencamp, 2011). Analyzing the temporal structure of chirping during courtship on a larger scale, we found that female chirp display indeed increased in tempo, starting from a very low rate, in the immediate time period around spawning. In contrast, male chirp rate remained stable (Fig. 4.5), but the relative proportion of long chirps increased to almost 100% of all emitted male chirps synchronously with the female's chirp rate increase.

Further, in the time period before and after spawning, male chirping is precisely triggered on female chirps (Fig. 4.6 D). This behavior clearly demonstrates that males are able to rapidly detect and react to female chirping, thereby following its rate accurately. At the same time it directly demonstrates the occurrence (and relevance) of communication, following the definition of animal communication by Wilson (1975)[1].

In contrast, the female's ability to detect and discriminate a male's small and long chirp is not directly shown, because the observed synchronous chirp rate increase could be controlled by the male fish alone and the available evidence for a female echo response is weak (Fig. 4.6 C). However, it is plausible that females are able to discriminate male chirp types. (i) On the background of large frequency differences, as they occur during male-female interaction (> 150 Hz), high frequency chirps have been shown to be conspicuous and reliable signals in P-unit activity (Benda et al., 2006). (ii) It would make little sense for a sender, the male, to switch to a new signal type that could not be discriminated by the receiver, the female, especially in a context as important as courtship. Neurophysiological studies demonstrated that small chirps and high frequency chirps are encoded by two distinct populations of pyramidal cells in the ELL's lateral segment, the I-cells and the E-cells, respectively (Marsat et al., 2009; Marsat and Maler, 2010). However, these studies were based on the assumptions that small chirps occur on the background of small frequency differences (5 Hz) between two communicating fish and that the durations of high frequency chirps do not exceed 50 ms. Both assumptions are inconsistent with our data on chirps occurring during courtship episodes (e.g., Fig. 4.4). A study by Vonderschen and Chacron (2011), using a larger and more naturalistic stimulus set, showed that separate populations of neurons in the torus semicularis encode the occurrence and the characteristics of chirps and thereby together are able to detect and discriminate various chirp types on various signal backgrounds. (iii) We do not have any data yet showing the relevance of the echo response for the female's disposition to spawn. But the fact that the echo response is conserved over individuals (Fig. 3.5 F,H) and species, as shown by the similar results from our field and laboratory studies, suggests a female preference for males exhibiting an echo response.

Our observations of synchronized chirping raise new questions. How is the male echo response acknowledged (on the behavioral side) and processed (on the neural side) by female fish? Are females less prone to mate with a male which locks to its chirps only weakly or not at all?

The female's ability to reliably detect various chirp types in dependence of signal intensity and EOD frequency difference could be tested analogous to Knudsen (1974), who determined behavioral response thresholds of *A. albifrons* in response to sine wave electric fields using a two-alternative forced choice paradigm. Testing the female's behavioral response to the echo chirping is less straight forward. The simplest approach would be to search for occasions, where the initiation of courtship fails and try to relate this to the occurrence and the parameters of the echo response. However, such events might be rare, if the echo response is a strongly selected trait. Another option would be to use closed loop experiments with spawning females, which could be identified on-line using our monitoring setup.

Generally, chirp activity increased starting with the onset of conductivity reduction (Fig. 4.2). This increase is especially apparent in males and its functional significance is yet undetermined. The early increase of chirping activity could be related to the establishment of a hierarchy among the males that was triggered by hormonal changes induced by the reduction of conductivity. This is consistent with the observation that large numbers of chirps were reported in the context of long agonistic interactions during the establishment of a hierarchy in *E. virescens* and generally during agonistic interactions in *A. leptorhynchus* under laboratory conditions (Hagedorn and Heiligenberg, 1985). It will be fascinating to analyze, if reproductive success, or participation in courtship, can be related to the early chirping interactions.

Another possibility is that the chirping activity preceding actual courtship has a priming effect on gonadal maturation. In contrast to 'releasing' signals that influence an receiver's immediate behavior, e.g., during courtship and spawning, 'priming' signals alter the recipient's endocrine and neuroendocrine system such that subsequent behavioral patterns are modified (Wilson and Bossert, 1963). E.g., in lizards ovarian maturation is accelerated by male courtship and its mimics (Crews, 1975). In some bird species,

song stimulation increases the reproductive efforts of females. In mockingbirds and canaries females exposed to high-quality male singing initiate nest-building faster and lay more and larger eggs (Kroodsma, 1976; Gil et al., 2004; Logan et al., 1990). If male signals are necessary to induce gonadal maturation can easily be tested by stimulating breeding conditions and monitoring gonadal maturation in a group of females only.

The neural pathways by which electric signals can influence the control of neuroendocrine processes and motivation have been described for *Eigenmannia* spec. by Keller et al. (1990): nEb is a subdivision of the nucleus electrosensorius, a diencephalic electrosensory-motor interface. nEb receives electrosensory information from the torus semicularis and projects to thalamic and hypothalamic nuclei that may provide electrosensory information to areas mediating motivational and neuroendocrine control. The control of reproduction by the hypothalamo-pituitary-gonadal axis is evolutionary conserved in vertebrates and in fish is closely associated with the serotonin system (Peter et al., 1990; Prasad et al., 2015).

It must be noted again, that technical reasons underlie the apparent decrease of male chirping activity after about day 50, which therefore is not discussed further at this point. Finally, the differences in the diurnal chirp activity of males and females are apparent (Fig. 4.3), but cause and function are yet undetermined.

Datasets like ours, combining electric with video recordings and automated analysis, allow for a systematic functional review of communication signals. The opportunities originating from our novel study design are a major improvement over conventional approaches, e.g., chirp chambers and staged dyadic interactions, for which it is difficult to assess the motivational state of the studied individuals. In contrast, our study design detects and works on spontaneous behavior and could even be used to select courting individuals for chirp chamber experiments or the timing of hormone sampling. This makes our study design a valuable supplement to the study of natural behavior and stimuli in the field.

CHAPTER 5

DISCUSSION

> *The brain is the chief architect, orchestrator and driver of behavior; behavior, in turn, is the principal function of the brain. Thus, if the problem of neuroscience is to understand brain function, then success hinges not only on explaining how neural systems work, but in linking this to behavior in a systematic way. Thus, behavioral data is not simply a tool for helping neuroscientists interpret brain data, but also the foundational problem of neuroscience.*
>
> *From* Gomez-Marin et al., 2014

In the introduction we stated and described the demand for data on relevant natural behavior and the corresponding sensory scenes. This data is a necessary basis for understanding the neural processing of sensory information, because it provides us with the knowledge on the scene analysis problems actually faced and solved by the animal's sensory system. The weakly electric fish is a well established model system for the study of the mechanisms underlying sensory processing (e.g., Heiligenberg, 1991a; Sawtell et al., 2005; Chacron et al., 2011). However, consistent data on the use of and response to electro-communication signals in ecologically relevant contexts were lacking (Smith, 2013), despite of the early recognition of the electric fish's aptitude for exactly such studies (Hagedorn and Heiligenberg, 1985). Accordingly, the central aim of this thesis was to provide the means for the tracking of electric fish behavior in their natural habitats. Further, we aimed to obtain data on the electrosensory context of natural interactions of electric fish.

In Chapter 2 we presented an automated tracking system allowing for the reliable and continuous tracking of wave-type electric fish based on the individual-specific EOD*f*s. The system extracts frequency modulations of the EOD on short and long time scales, and estimates location and orientation of the tracked fish. Consequently, our system allows for the automated analysis of unprecedented amounts of EOD data, thereby providing the basis for better statistics on electric fish behavior and paving the way for new types of studies. Further, because the outputs of our analysis are machine-readable, our tracking system should also be considered as a step towards the machine aided analysis of electric fish behavior. The development of the presented tracking system therefore is a main result of this thesis.

We acquired data on natural communication of the ghost knifefish, *A. rostratus*, during its reproductive period, by deploying our tracking system in the Panamanian rain forest (Chapter 3). We tracked individuals and characterized dyadic interactions and the corresponding electro-communication scenes. Two types of dyadic interactions were analyzed: male-female interactions with long durations and large numbers of emitted chirps and brief male-male interactions with only few chirps emitted. Male-female interactions were later identified as courtship and spawning and followed a stereotyped pattern that was repeated many times. We showed that almost all chirps, independent of context, were emitted in close proximity to a conspecific. During courtship, male chirps were preferentially generated and precisely timed after female chirps, thereby generating a so-called echo response. Our data also showed that competing male intruders can be detected and responded to over larger distances of up to 170 cm, even in the

presence of a much stronger EOD of a nearby female conspecific. For the observed interactions we extracted frequency differences and estimated effective signal intensities, and related those to the response properties of the P-unit electro-receptors. Surprisingly, we found that in many relevant communication situations the electro-receptors will be driven only weakly by electric communication signals, either because of a frequency mismatch in courtship or because of large interaction distances in agonistic contexts. Our data also allowed for a new level of abstraction of natural social interactions and e.g., revealed that a given female mates with several competing males over the course of the night. This study is the first account for the detailed monitoring and characterization of electric fish movement and communication in their natural habitat.

To determine the behavioral context of the male-female interaction observed in Panamá, we conducted a long-term breeding experiment in the laboratory with the closely related species *A. leptorhynchus* (Chapter 4). We used our tracking software to identify male-female communication scenes similar to those observed in the field. Video footage synchronized on such events showed courtship and spawning, an interpretation which was reconfirmed by the finding of fertilized eggs on the mornings following these interactions. Sequence and dynamics of the chirping during courtship closely matched that observed in the field, although species-specific differences were found. We found that both the female long chirp signaling spawning and the quick and precisely timed male echo response to female chirps are conserved across species. However, in contrast to *A. rostratus*, *A. leptorhynchus* additionally emitted high frequency chirps of varied durations during courtship.

Our studies clearly demonstrated our tracking system's aptitude for the automated tracking of electric fish movement and communication over extended periods of time and space, even in previously inaccessible natural environments. Applying this system we revealed the properties of natural communication situations. We then demonstrated how our system can be used to further characterize the behaviors observed in the field in a tailor-made long-term laboratory study.

Machine-aided analysis of behavior

The importance of tracking and quantification of behavior increased strongly in recent years, providing many current examples of machine-based tracking of animals. New techniques for circuit mapping and manipulation (e.g., Luo et al., 2010; Leifer et al., 2011) provide the means to establish a causal relationship between neural activity and behavior, but therefore crucially depend on the ability to quantitatively track animal behavior. This relationship was driver for the development of visual tracking tools for a range of model organisms (e.g., C. elegans: Swierczek et al., 2011; Drosophila: Dankert et al., 2009; zebrafish: Green et al., 2012). Independent of optogenetics, new tools for the tracking of more exotic animals were developed (e.g., electric fish: Hofmann et al., 2014; Jun et al., 2014a; Steinbach, 1970; bats: Hiryu et al., 2007; Yartsev and Ulanovsky, 2013; for a review of acoustic tracking see Blumstein et al., 2011). Electric fish, and here in particular wave-type fish, are especially well suited for tracking. These fish permanently generate an electric organ discharge that can readily and cheaply be recorded and analyzed for identity and individual location and communication signals.

Our automated analysis of EODs yields abstract data, i.e. EOD*f* and movement traces and the timestamps and durations of communication signals. This is helpful and even necessary to analyze behaviors in large datasets: data from multi-channel systems like ours are too large and too high dimensional for manual review by a human observer. Movement traces are hard to extract manually and even communication signals are so short that one would need to search for them on short time scales and on many channels, a time and labor intensive and practically impossible endeavor, if one considers their vast numbers. In this perspective, our computationally aided analysis of electric fish behavior gives us access to new spatial and temporal scales of electric fish behavior.

However, it must be noted that our system can only find communication signals matching the parameters of its detectors. Because there might be many signals we do not know yet, maybe some as exclusive and rare as the female long chirp, it remains essential to pay close attention to the underlying raw-data, especially in adequate spectral representations, to find new and unknown signals. Human observers remain the best detectors of novel patterns at our disposal.

Tracking of movement and communication is the first step in the understanding of animal behavior, but behavior includes both a mechanistic and a functional account. Therefore, what necessarily follows is the abstraction from datum to factum, i.e. the annotation of actions, activities and functions, and their detailed analysis. Our system automatically performs the first and, with the classification of distinct communication signals, in parts the second step. However, most of the annotation and all of the subsequent analysis of behavior is done manually, because these steps still need the creativity, care and insight of a human observer. This is a characteristic that our system shares with the computational analysis of behavior from visual recordings: software that generalizes well across differing setups is still rare (but see Prez-Escudero et al., 2014).

The performance and consistency of a human observer strongly depends on their attention and experience. Therefore, the ultimate challenge is to develop a framework and the computational capability to identify and quantify behavior, which is the aim of the newly emerging field of Computational Ethology, with all its tailing opportunities and dangers (Anderson and Perona, 2014; Gomez-Marin et al., 2014). The biggest and most obvious drawback of automated behavioral analysis is the increased distance of the scientist to data generation and analysis. The field of ethology progressed, because scientists extensively observed and annotated behavioral states and actions under natural conditions and gained deep insights into the animal's behavior in the process. But while classical ethology often relied on ad hoc behavioral categories and summary statistics, thereby reducing dimensionality already during the recording process, its modern counterpart provides us with the possibility to repeatedly revisit large multidimensional datasets, each time refining or changing the questions asked.

For our tracking system, manual identification and annotation of behavior remains a necessary task, but as soon as the characteristics of an interaction are known, detectors can be defined allowing for an automated search in the datasets for the behavior in question. E.g., we learned that in *Apteronotus* courtship and spawning culminates in the abrupt increase of female chirp rate and the generation of a long chirp, and we already demonstrated our ability to find spawning events only by searching for the long chirps. If we would like to ask the question, if the synchronization of courtship ever failed, we could define a detector that searches for events of abrupt increases of chirp rate, which are lacking the female long chirp. Or, we could ask if a male's courtship is ever rejected by a female, by searching for males that extensively chirp in close proximity to a female, but never actually participate in spawning. If such events are found, we could then dive deeper into the dataset to check, e.g., if the unsuccessful male's chirping differs from those of successful males, which could then be related to the properties of neural processing of chirps in females. Rather than fully automated, such an analysis is machine-aided and the scientist retains many opportunities to review the underlying data in detail, of course at the cost of throughput. Such an approach reduces the effort of data analysis and allows for answering new types of questions.

EOD-based tracking

There are obvious limits to EOD-based tracking. Although many behaviors of electric fish are exclusively electric in nature (e.g., electro-communication and the jamming avoidance response), direct evidence for physical interactions that could easily be tracked visually (Triefenbach and Zakon, 2008) is inaccessible and has to be inferred jointly from EOD signals, context, and movement dynamics. While it is possible to combine electric and video recordings in the laboratory, providing us with the best of two worlds (Chapter 4), our field setup is limited to EOD recordings only. The drawback is undeniable, but is more than compensated by the direct access to the communication signals embedded in the fish's EOD. None of the main (mice, rat, Drosophila, and C. elegans) and few of the more exotic animal model systems share this advantage (but mind the bat: Ulanovsky and Moss, 2008; Yartsev and Ulanovsky, 2013). This advantage ideally meets the electric fish's role as a model system for the analysis of the neural mechanisms underlying the processing of communication signals.

Another limit of EOD-based tracking is its scalability. A 64-channel system covering a few square meters generates several hundred of gigabytes of uncompressed data each day. Data can be reduced to about 50% using lossless compression, e.g., FLAC, and to about 10 – 25% using reasonably lossy

compression, e.g., MPEG-1 Audio Layer III, 128 – 320 kbit/s. Even then, the amounts of data generated when monitoring large areas are huge, but the same is true for visual recordings: 24-hours of HD-quality recording with a single camera generate about 80 Gb of data (sample-rates: 15 Hz at night, 25 Hz during day; medium compression). Several solutions, independent of technological advance, are possible. (i) A circular buffer-based system could identify relevant parts of data only, e.g., channels with signal amplitudes above a pre-set threshold, and save only these parts. (ii) Online analysis could process and reduce data on-line and save only abstract data. (iii) Different experiment designs could use different strategies to reduce data. e.g., long-term transect recordings in the field with many electrodes distributed along the stream banks could focus on nocturnal recordings and save daylight activity, i.e. when fish remain at their hiding places, in short patches only. Designs using large array-like setups to study spatial interactions could use a full-take strategy at night, but during the day would save only data from electrodes close to the stream banks or from those with sufficiently large signals.

5.1 Implications for neuroscience

In Chapter 3, we reported that the electrosensory system is often activated only weakly by relevant signals emitted by either competitors or mating partners. However, fish behavior demonstrated that these weak signals are nevertheless successfully processed. This reveals the system's impressive sensitivity and raises the question why some apteronotid species evolved such a pronounced sexual dimorphism in EOD*f* that potentially impairs neural encoding of important signals. In apteronotid species sexual dimorphism in EOD*f* is evolutionary labile and in many species EOD*f* does not differ between the sexes (e.g., Ho et al., 2010; Zhou and Smith, 2006), whereas other species show the exact opposite from *A. leptorhynchus*, e.g., *A. albifrons*. In addition, chirp structure varies strongly across apteronotid species (Turner et al., 2007), from simple chirps with a single frequency peak to complex and multi-peaked chirps (e.g., Dunlap and Larkins-Ford, 2003). These properties make the genus *Apteronotus* a formidable subject for comparative studies of the evolutionary aspects of neural coding.

Implications of receptor frequency tuning and small signal intensities

We reported that, during natural interactions of dyads, chirps were emitted at distances smaller than 32 cm, independent of the sex of sender and receiver and their EOD*f* differences (Fig. 3.9 C). Fotowat et al. (2013) showed that during interactions of dyads the resulting EOD AMs at the skin of the fish, i.e. the beat contrast that is encoded by the P-unit electroreceptors, drop below 20% contrast at distances greater than 23 cm and below 5% contrast at distances greater than 30 cm. Because these measurements were performed in a small tank with shallow water, i.e. under conditions that extend the range of the electric field, these results should be considered as an upper limit. In summary, it seems that chirps are generally emitted at beat contrasts greater than 5%. However, it should be considered that because of the complex electric field of a nearby conspecific the receptors distributed over the fish's skin are exposed to a full range of intensities of amplitude modulations that could be even much lower than the estimated 5% contrast. Studies on the processing of chirps commonly use EOD beat amplitudes of 10 – 20%, thereby roughly matching the lower range of the estimated intensities (e.g., Marsat and Maler, 2010; Walz et al., 2014).

The signal received at the fish's skin is further scaled by the frequency tuning of the tuberous electroreceptors (see Fig. 3.9 B, E; Hopkins, 1976; Nelson, 2011; Chacron et al., 2005). Beat frequencies between 60 – 100 Hz, i.e. within the range of same-sex interactions, are well transmitted, whereas, e.g., beat frequencies greater than 200 Hz, common for opposite-sex interactions, are substantially scaled down. Because of the behavioral responses to small chirps in our recordings of male-female interactions in Panamá, we can assume that both, the 400 Hz beat, at least at this close distance, and the chirps riding on this beat are well detected. However, we cannot exclude that chirps emitted under these conditions are detectable at even larger distances, but are emitted on short distances for other, behavioral reasons. This appears to be the case during male-male interactions with small beat frequencies. In these situa-

tions chirps were emitted only on short distances, although chirps embedded in small beats should be detectable even at larger distances, because the receptors respond much stronger to small than to large beat frequencies. Behavioral reasons, e.g., physical interactions, are the likely cause for the emission of chirps on short distances.

Studies on the sensory processing of chirps commonly use chirp stimuli at beat frequencies below 256 Hz for small chirps (Benda et al., 2006; Marsat and Maler, 2010) and up to 400 Hz for high frequency chirps (Vonderschen and Chacron, 2011). However, our results clearly demonstrate that, at least in *A. rostratus*, small chirps emitted at higher EOD*f* differences are successfully detected by the electrosensory system. Therefore, future studies on chirp encoding should incorporate small chirp stimuli at large EOD*f* differences. This should be supplemented by behavioral experiments determining the absolute detection threshold of different chirp types in dependence of beat frequency.

In general, many important electric signals seem to cause very small receptor responses and, accordingly, low signal-to-noise ratios. Accordingly, one might expect neural adaptations that enhance the detectability of communication signals. Previous studies in other sensory systems demonstrated that nervous systems are able to extract weak signals using stochastic resonance (e.g., Douglass et al., 1993; Levin and Miller, 1996; Collins et al., 1996; Linkenkaer-Hansen et al., 2004). Another proposed mechanism enhancing weak sensory inputs is Bayesian inference. In this framework, prior knowledge on sensory scenes, mediated by massive feedback from higher brain areas, is supposed to help disambiguating weak sensory inputs (e.g., Lee and Mumford, 2003; Lochmann and Deneve, 2011).

Feedback connections are very prominent in the electrosensory system, e.g., to ELL pyramidal neurons from the nucleus praeminentialis dorsalis (NPd, the direct pathway; Sas and Maler, 1983) and from eminentia granularis pars posterior (EGp, the indirect pathway; Sas and Maler, 1987). Previous work already demonstrated how the indirect pathway enhances chirp detection by canceling out slow (< 20 Hz) predictable signals (Marsat and Maler, 2012). Accordingly, it would be fascinating to use the electric fish as a model system for studying if and how feedback from higher brain areas can further facilitate the detection of weak communication signals, e.g., weak EODs of other conspecifics and small chirps embedded in EODs with large EOD*f* differences.

Further implications for chirp encoding

The short story of chirp function in *A. leptorhynchus* is that small chirps are considered signals emitted during same-sex agonistic interactions by males and females, while high frequency chirps are emitted during courtship by males (e.g., Bastian et al., 2001; Cuddy et al., 2012; Triefenbach and Zakon, 2003). This view is supported by a neurophysiological study by Benda et al. (2006) reporting that in P-unit output small chirps are conspicuous on the background of small EOD*f* differences (< 30 Hz), while in contrast high frequency chirps are conspicuous signals on the background of large EOD*f* differences (~ 50 – 200 Hz).

Our studies did not yet systematically characterize the parameters of the found chirps, but one conflict of our observations with the established view is apparent. In our field data *A. rostratus* generates only small chirps during all interactions, independent of the sex of sender and the of EOD*f* differences. In our laboratory data of *A. leptorhynchus* males generate high frequency chirps of varied durations, while females generate mostly short low frequency chirps. In both datasets, males demonstrated their ability to detect and react to the putative 'inconspicuous' small chirps over the large dFs occurring during courtship (up to ~ 420 Hz) by performing their consistent and precise echo response. These results strongly suggest that our understanding of usage, function, and encoding of chirps is still incomplete.

Finally, there are good reasons for performing neurophysiological experiments on the encoding of chirps on reproductively active fish. On the electro-motor side, substantial parts of the PPnC are reconfigured during the change into reproductive state (Zupanc and Maler, 1997). Among others, these changes are mediated by serotonin, a neuromodulator known to be involved in the control of reproduction (Prasad et al., 2015; Smith and Combs, 2008), and that is also known to influence chirping behavior in females. On the electrosensory side, serotonin modulates the processing of electric signals in the ELL and has been predicted to enhance the detection of same-sex EOD*f*s, while at the same time improving

the detection of chirps emitted by the other sex (Deemyad et al., 2011). Therefore, when the goal is to understand the processing of electro-communication signals, only studying reproductively active fish guarantees that one probes the neural structures in a relevant condition. Otherwise, one risks missing important mechanisms improving the encoding and discrimination of electric signals.

Implications of the echo response

We observed a distinct male echo response to female chirps both in the field and in our laboratory breeding study. All males exhibited a pronounced reduction in chirp rate at a latency of about 66 ms and increase at 160 ms and 215 ms, for *A. rostratus* and *A. leptorhynchus*, respectively. The echo response observed in the field was less pronounced than that in the laboratory. This effect might be species or context specific, but it could also be caused by the difference in the analysis: in the field study all chirps of a dyad were used for the cross-correlation, while in the laboratory only chirps emitted 60 s before and after a female long chirp were considered.

The echo response was reported before in *Apteronotus* among fighting males (Hupé and Lewis, 2008; Zupanc et al., 2006) and in a playback study (Salgado and Zupanc, 2011). The timescale reported by Hupé and Lewis matches well that observed in our field and laboratory studies, while the timescales reported by the other studies were much longer with response times up to 600 ms. The functional significance of the echo response during male-male interactions is unknown and it's not clear, if this behavior occurs during natural interactions. Male-male interactions of *A. rostratus* observed in Panamá were much shorter (tens of seconds up to a few minutes) than observed in laboratory studies. In the context of our results, it appears possible that the neural mechanism underlying the male echo response is a trait strongly selected by females. Accordingly, the echo response observed during agonistic behavior may be a mere consequence of female preference or a laboratory artifact caused by the impossibility to evade each other imposed by small tanks.

Two reasons come to mind, why females might require males to lock precisely to their chirps. First, the echo response demonstrates a male's ability to synchronize gamete release during spawning to the female's chirps. The latter is essential as the data from this and previous breeding experiments (Hagedorn and Heiligenberg, 1985; Kirschbaum and Schugardt, 2002) suggest that females produce and spawn up to a few tens of large eggs about every 14 days. The female investment is much larger than the male investment, because it is much more expensive to produce eggs than sperm. In this perspective, the extensive male chirping preceding spawning would have at least two functions, i.e. (i) to stimulate a female into a receptive state and (ii) to prove a male's ability to detect and lock to the female's chirps. This might resolve the debate about the costs of extensive male chirping (Reardon et al., 2011). It would not be the chirp itself that is energetically costly, but inaccurately timed chirping would impose a kind of opportunity cost. Second, the echo response might be a mechanism to ensure mating with a member of the same species. In our field study of *A. rostratus* we find a preferred response time of about 160 ms. In contrast, in our breeding study with *A. leptorhynchus* we find a response time of 215 ms, although it must be noted that only 17 spawnings of a single male were analyzed. The difference of 55 ms is apparent and it might carry functional meaning. The timing of chirp response might provide an additional electrosensory selection mechanism that reduces the risk to generate hybrids in regions where several apteronotid species occur syntopic. The two arguments are not exclusive, as the echo response might prove a male's ability to synchronize to the female's chirps and at the same time can help to find a member of the right species by its precise latency. However, it appears as if syntopy of multiple *Apteronotus* species is not a regular phenomenon (Carlos D. Santana, personal communication).

What can we learn from the time course of the echo response? The latency of the leading inhibition is in both species about 66 ms, suggesting similar processing. Where does the inhibition come from? The fastest pathway from the P-units to the electric organ is: to ELL (5-6 ms) to torus semicularis (3-4 ms) to nucleus electrosensorius (5 ms) to PPnC (5 ms) to pacemaker nucleus (5 ms) to spinal cord (5 ms), totaling to about 30 ms (Vonderschen and Chacron, 2011; L. Maler and M. Chacron, personal communication). This estimated latency is much smaller than the latency of the observed inhibition, suggesting a more indirect processing pathway. A possible indirect route could e.g., involve processing

in the telencephalon. An important question is the target of the observed inhibition. This would likely be the chirp eliciting neurons in the PPnC, because in the nucleus electrosensorius no cells have yet been found that are able to elicit chirping. In case of the PPnC, a good candidate source of inhibitory projections is the subpallium (Wong, 1997). Mueller and Guo (2009) reported strong expression of the GABA synthesizing protein GAD in the subpallium. The subpallium is homologous to the basal ganglia of mammals and is conserved across teleosts (Ganz et al., 2012; Harvey-Girard et al., 2013).

5.2 Behavior, ecology and evolution

A fact often stated by neurophysiologists working on *A. leptorhynchus* is that the characteristics of natural electric signals are well known. This view is founded on a plethora of laboratory studies, some describing the dependence of chirping on a range of parameters of EOD mimics (e.g., Dunlap and Larkins-Ford, 2003), others the influence of hormones (e.g., Dunlap, 2002) and some the chirping during staged encounters (e.g., Hupé and Lewis, 2008; Triefenbach and Zakon, 2008) and courtship (Hagedorn and Heiligenberg, 1985). Although some studies provided very elaborated naturalistic environments (e.g., Black-Cleworth, 1970), all of these experiments were performed on captive fish in tanks.

In contrast, usually much fewer field studies on natural behavior are cited, and here mostly the works of Carl Hopkins (Hopkins, 1972, 1974a,b; Hopkins and Heiligenberg, 1978), Mary Hagedorn (Hagedorn, 1986, 1988), and Schwassmann (Schwassmann, 1976, 1978). These works revealed much about ecology, life history and species specific distributions of EOD*f* of gymnotiform fish (e.g., Fig. 1.2). However, because most of these studies were both very labor intensive and yet restricted in their means to monitor the behavior of free roaming fish, many observations remain anecdotal. Therefore, it is likely that many natural electric signals and their function are not yet fully characterized and understood.

While the laboratory is well suited to characterize properties of the electrosensory system in detail (e.g., Knudsen, 1974), the wide range of its capabilities is best revealed in a natural environment. Accordingly, the full spectrum of electric signals is best extracted from naturally occurring communication situations that provide the signal's natural context. This is precisely the purpose of our tracking system.

The difference between laboratory and field settings is well illustrated by the differences we observed in mating behavior. In agreement with Hagedorn and Heiligenberg, the preliminary data from our breeding experiments suggests a clear-cut male hierarchy in breeding tanks, such that the largest fish participated in spawnings (with the difference that he did not have the highest EOD*f*). In contrast, in our field data we found that several males were spawning with a single female over the course of a night (for an overview, see Fig. 3.10). Although we found competition among males, no clear-cut hierarchy based on EOD*f* was observed and it seems that a male that is reproductively successful on one day can be much less successful on another. Of course, a much larger dataset is necessary to confirm this pattern.

Another example is agonistic behavior, which in the laboratory is observed during staged encounters (e.g., Triefenbach and Zakon, 2008; Hupé and Lewis, 2008) and before courtship in breeding experiments (Hagedorn and Heiligenberg, 1985). In staged encounters, agonistic behavior was commonly observed to continue for several minutes, before the combatants were eventually separated, and during courtship almost continuously over sequential nights and in both contexts interactions were accompanied by chirping. In contrast, agonistic behavior in our field study was, with a single exception, exclusively observed during situations reminiscent of resident-intruder situations interrupting courtship. Common durations for interactions were a few tens of seconds and, more rarely, several minutes. During these interactions, only few chirps were emitted and the losing fish retreated eventually. These contrasting observations suggest that the impossibility to retreat escalates conflicts such that the resulting behavior is not representative for natural behavior and hard to interpret. Consequently, more naturalistic setups (e.g., Black-Cleworth, 1970) allowing for long-term tracking of behavior are necessary to create representative data.

Large differences between the behavior in the field and in laboratory studies have also been reported for other animals. e.g., male insects have long been assumed to dominate their female partners after mating by aggressive behavior to restrict their access to other males (Alcock, 1994). After performing an

extensive study of crickets in a natural environment, Rodriguez-Munoz et al. (2011) report that instead of restricting their female partners, the presence of male crickets after mating drastically decreases female predation rate at the cost of an increase of their own.

The wild cricket project (Rodriguez-Munoz et al., 2010, 2011) depicts an interesting approach that might serve as an example for electric fish research. In a joint effort of multiple laboratories with differing evolutionary and ecological interests, the behavior and genetics of tagged animals and their descendants are monitored over years. This approach allows to test evolutionary hypotheses developed in the laboratory in a natural population, and helps e.g., to reveal if traits found to be successful in the laboratory are similarly successful in the wild. Accordingly, electric fish populations could be monitored electrically, genetically, and using implanted NFC tags over long periods of time. Spatially detailed electric recordings (e.g., Chapter 3) could be complemented by transect-like recordings with many electrodes distributed along a stream's banks, revealing interactions and their signals and diurnal to annual movements of many sympatric electric fish species. This way, the potential of electric fish for studying evolutionary questions (e.g., Zakon et al., 2006) could be further extended.

Slow frequency modulations: rises and drops

Rises were hypothesized to be general signals of social stress or signals of dominance or appeasement and subordinance (Serrano-Fernandez, 2003; Tallarovic and Zakon, 2002, 2005; Smith, 2013). In laboratory recordings of *A. leptorhynchus* rises occur frequently (see Fig. 2.2) and can be distinguished coarsely in transient yodels and longer gradual rises. In contrast, in our field data of *A. rostratus* only a single rise emitted by a single retreating male was found. This could be a behavioral difference between species, similar to the difference in chirp-types used during courtship (small chirps in *A. rostratus* vs. high frequency chirps in *A. leptorhynchus*). Or it could be a general difference between a relatively small tank setup and a spacious natural habitat. In this perspective, a tank setup offers limited opportunities to evade conflict or even the presence of conspecifics, thereby increasing social stress. In contrast, in a natural habitat competition for mates and other resources is likely to cause social stress, but at the same time the fish can evade conflicts. This view is consistent with the ecology of *A. rostratus* in its Panamanian habitat: fish live solitary and widely distributed along the stream banks and meet only at night.

Are rises a form of directed communication, like chirps appear to be, or rather a broadcast signal, like an alarm signal? In EOD recordings from the laboratory rises often appear to be synchronized among fish of the same sex, suggesting a directed signal, and were found to be initiated by both higher and lower EOD*f* fish (Fig. 2.2; Tallarovic and Zakon, 2005). Synchronized frequency drops were observed, too (Fig. 2.2 C). This observation is particularly interesting: (i) it suggests an interaction and a directed signal within the same sex. (ii) To my knowledge, slow transient reductions of EOD*f* and the neural mechanisms controlling them have not yet been reported for *Apteronotus* (Heiligenberg et al., 1996; Juranek and Metzner, 1997; Metzner, 1999). However, fast transient dips with a duration of 100-200 ms have previously been reported by Tallarovic and Zakon, 2002 in female *A. leptorhynchus*.

Individual recognition

In the field we observed that a losing male would return several times over the course of tens of minutes (Fig. 3.9 D). In this case, the resident male started his attack on the intruder over increasingly larger distances, suggesting that he recognized the intruder. Over large distances the only cue available to the resident male is EOD*f*. This matches well the observations of Harvey-Girard et al. (2010), who reported that *A. leptorhynchus* can learn to identify conspecifics based on their EOD*f*. Because EOD*f* changes continuously, behaviorally and driven by changes of water temperature, individual recognition based on EOD*f* is most suited for short time scales like those in the example of the repeated resident-intruder situation.

5.3 Open ends

In our field data (Chapter 3) we tracked four sympatric species of electric fish in a small stream in Panamá and focused on one, *A. rostratus*. The movement traces of the other species were not evaluated in detail, but it appears as if inter-species interactions occurred that would be fascinating to follow up. e.g., we observed the cessation of courtship of *A. rostratus*, when a *Sternopygus* approached the courting dyad. The female retreated into the stream's bank, while the male swam briskly upstream. Also, co-localizations of *Apteronotus* and *Eigenmannia* occurred repeatedly. In conclusion, these datasets certainly contain many more fascinating aspects of electric fish behavior and encourage more extensive studies of signals and interactions in a natural environment.

The goal of the presented long-term monitoring of fish in the laboratory (Chapter 4) was to identify the function of the long chirps and the associated communication scenes observed in our field study in Panamá. Because of this framework, we did not analyze the data in respect to individual activity. However, the data reviewed so far promises many more interesting insights in electric fish behavior. Therefore, the dataset should be re-analyzed in respect to individual activity and communication signals that could then be studied in respect to individual interactions, advertisement for upcoming courtship, the establishment of hierarchy, agonistic behavior etc. This task should be supported by a detailed automatic parametrization of chirps, that will help us to learn more about context-specific communication patterns. The availability of high-resolution video recordings continuous over many months will facilitate a systematic functional review of the classified communication signals.

Among the fascinating aspects of this dataset are the differences between male and female chirping. Male chirping increased with conductivity reduction of the tank water and was concentrated on the dark hours. The work of Hagedorn and Heiligenberg (1985) suggests a relationship of male chirping with the establishment of a dominance hierarchy among males, a hypothesis that could be systematically tested with our dataset. In contrast, the temporal distribution of chirps emitted by females differs strongly from that of males: females emitted chirps in similar proportions during the light and dark period. Additionally, and in contrast to the common view of female chirping, females emitted chirps long before the occurrence of and on days without courtship and spawning. Because *Apteronotus* females do not seem to establish a hierarchy that might serve to explain extensive female chirping, our findings suggest yet unknown functions for female chirping that could be studied on this dataset.

Eventually, the approach of our laboratory monitoring should be extended towards a naturalistic setting similar to that of Black-Cleworth, 1970. Small groups of electric fish could be monitored visually and electrically in a very large tank separated in micro environments, e.g., spawning substrates, hiding places and feeding stations. Interesting communication situations could be identified based on EOD analysis and then further analyzed incorporating visual tracking tools. This will permit for analyzing spontaneous behaviors in a less restricted environment that allows the animals to evade each other. Large datasets generated in such environments will likely contain many similar events that could then be analyzed with the same statistical rigor as experiments run under tightly controlled conditions, but with the benefit of less restricted and more natural behavior.

The tracking system for electric fish presented in this thesis provides many exciting opportunities, the most exciting certainly being the extended automated and non-invasive tracking of electric fish movements and communication interactions in the natural habitat. In our studies we demonstrated how this system can help extending our knowledge of natural communication situations. This novel approach has made possible a new kind of interplay of laboratory and field studies that promises to reveal many additional fascinating aspects of electric fish biology and of the constraints acting on the evolution of sensory systems.

Supplemental materials

Audio, animations, and video

Supporting media files are available on the attached data storage medium.

Filename: audio_courtship_communication-field_data.wav

Audio S 1: AUDIO TRACE OF THE COURTSHIP SEQUENCE SHOWN IN FIG. 3.3 A. A male (930 Hz) generated a series of small chirps. Eventually, the female (620 Hz) fish joins in, increases chirp rate and finishes with a big chirp (see Fig. 3.3 A), which is acknowledged by the male with a small chirp doublet.

Filename: movie_voltage_traces_and_position_estimate.mp4

Movie S 2: EXAMPLE OF RAW VOLTAGE RECORDINGS AND CORRESPONDING POSITION ESTIMATE OF A SINGLE FISH, *Eigenmannia humboldtii*, PASSING THROUGH THE ARRAY OF ELECTRODES. The head and tail area of its surrounding electric field are of inverse polarity, which is why the polarity of the recorded EOD switches as the fish passes an electrode. Note the irregular occuring discharge patterns on all electrodes. Previous studies (Hopkins, 1973) attributed similar discharge patterns to propagating distant lightning. The animation is played back at real-time.

Filename: movie_courtship_and_intruder-field_data.mp4

Movie S 3: ANIMATION OF THE COURTSHIP AND AGRESSION BEHAVIOR SHOWN IN FIG. 3.3 B–D. A courting dyad is engaged in intense chirp activity (transparent circles and 50 ms beeps at the fish's baseline EODf). An intruder male (red circles indicate position during the last 5 seconds, black ring marks current position) first lingers at a distance of one meter. When it approaches further, courting is interrupted and the resident male engages the intruder. Just before the male intruder retreats it emits a series of small chirps, and subsequently leaves the recording area. The resident male returns to the female and resumes to emit chirps. Eventually, the female responds with small chirps followed by a single big chirp (large empty circle and a 500 ms beep at the female's baseline EODf). Then both fish cease chirp activity and the male resumes to emit chirps after a few seconds. The animation is played back at 2× real-time. See movie S 4 for the raw electrode traces of the same scene.

Filename: movie_courtship_and_intruder-voltage_traces-field_data.mp4

Movie S 4: RAW VOLTAGE TRACES OF THE COURTSHIP AND AGGRESSION BEHAVIOR SHOWN IN MOVIE S 3. The video is played back at 2× real-time.

Filename: movie_repetitive_intruder-field_data.mp4

Movie S 5: ANIMATION OF A COURTSHIP SEQUENCE WITH MULTIPLE ATTEMPTS OF AN INTRUDING MALE TO APPROACH THE COURTING DYAD. The resident male drives the intruder three times away, starting the approach at increasingly greater distances (marked in Fig. 3.9 D, bottom no. 1–3). *Apteronotus rostratus* are marked by circles, *Eigenmannia humboltii* by squares. The animation is played back at 2× real-time.

Filename: movie_courtship-breeding_tank.avi

Movie S 6: SPAWNING OF THE CLOSELY RELATED SPECIES *Apteronotus lepthorhynchus* DURING A BREEDING EXPERIMENT. The overall sequence of chirp production is very similar to the courtship motiv observed in *A. rostratus*. However, male *A. lepthorhynchus* increasingly generate a second type of chirp, a variety of a big chirp, as spawning approaches. The video shows a big male (770 Hz) courting a smaller female (590 Hz) supported by audio created from concurrent EOD recordings. Both fish generate chirps at an increased rate (about 1.5 Hz), just before the male thrusts its snout against the female, which responds with a big chirp, clearly noticeable from the audio trace. Subsequently, the male retreats to a tube and the female hovers around the substrate, where the spawned egg was found.

Bibliography

Albert S, Crampton W (2005) Diversity and phylogeny of neotropical electric fishes (gymnotiformes). In *Electroreception* pages 360–409. Springer.

Alcock J (1994) Postinsemination associations between males and females in insects: the mate-guarding hypothesis. *Annu Rev Entomol* 39: 1–21.

Anderson D, Perona P (2014) Toward a Science of Computational Ethology. *Neuron* 84: 18–31.

Arnott G, Elwood R (2008) Information gathering and decision making about resource value in animal contests. *Anim Behav* 76: 529–542.

Assad C, Rasnow B, Stoddard P, Bower J Oct (1998) The electric organ discharges of the gymnotiform fishes: Ii. *Eigenmannia*. *J Comp Physiol A* 183: 419–432.

Barlow H (1972) Single units and sensation: A neuron doctrine for perceptual psychology? *Perception* 1: 371–394.

Bass A (1986) *Electric organs revisited: evolution of a vertebrate communication and orientation organ*. Wiley, New York.

Bastian J, Chacron M, Maler L (2004) Plastic and nonplastic pyramidal cells perform unique roles in a network capable of adaptive redundancy reduction. *Neuron* 41: 767–779.

Bastian J, Schniederjan S, Nguyenkim J (2001) Arginine vasotocin modulates a sexually dimorphic communication behavior in the weakly electric fish apteronotus leptorhynchus. *J Exp Biol* 204: 1909–1923.

Bastian J, Zakon H (2005) Plasticity of sense organs and brain. In *Electroreception* pages 195–228. Springer.

Bauer R (1979) Electric organ discharge (eod) and prey capture behaviour in the electric eel, electrophorus electricus. *Behav Ecol Sociobiol* 4: 311–319.

Benda J, Longtin A, Maler L (2006) A synchronization-sesynchronization sode for natural communication signals. *Neuron* 52: 347–358. ISSN 08966273.

Bennett M (1971) Electric organs. *Fish physiology* 5: 347–491.

Bennett M, Wurzel M, Grundfest H (1961) The electrophysiology of electric organs of marine electric fishes i. properties of electroplaques of torpedo nobiliana. *J Gen Physiol* 44: 757–804.

Berman N, Maler L (1999) Neural architecture of the electrosensory lateral line lobe: adaptations for coincidence detection, a sensory searchlight and frequency-dependent adaptive filtering. *J Exp Biol* 202: 1243–1253.

Betsch B, Einhaeuser W, Koerding K, Koenig P (2004) The world from a cat's perspective–statistics of natural videos. *Bio Cyb* 90: 41–50.

Black-Cleworth P (1970) The role of electrical discharges in the non-reproductive social behaviour of gymnotus carapo (gymnotidae, pisces). *Anim Behav Monographs* 3: 1–IN1.

Blumstein D, Mennill D, Clemins P, Girod L, Yao K, Patricelli G, Deppe J, Krakauer A, Clark C, Cortopassi K, others (2011) Acoustic monitoring in terrestrial environments using microphone arrays: applications, technological considerations and prospectus. *Journal of Applied Ecology* 48: 758–767.

Bradbury J, Vehrencamp S (2011) *Principles of animal communication*. Sinauer Sunderland 2nd edition.

Bullock T (1969) Species differences in effect of electroreceptor input on electric organ pacemakers and other aspects of behavior in electric fish; pp. 85–101. *Brain Behav Evolut* 2: 85–101.

Bullock T May (1970) The reliability of neurons. *J Gen Physiol* 55: 565–584.

Bullock T (1982) Electroreception. *Annu Rev Neurosci* 5: 121–170.

Bullock T (1984) Comparative neuroscience holds promise for quiet revolutions. *Science* 225: 473–478.

Bullock T, Behrend K, Heiligenberg W (1975) Comparison of the jamming avoidance responses in gymnotoid and gymnarchid electric fish: a case of convergent evolution of behavior and its sensory basis. *J Comp NeurolComp Physiol A* 103: 97–121.

Bullock T, Bodznick D, Northcutt R (1993) The phylogenetic distribution of electroreception: evidence for convergent evolution of a primitive vertebrate sense modality. In *How do Brains Work?* pages 581–602. Springer.

Bullock T, H R, Scheich H (1972) The jamming avoidance response of high frequency electric fish. II. Quantitative aspects. *J Comp Physiol* 77: 23–48. ISSN 0340-7594.

Bullock T, Heiligenberg W, editors (1986) *Electroreception*. Wiley, New York.

Caputi A, Carlson B, Macadar O (2005) Electric organs and their control. In *Electroreception* pages 410–451. Springer.

Carlson BA, Hasan SM, Hollmann M, Miller DB, Harmon LJ, Arnegard ME (2011) Brain evolution triggers increased diversification of electric fishes. *Science* 332: 583–586.

Catania K (2014) The shocking predatory strike of the electric eel. *Science* 346: 1231–1234.

Chacron M, Doiron B, Maler L, Longtin A, Bastian J (2003) Non-classical receptive field mediates switch in a sensory neuron's frequency tuning. *Nature* 423: 77–81.

Chacron M, Longtin A, Maler L (2011) Efficient computation via sparse coding in electrosensory neural networks. *Curr Opin Neurobiol* 21: 752–760.

Chacron MJ, Fortune ES (2010) Subthreshold membrane conductances enhance directional selectivity in vertebrate sensory neurons. *Journal of neurophysiology* 104: 449–462.

Chacron MJ, Maler L, Bastian J (2005) Electroreceptor neuron dynamics shape information transmission. *Nature Neurosci* 8: 673–678.

Changeux JP (1993) Chemical signaling in the brain. *Sci Am* 269: 58–58.

Chen L, House J, Krahe R, Nelson M Apr (2005) Modeling signal and background components of electrosensory scenes. *J Comp Physiol A* 191: 331–345.

Collins J, Imhoff T, Grigg P (1996) Noise-enhanced information transmission in rat sa1 cutaneous mechanoreceptors via aperiodic stochastic resonance. *J Neurophysiol* 76: 642–645.

Crampton W, Albert J (2006) Evolution of electric signal diversity in gymnotiform fishes. *Communication in fishes* 2: 647–731.

Crews D (1975) Effects of different components of male courtship behaviour on environmentally induced ovarian recrudescence and mating preferences in the lizard, anolis carolinensis. *Animal Behaviour* 23: 349–356.

Crick F (1984) Function of the thalamic reticular complex: the searchlight hypothesis. *Proc Natl Acad Sci USA* 81: 4586–4590.

Cuddy M, Aubin-Horth N, Krahe R (2012) Electrocommunication behaviour and non invasively-measured androgen changes following induced seasonal breeding in the weakly electric fish, apteronotus leptorhynchus. *Horm Behav* 61: 4–11.

Czech-Damal N, Liebschner A, Miersch L, Klauer G, Hanke F, Marshall C, Dehnhardt G, Hanke W (2012) Electroreception in the guiana dolphin (sotalia guianensis). *Proceedings of the Royal Society of London B: Biological Sciences* 279: 663–668.

Dankert H, Wang L, Hoopfer E, Anderson D, Perona P (2009) Automated monitoring and analysis of social behavior in drosophila. *Nature methods* 6: 297–303.

Dawkins M, Guilford T (1994) Design of an Intention Signal in the Bluehead Wrasse (*Thalassoma bifasciatum*). *Proc Royal Soc B* 257: 123–128. ISSN 0962-8452.

de Santana C, Vari R (2013) Brown ghost electric fishes of the *Apteronotus leptorhynchus* species-group (Ostariophysi, Gymnotiformes); monophyly, major clades, and revision. *Zool J Linnean Soc* 168: 564–596. ISSN 00244082.

Deemyad T, Maler L, Chacron M (2011) Inhibition of sk and m channel-mediated currents by 5-ht enables parallel processing by bursts and isolated spikes. *J Neurophysiol* 105: 1276–1294.

Douglass J, Wilkens L, Pantazelou E, Moss F, others (1993) Noise enhancement of information transfer in crayfish mechanoreceptors by stochastic resonance. *Nature* 365: 337–340.

Dulka J, Maler L (1994) Testosterone modulates female chirping behavior in the weakly electric fish, apteronotus leptorhynchus. *J Comp Physiol A* 174: 331–343.

Dulka J, Nickla J (2001) Direct evidence that male and female chirps synchronize spawning in the weakly electric brown ghost knifefish, apteronotus leptorhynchus. Neurobiology of Electrosensory Organisms, Bonn.

Dunlap K (2002) Hormonal and body size correlates of electrocommunication behavior during dyadic interactions in a weakly electric fish, apteronotus leptorhynchus. *Horm Behav* 41: 187–194.

Dunlap K, Larkins-Ford J (2003) Diversity in the structure of electrocommunication signals within a genus of electric fish, apteronotus. *J Comp Physiol A* 189: 153–161.

Dunlap K, Oliveri L (2002) Retreat site selection and social organization in captive electric fish, apteronotus leptorhynchus. *J Comp Physiol A* 188: 469–477.

Dunlap K, Smith G, Yekta A (2000) Temperature dependence of electrocommunication signals and their underlying neural rhythms in the weakly electric fish, *Apteronotus leptorhynchus*. *Brain Behav Evol* 55: 152–162. ISSN 0006-8977.

Dunlap K, Thomas P, Zakon H July (1998) Diversity of sexual dimorphism in electrocommunication signals and its androgen regulation in a genus of electric fish, *Apteronotus*. *J Comp Physiol A* 183: 77–86.

Dye J (1987) Dynamics and stimulus-dependence of pacemaker control during behavioral modulations in the weakly electric fish, apteronotus. *J Comp Physiol A* 161: 175–185.

Eagleman DM (2001) Visual illusions and neurobiology. *Nature Rev Neurosci* 2: 920–926.

Engler G, Fogarty C, Banks J, Zupanc G (2000) Spontaneous modulations of the electric organ discharge in the weakly electric fish, *Apteronotus leptorhynchus*: A biophysical and behavioral analysis. *J Comp Physiol A* 186: 645–660. ISSN 03407594.

Engler G, Zupanc G (2001) Differential production of chirping behavior evoked by electrical stimulation of the weakly electric fish, *Apteronotus leptorhynchus*. *J Comp Physiol A* 187: 747–756.

Feldberg W, Fessard A, Nachmansohn D (1940) The cholinergic nature of the nervous supply to the electric organ of the torpedo (torpedo marmorata). *J Physiol* 97: 3–4.

Fortune ES, Rose GJ (1997) Passive and active membrane properties contribute to the temporal filtering properties of midbrain neurons in vivo. *The Journal of neuroscience* 17: 3815–3825.

Fotowat H, Harrison R, Krahe R (2013) Statistics of the electrosensory input in the freely swimming weakly electric fish *Apteronotus leptorhynchus*. *J Neurosci* 33: 13758–13772. ISSN 1529-2401.

Franchina C, Stoddard P (1998) Plasticity of the electric organ discharge waveform of the electric fish *Brachyhypopomus pinnicaudatus* I. Quantification of day-night changes. *J Comp Physiol A* 183: 759–768. ISSN 03407594.

Friedman M, Hopkins C (1996) Tracking individual mormyrid electric fish in the field using electric organ discharge waveforms. *Anim Behav* 51: 391–407. ISSN 00033472.

Froudarakis E, Berens P, Ecker A, Cotton R, Sinz F, Yatsenko D, Saggau P, Bethge M, Tolias A (2014) Population code in mouse v1 facilitates readout of natural scenes through increased sparseness. *Nature Neurosci* 17: 851–857.

Fugère V, Krahe R (2010) Electric signals and species recognition in the wave-type gymnotiform fish apteronotus leptorhynchus. *J Exp Biol* 213: 225–236.

Fugère V, Ortega H, Krahe R (2011) Electrical signalling of dominance in a wild population of electric fish. *Biol Lett* 7: 197–200. ISSN 1744-9561.

Galzi J, Revah F, Bessis A, Changeux J (1991) Functional architecture of the nicotinic acetylcholine receptor: from electric organ to brain. *Annu Rev Pharmacol Toxicol* 31: 37–72.

Ganz J, Kaslin J, Freudenreich D, Machate A, Geffarth M, Brand M (2012) Subdivisions of the adult zebrafish subpallium by molecular marker analysis. *J Comp Neurol* 520: 633–655.

Gil D, Leboucher G, Lacroix A, Cue R, Kreutzer M (2004) Female canaries produce eggs with greater amounts of testosterone when exposed to preferred male song. *Horm Behav* 45: 64–70.

Glynn I (1963) 'transport adenosinetriphosphatase'in electric organ. the relation between ion transport and oxidative phosphorylation. *J Physiol* 169: 452–465.

Gollisch T, Meister M (2010) Eye smarter than scientists believed: neural computations in circuits of the retina. *Neuron* 65: 150–164.

Gomez-Marin A, Paton J, Kampff A, Costa R, Mainen Z (2014) Big behavioral data: psychology, ethology and the foundations of neuroscience. *Nature Neuroscience* 17: 1455–1462.

Green J, Collins C, Kyzar E, Pham M, Roth A, Gaikwad S, Cachat J, Stewart A, Landsman S, Grieco F, others (2012) Automated high-throughput neurophenotyping of zebrafish social behavior. *Journal of neuroscience methods* 210: 266–271.

Hagedorn M (1986) The ecology, courtship, and mating of gymnotiform electric fish. In *Electroreception* pages 497–525. Wiley, New York.

Hagedorn M (1988) Ecology and behavior of a pulse-type electric fish hypopomus occidentalis in a fresh-water stream in panama. *Copeia* 2: 324–335.

Hagedorn M, Heiligenberg W (1985) Court and spark: electric signals in the courtship and mating of gymnotid fish. *Anim Behav* 33: 254–265.

Harvey-Girard E, Giassi A, Ellis W, Maler L (2013) Expression of the cannabinoid cb1 receptor in the gymnotiform fish brain and its implications for the organization of the teleost pallium. *J Comp Neurol* 521: 949–975.

Harvey-Girard E, Tweedle J, Ironstone J, Cuddy M, Ellis W, Maler L (2010) Long-term recognition memory of individual conspecifics is associated with telencephalic expression of egr-1 in the electric fish apteronotus leptorhynchus. *J Comp Neurol* 518: 2666–2692.

Heiligenberg W (1991)a *Neural nets in electric fish*. MIT press Cambridge, MA.

Heiligenberg W (1991)b *Neural nets in electric fish.* MIT Press Cambridge, MA.

Heiligenberg W, Wong C, Metzner W, Keller C (1996) Motor control of the jamming avoidance response of apteronotus leptorhynchus: evolutionary changes of a behavior and its neuronal substrates. *J Comp Physiol A* 179: 653–674.

Hiryu S, Hagino T, Riquimaroux H, Watanabe Y (2007) Echo-intensity compensation in echolocating bats (pipistrellus abramus) during flight measured by a telemetry microphone. *The Journal of the Acoustical Society of America* 121: 1749–1757.

Ho W, Fernandes C, Alves-Gomes J, Smith G (2010) Sex differences in the electrocommunication signals of the electric fish apteronotus bonapartii. *Ethology* 116: 1050–1064.

Ho W, Rack J, Smith G (2013) Divergence in androgen sensitivity contributes to population differences in sexual dimorphism of electrocommunication behavior. *Horm Behav* 63: 49–53.

Hofmann V, Geurten B, Sanguinetti-Scheck J, Gomez-Sena L, Engelmann J (2014) Motor patterns during active electrosensory acquisition. *Frontiers in behavioral neuroscience* 8.

Hopkins C (1972) Sex differences in electric signaling in an electric fish. *Science* 176: 1035–1037.

Hopkins C (1973) Lightning as background noise for communication among electric fish. *Nature* 242: 268–270.

Hopkins C (1974)a Electric communication: functions in the social behavior of eigenmannia virescens. *Behaviour* 50: 270–304.

Hopkins C (1974)b Electric communication in the" reproductive behavior of stemopygus macmms (gymnotoidei). *Z. TierpsychoL* 35: 518–535.

Hopkins C (1976) Stimulus filtering and electroreception: tuberous electroreceptors in three species of gymnotoid fish. *J Comp Physiol* 111: 171–207.

Hopkins C, Heiligenberg WF (1978) Evolutionary designs for electric signals and electroreceptors in gymnotoid fishes of surinam. *Behavioral Ecology and Sociobiology* 3: 113–134.

Hoshimiya N, Shogen K, Matsuo T, Chichibu S (1980) The *Apteronotus* eod field: waveform and eod field simulation. *J Comp Physiol A* 135: 283–290.

Hromadka T, DeWeese M, Zador A, others (2008) Sparse representation of sounds in the unanesthetized auditory cortex. *PLoS Biol* 6: e16.

Hughes N, Kelly L (1996) New techniques for 3-d video tracking of fish swimming movements in still or flowing water. *Can J Fish Aquat Sci* 53: 2473–2483.

Hupé G, Lewis J (2008) Electrocommunication signals in free swimming brown ghost knifefish, *Apteronotus leptorhynchus*. *J Exp Biol* 211: 1657–1667.

Jun J, Longtin A, Maler L (2012) Precision measurement of electric organ discharge timing from freely moving weakly electric fish. *J Neurophysiol* 107: 1996–2007. ISSN 1522-1598.

Jun J, Longtin A, Maler L (2013) Real-time localization of moving dipole sources for tracking multiple free-swimming weakly electric fish. *PLoS ONE* 8. ISSN 19326203.

Jun J, Longtin A, Maler L (2014)a Enhanced sensory sampling precedes self-initiated locomotion in an electric fish. *J Exp Biol* 217: 3615–3628.

Jun J, Longtin A, Maler L (2014)b Long-term behavioral tracking of freely swimming weakly electric fish. *JoVE* NA: e50962—-e50962.

Juranek J, Metzner W (1997) Cellular characterization of synaptic modulations of a neuronal oscillator in electric fish. *J Comp Physiol A* 181: 393–414.

Kalmijn A (1966) Electro-perception in sharks and rays. *Nature* 212: 1232–1233.

Kawasaki M, Rose G, Heiligenberg W (1988) Temporal hyperacuity in single neurons of electric fish. *Nature* 336: 173–176.

Keller C, Maler L, Heiligenberg W (1990) Structural and functional organization of a diencephalic sensory-motor interface in the gymnotiform fish, eigenmannia. *Journal of Comparative Neurology* 293: 347–376.

Kelly M, Babineau D, Longtin A, Lewis J (2008) Electric field interactions in pairs of electric fish: modeling and mimicking naturalistic inputs. *Biol Cybern* 98: 479–490.

Kern R, Van Hateren J, Michaelis C, Lindemann J, Egelhaaf M (2005) Function of a fly motion-sensitive neuron matches eye movements during free flight. *PLoS Biol* 3: 1130.

Kersten D, Mamassian P, Yuille A (2004) Object perception as bayesian inference. *Annu Rev Psychol* 55: 271–304.

Kirschbaum F (1983) Myogenic electric organ precedes the neurogenic organ in apteronotid fish. *Naturwissenschaften* 70: 205–207.

Kirschbaum F, Schugardt C (2002) Reproductive strategies and developmental aspects in mormyrid and gymnotiform fishes. *J Physiol Paris* 96: 557–566. ISSN 09284257.

Kirschbaum F, Westby G (1975) Development of the electric discharge in mormyrid and gymnotid fish (*Marcusenius* sp. and *Eigenmannia virescens*). *Experientia* 31: 1290–1294. ISSN 00144754.

Knudsen E (1974) Behavioral thresholds to electric signals in high frequency electric fish. *J Comp Physiol A* 91: 333–353.

Knudsen E (1975) Spatial aspects of the electric fields generated by weakly electric fish. *J Comp Physiol A* 99: 103–118.

Knutsen P, Biess A, Ahissar E (2008) Vibrissal kinematics in 3d: tight coupling of azimuth, elevation, and torsion across different whisking modes. *Neuron* 59: 35–42.

Krahe R, Gabbiani F (2004) Burst firing in sensory systems. *Nature Rev Neurosci* 5: 13–23.

Krahe R, Maler L (2014) Neural maps in the electrosensory system of weakly electric fish. *Curr Opin Neurobiol* 24: 13–21.

Kramer B, Kirschbaum F, Markl H (2013) Species specificity 0f electric organ discharges in a sympatric group of gymnotoid fish from manaus (amazonas). In *Sensory Physiology of Aquatic Lower Vertebrates: Satellite Symposium of the 28th International Congress of Physiological Sciences, Keszthely, Hungary, 1980* 31 page 195. Elsevier.

Kroodsma D (1976) Reproductive development in a female songbird: differential stimulation by quality of male song. *Science* 192: 574–575.

Ladich F (2007) Females whisper briefly during sex: context- and sex-specific differences in sounds made by croaking gouramis. *Anim Behav* 73: 379–387. ISSN 00033472.

Langner G, Scheich H (1978) Active phase coupling in electric fish: Behavioral control with microsecond precision. *Journal of comparative physiology* 128: 235–240.

Lavoue S, Miya M, Arnegard M, Sullivan J, Hopkins C, Nishida M (2012) Comparable ages for the independent origins of electrogenesis in african and south american weakly electric fishes. *PLoS One* 7: e36287–e36287.

Lee T, Mumford D (2003) Hierarchical bayesian inference in the visual cortex. *JOSA A* 20: 1434–1448.

Leifer A, Fang-Yen C, Gershow M, Alkema M, Samuel AD (2011) Optogenetic manipulation of neural activity in freely moving caenorhabditis elegans. *Nature methods* 8: 147–152.

Levin J, Miller J (1996) Broadband neural encoding in the cricket cereal sensory system enhanced by stochastic resonance. *Nature* 380: 165–168.

Lewicki M (2002) Efficient coding of natural sounds. *Nature Neurosci* 5: 356–363.

Lewicki M, Olshausen B, Surlykke A, Moss C (2014) Scene analysis in the natural environment. *Front Psychol* 5: 1–21. ISSN 16641078.

Linkenkaer-Hansen K, Nikulin V, Palva S, Ilmoniemi R, Palva J (2004) Prestimulus oscillations enhance psychophysical performance in humans. *J Neurosci* 24: 10186–10190.

Lissmann H, Machin K (1958) The mechanism of object location in gymnarchus niloticus and similar fish. *J Exp Biol* 35: 451–486.

Lobel P (1992) Sounds produced by spawning fishes. *Environ Biol Fishes* 33: 351–358. ISSN 03781909.

Lochmann T, Deneve S (2011) Neural processing as causal inference. *Curr Opin Neurobiol* 21: 774–781.

Logan C, Hyatt L, Gregorcyk L (1990) Song playback initiates nest building during clutch overlap in mockingbirds, mimus polyglottos. *Anim Behav* 39: 943–953.

Luo L, Gershow M, Rosenzweig M, Kang K, Fang-Yen C, Garrity P, Samuel A (2010) Navigational decision making in drosophila thermotaxis. *J Neurosci* 30: 4261–4272.

Maciver M, Sharabash N, Nelson M (2001) Prey-capture behavior in gymnotid electric fish: motion analysis and effects of water conductivity. *Journal of experimental biology* 204: 543–557.

Maler L, Finger T, Karten H (1974) Differential projections of ordinary lateral line receptors and electroreceptors in the gymnotid fish, *Apteronotus (Sternarchus) albifrons*. *J Comp Neurol* 158: 363–382.

Markham M, McAnelly M, Stoddard P, Zakon H (2009) Circadian and social cues regulate ion channel trafficking. *PLoS Biology* 7. ISSN 15449173.

Marsat G, Maler L (2010) Neural heterogeneity and efficient population codes for communication signals. *J Neurophysiol* 104: 2543–2555.

Marsat G, Maler L (2012) Preparing for the unpredictable: adaptive feedback enhances the response to unexpected communication signals. *J Neurophysiol* 107: 1241–1246.

Marsat G, Proville R, Maler L (2009) Transient signals trigger synchronous bursts in an identified population of neurons. *J Neurophysiol* 102: 714–723.

McDermott JH (2009) The cocktail party problem. *Curr Biol* 19: R1024–R1027.

Metzner W (1999) Neural circuitry for communication and jamming avoidance in gymnotiform electric fish. *J Exp Biol* 202: 1365–1375.

Meyer J, Leong M, Keller C (1987) Hormone-induced and maturational changes in electric organ discharges and electroreceptor tuning in the weakly electric fish *Apteronotus*. *J Comp Physiol A* 160: 385–394. ISSN 03407594.

Möhres F (1957) Elektrische entladungen im dienste der revierabgrenzung bei fischen. *Naturwissenschaften* 44: 431–432.

Moller P (1995) *Electric fishes: history and behavior* 17. Chapman & Hall London.

Moortgat K, Keller C, Bullock T, Sejnowski T (1998) Submicrosecond pacemaker precision is behaviorally modulated: the gymnotiform electromotor pathway. *Proc Natl Acad Sci USA* 95: 4684–4689. ISSN 0027-8424.

Mueller T, Guo S (2009) The distribution of gad67-mrna in the adult zebrafish (teleost) forebrain reveals a prosomeric pattern and suggests previously unidentified homologies to tetrapods. *J Comp Neurol* 516: 553–568.

Murray J (1995) Spectral and temporal analysis of male and female courtship signals in the gymnotiform electric fish apteronotus leptorhynchus. page 412. 4th Internatl. Congress Neuroethology, Cambridge.

Murray R (1960) Electrical sensitivity of the ampullae of lorenzini. *Nature* 187: 957.

Nelson M, Xu Z, Payne J (1997) Characterization and modeling of P-type electrosensory afferent responses to amplitude modulations in a wave-type electric fish. *J Comp Physiol A* 181: 532–544. ISSN 03407594.

Nelson ME (2005) Target detection, image analysis, and modeling. In *Electroreception* pages 290–317. Springer.

Nelson ME (2011) Electric fish. *Current Biology* 21: R528–R529.

Nelson ME, MacIver MA (1999) Prey capture in the weakly electric fish *Apteronotus albifrons*: sensory acquisition strategies and electrosensory consequences. *J Exp Biol* 202: 1195–1203.

Noldus L, Spink A, Tegelenbosch R (2001) EthoVision: a versatile video tracking system for automation of behavioral experiments. *Behav Res Meth Ins C* 33: 398–414. ISSN 0743-3808.

Olshausen B, Field D (1996) Emergence of simple-cell receptive-field properties by learning a sparse code for natural images. *Nature* 381: 607–609.

Oswald A, Chacron M, Doiron B, Bastian J, Maler L (2004) Parallel processing of sensory input by bursts and isolated spikes. *J Neurosci* 24: 4351–4362.

Parker G, Van Heusen A (1917) The responses of the catfish, amiurus nebulosus, to metallic and non-metallic rods. *Am J Physiol* 44: 405–420.

Peter R, Yu K, Marchant T, Rosenblum P (1990) Direct neural regulation of the teleost adenohypophysis. *J Exp Zool* 256: 84–89.

Poggio T, Koch C (1985) Ill-posed problems in early vision: from computational theory to analogue networks. *Proc Royal Soc B* 226: 303–323.

Prasad P, Ogawa S, Parhar I (2015) Role of serotonin in fish reproduction. *Front Neurosci* 9: 195.

Prez-Escudero A, Vicente-Page J, Hinz R, Arganda S, de Polavieja G (2014) idtracker: tracking individuals in a group by automatic identification of unmarked animals. *Nature methods* 11: 743–748.

Rasnow B, Assad C, Bower J (1993) Phase and amplitude maps of the electric organ discharge of the weakly electric fish, *Apteronotus leptorhynchus*. *J Comp Physiol A* 172: 481–491. ISSN 03407594.

Reardon E, Parisi A, Krahe R, Chapman L (2011) Energetic constraints on electric signalling in wave-type weakly electric fishes. *J Exp Biol* 214: 4141–4150.

Rodriguez-Munoz R, Bretman A, Slate J, Walling C, Tregenza T (2010) Natural and sexual selection in a wild insect population. *Science* 328: 1269–1272.

Rodriguez-Munoz R, Bretman A, Tregenza T (2011) Guarding males protect females from predation in a wild insect. *Curr Biol* 21: 1716–1719.

Rose G, Heiligenberg W (1984) Temporal hyperacuity in the electric sense of fish. *Nature* 318: 178–180.

Salgado J, Zupanc G (2011) Echo response to chirping in the weakly electric brown ghost knifefish (*Apteronotus leptorhynchus*): role of frequency and amplitude modulations . *Can J Zool* 89: 498–508.

Sas E, Maler L (1983) The nucleus praeeminentialis: a golgi study of a feedback center in the electrosensory system of gymnotid fish. *J Comp Neurol* 221: 127–144.

Sas E, Maler L (1987) The organization of afferent input to the caudal lobe of the cerebellum of the gymnotid fish apteronotus leptorhynchus. *Anat Embryol* 177: 55–79.

Saunders J, Bastian J (1984) The physiology and morphology of two types of electrosensory neurons in the weakly electric fishapteronotus leptorhynchus. *Journal of Comparative Physiology A* 154: 199–209.

Sawtell N, Williams A, Bell C (2005) From sparks to spikes: information processing in the electrosensory systems of fish. *Curr Opin Neurobiol* 15: 437–443.

Scheich H, Langner G, Tidemann C, Coles R, Guppy A (1985) Electroreception and electrolocation in platypus. *Nature* 319: 401–402.

Schwartz O, Simoncelli E (2001) Natural signal statistics and sensory gain control. *Nature Neurosci* 4: 819–825.

Schwassmann H (1976) *Ecology and taxonomic status of different geographic populations of Gymnorhamphichtys hypostomus Ellis (Pisces, Cypriniformes, Gymnotoidei)*.

Schwassmann H (1978) *Times of annual spawning and reproductive strategies in Amazonian fishes*.

Serrano-Fernandez P (2003) Gradual frequency rises in interacting black ghost knifefish, apteronotus albifrons. *JComp Physiol A* 189: 685–692.

Sharafi N, Benda J, Lindner B (2013) Information filtering by synchronous spikes in a neural population. *J Comput Neurosci* 34: 285–301.

Silva A, Quintana L, Perrone R, Sierra F (2008) Sexual and seasonal plasticity in the emission of social electric signals. Behavioral approach and neural bases. *J Physiol Paris* 102: 272–278. ISSN 09284257.

Simoncelli EP, Olshausen BA (2001) Natural image statistics and neural representation. *Annu Rev Neurosci* 24: 1193–1216.

Singh N, Theunissen F (2003) Modulation spectra of natural sounds and ethological theories of auditory processing. *J Acoust Soc Am* 114: 3394–3411.

Smith C (2008) *Biology of sensory systems*. John Wiley & Sons.

Smith G (2013) Evolution and hormonal regulation of sex differences in the electrocommunication behavior of ghost knifefishes (Apteronotidae). *J Exp Biol* 216: 2421–33. ISSN 1477-9145.

Smith GT, Combs N (2008) Serotonergic activation of 5ht 1a and 5ht 2 receptors modulates sexually dimorphic communication signals in the weakly electric fish apteronotus leptorhynchus. *Hormones and behavior* 54: 69–82.

Stamper SA, Roth E, Cowan NJ, Fortune ES (2012) Active sensing via movement shapes spatiotemporal patterns of sensory feedback. *The Journal of experimental biology* 215: 1567–1574.

Steinbach A (1970) Diurnal movements and discharge characteristics of electric gymnotid fishes in the Rio Negro, Brazil. *Biol Bull* 138: 200–210.

Stoddard P, Markham M, Salazar V, Allee S Jan. (2007) Circadian rhythms in electric waveform structure and rate in the electric fish *Brachyhypopomus pinnicaudatus*. *Physiol Behav* 90: 11–20. ISSN 00319384.

Swierczek NA, Giles A, Rankin C, Kerr R (2011) High-throughput behavioral analysis in c. elegans. *Nature methods* 8: 592–598.

Tallarovic S, Zakon H (2002) Electrocommunication signals in female brown ghost electric knifefish, apteronotus leptorhynchus. *J Comp Physiol A* 188: 649–657.

Tallarovic S, Zakon H (2005) Electric organ discharge frequency jamming during social interactions in brown ghost knifefish, apteronotus leptorhynchus. *Anim Behav* 70: 1355–1365.

Theunissen F, Sen K, Doupe A (2000) Spectral-temporal receptive fields of nonlinear auditory neurons obtained using natural sounds. *J Neurosci* 20: 2315–2331.

Todd B, Andrews D (1999) The identification of peaks in physiological signals. *Comput Biomed Res* 32: 322–335. ISSN 0010-4809.

Triefenbach F, Zakon H (2003) Effects of sex, sensitivity and status on cue recognition in the weakly electric fish apteronotus leptorhynchus. *Anim Behav* 65: 19–28.

Triefenbach F, Zakon H (2008) Changes in signalling during agonistic interactions between male weakly electric knifefish, apteronotus leptorhynchus. *Animal Behaviour* 75: 1263–1272.

Turner C, Derylo M, de Santana C, Alves-Gomes J, Smith G (2007) Phylogenetic comparative analysis of electric communication signals in ghost knifefishes (Gymnotiformes: Apteronotidae). *J Exp Biol* 210: 4104–4122. ISSN 0022-0949.

Ulanovsky N, Moss C (2008) What the bat's voice tells the bat's brain. *Proceedings of the National Academy of Sciences* 105: 8491–8498.

Vinje W, Gallant J (2002) Natural stimulation of the nonclassical receptive field increases information transmission efficiency in v1. *J Neurosci* 22: 2904–2915.

Vonderschen K, Chacron MJ (2011) Sparse and dense coding of natural stimuli by distinct midbrain neuron subpopulations in weakly electric fish. *J Neurophysiol* 106: 3102–3118.

Walz H, Grewe J, Benda J (2014) Static frequency tuning properties account for changes in neural synchrony evoked by transient communication signals. *J Neurophysiol* 112: 752–765. ISSN 1522-1598.

Walz H, Hupé G, Benda J, Lewis J (2013) The neuroethology of electrocommunication: how signal background influences sensory encoding and behaviour in Apteronotus leptorhynchus. *J Physiol Paris* 107: 13–25.

Whittaker VP (1992) *The cholinergic neuron and its target: the electromotor innervation of the electric ray" Torpedo" as a model*. Birkhauser.

Wilson E (1975) *Sociobiology: The New Synthesis*. Harvard University Press Camridge MA.

Wilson E, Bossert W (1963) Chemical communication among animals. *Recent progress in hormone research* 19: 673.

Wong CJ (1997) Afferent and efferent connections of the diencephalic prepacemaker nucleus in the weakly electric fish, eigenmannia virescens: interactions between the electromotor system and the neuroendocrine axis. *J Comp Neurol* 383: 18–41.

Wright S, Nocedal J (1999) *Numerical optimization* 2. Springer New York.

Yartsev M, Ulanovsky N (2013) Representation of three-dimensional space in the hippocampus of flying bats. *Science* 340: 367–372.

Young M, Yamane S (1992) Sparse population coding of faces in the inferotemporal cortex. *Science* 256: 1327–1331.

Zakon H (1986) The electroreceptive periphery. In *Electroreception* pages 103–156. Wiley, New York.

Zakon H, Lu Y, Zwickl D, Hillis D (2006) Sodium channel genes and the evolution of diversity in communication signals of electric fishes: convergent molecular evolution. *Proc Natl Acad Sci USA* 103: 3675–3680.

Zakon H, Oestreich J, Tallarovic S, Triefenbach F (2002) EOD modulations of brown ghost electric fish: JARs, chirps, rises, and dips. *J Physiol Paris* 96: 451–458. ISSN 09284257.

Zhou M, Smith G (2006) Structure and sexual dimorphism of the electrocommunication signals of the weakly electric fish, adontosternarchus devenanzii. *J Exp Biol* 209: 4809–4818.

Zupanc G (2002) From oscillators to modulators: behavioral and neural control of modulations of the electric organ discharge in the gymnotiform fish, apteronotus leptorhynchus. *J Physiol Paris* 96: 459–472.

Zupanc G, Bullock T (2005) From electrogenesis to electroreception: an overview. In *Electroreception* pages 5–46. Springer.

Zupanc G, Maler L (1993) Evoked chirping in the weakly electric fish apteronotus leptorhynchus: a quantitative biophysical analysis. *Can J Zool* 71: 2301–2310.

Zupanc G, Maler L (1997) Neuronal control of behavioral plasticity: the prepacemaker nucleus of weakly electric gymnotiform fish. *J Comp Physiol A* 180: 99–111.

Zupanc G, Sirbulescu R, Nichols A, Ilies I Feb. (2006) Electric interactions through chirping behavior in the weakly electric fish, *Apteronotus leptorhynchus*. *J Comp Physiol A* 192: 159–173.